A DETAILED FRACTURE ANALYSIS OF TRIASSIC KINGRIALI FORMATION IN THE WESTERN SALT RANGE AND TRANS INDUS RANGES (SURGHAR RANGE), PAKISTAN

BY

ADNAN SAMIULLAH

DEPARTMENT OF EARTH SCIENCES,

QUAID-I-AZAM UNIVERSITY ISLAMABAD, PAKISTAN

SESSION 2021-2023

A DETAILED FRACTURE ANALYSIS OF TRIASSIC KINGRIALI FORMATION IN THE WESTERN SALT RANGE AND TRANS INDUS RANGES (SURGHAR RANGE), PAKISTAN

A Dissertation Submitted to the Department of Earth Sciences, Qusid-I-Azam University Islamabad, Pakistan for Partial Fulfillment of Requirement for the Degree of MPhil in Geology

By

ADNAN SAMIULLAH

Supervised By

DR. MUTLOOB HUSSAIN

DEPARTMENT OF EARTH SCIENCES,

QUAID-I-AZAM UNIVERSITY ISLAMABAD, PAKISTAN

SESSION 2021-2023

CERTIFICATE

It is certified that **Mr. Adnan Samiullah S/o Hayat Ullah Khan (Registration No. 02112113005)** carried out the work contained in this dissertation under my supervision and accepted in its present form by Department of Earth Sciences as satisfying the requirements for the award of **M.Phil Degree in Geology.**

RECOMMENDED BY

Dr. Mutloob Hussain
Associate Professor/Supervisor _____

Dr. Asghar Ali
External Examiner _____

Prof. Dr. Mumtaz M. Shah
Chairperson _____

DEPARTMENT OF EARTH SCIENCES
QUAID-I-AZAM UNIVERSITY
ISLAMABAD

DEDICATED

TO

TO MY BELOVED FATHER, LATE MOTHER,
FAMILY AND FRIENDS

ABSTRACT

The current research studies carried out on Kingriali Formation western Salt Range (Nammal Gorge and Zaluch Nala) and Trans Indus Ranges (Surghar Range) to understand the structure architecture of the area. The stratigraphic sequence exposed in study area ranging in age from the Permian to Miocene/Pliocene, resulting from the collision of the Indian plate with the Eurasian plate, north-south compressional stresses caused considerable deformation. Fracture analysis of Triassic Kingriali Formation is carried out in research area i.e., Nammal Gorge, Zaluch Nala, and Surghar Range section. Using Circular Inventory Method, the petrophysical properties e.g., fracture density, fracture porosity and fracture permeability are calculated. These calculated data are plotted crossly on graphs to determine the relationship between them. The relationship between fracture density and fracture porosity/fracture porosity and fracture permeability is uniform, whereas the relationship between fracture density and fracture permeability is not. The reservoir potential for each formation was evaluated qualitatively using the Naturally Fracture Reservoir (NFR) classification. Which represent that Kingriali formation is type-3 to type-1 type reservoir in study area. The fracture system varies in different sections therefore Nammal Gorge and Surghar Range Section have high reservoir potential while Zaluch Nala Section have comparatively low reservoir potential. The maximum stress direction (δ1) of 23 stations lies in NW direction 6 stations in NE direction while 1 station lies in SE direction. This indicates that the deformation i.e., fold, fault, joint and fracture in study area is due to the North-South compressional stresses.

ACKNOWLEDGMENTS

First and foremost, I am deeply grateful to Almighty Allah who made me able to complete this research work successfully. Countless salutations are upon the Holy Prophet Muhammad (S.A.W), the foundation of knowledge who always guided His Ummah to seek knowledge.

I would like to express deepest gratitude and appreciation to my supervisor **Associate Professor Dr. Mutloob Hussain** for his sincere help, continuous guidance, and precious remarks throughout the research work. I am grateful to **Professor Dr. Mumtaz Muhammad Shah** Chairman Department of Earth Sciences Quaid I Azam University Islamabad**,** for their help, facilitation, encouragement, and motivation.

I am also highly obliged to Dr. Mukhtar, Dr. Yaseen Muhammad and Dr. Imran Ahmed for their useful suggestion and assistance in my research work.

I am also thankful to Zubair Ahmed, Zia ul Islam, Danish Farooq, Fayaz, Farhan, Wasif Ullah, Asad, Azaz Raza and Abdul Bari Qanit for their help during my Research work.

I am thankful to our friends and classmates for their help and discussions during this research. Last, but not the least, I am deeply grateful to our parents, brothers and sisters for their unconditional love, care and support who always encouraged me to conclude this research. May Allah bless them all who helped me in my research studies (Ameen).

TABLE OF CONTENTS

ABSTRACT i
ACKNOWLEDGMENTS ii
TABLE OF CONTENTS iii
LIST OF FIGURES vii
LIST OF TABLES xi
CHAPTER 01 1
INTRODUCTION 1
1.1 Location and Accessibility 1
1.2 Previous Work 3
1.3 Present work 3
1.4 Aim and Objectives 3
1.5 Methodology 4
1.5.1 Field Work 4
1.5.2 Laboratory Work 4
1.6 Significance of the Study 4
CHAPTER 02 5
GEOLOGY AND TECTONIC FRAMEWORK 5
2.1 History of the Indian Plate 5
2.2 Geology and tectonics of northern part of Pakistan 6
2.3 Main Karakoram Thrust (MKT) 7
2.4 Kohistan Island Arc (KIA) 7
2.5 Main Mantle Thrust (MMT) 8
2.6 Northern Deformed Fold and Thrust Belt (NDFTB) 8
2.7 Main Boundary Thrust (MBT) 8
2.8 Southern Deformed Fold and Thrust Belt (SDFTB) 8
2.9 Potwar Plateau 9
2.10 Kohat Plateau 9
2.11 Salt Range Thrust (SRT) and Trans Indus Range Thrust (TIRT) 9
2.12 Punjab Foreland 10
2.13 Tectonic setup of the study Area 12
CHAPTER 03 14
GENERALIZED STRATIGRAPHY AND STRUCTURAL FARMWORK 14
3.1 Stratigraphy of Nammal Gorge Section 14
3.1.1 Wargal Limestone 14

3.1.2 Chiddru Formation 14
3.1.3 Mianwali Formation 15
3.1.4 Tredian Formation 15
3.1.5 Kingriali Formation 15
3.1.6 Datta Formation 16
3.1.7 Shinawari Formation 16
3.1.8 Chichali Formation 17
3.1.9 Hangu Formation 17
3.1.10 Lockhart Limestone 17
3.1.11 Patala Formation 17
3.1.12 Nammal Formation 18
3.1.13 Sakessar Limestone 18
3.2 Stratigraphy of Zaluch Nala Section 19
3.2.1 Tobra Formation 19
3.2.2 Warchha Sandstone 19
3.2.3 Sardhai Formation 19
3.2.4 Amb Formation 20
3.2.5 Samana Suk Formation 20
3.2.6 Chichali Formation 20
3.2.7 Lumshiwal Formation 20
3.3 Surghar Range Section 21
3.3.1 Chinji Formation 21
3.3.2 Nagri Formation 21
3.3.3 Dhok Pathan Formation 22
3.4 Structural Framework 24
3.4.1 Folded and faulted/thrusted Structure 24
CHAPTER 04 26
FRACTURE ANALYSIS 26
4.1 Fracture 26
4.2 Causes of fracture 26
4.3 Folding and Fracture 26
4.4 Release Fracture 26
4.5 Extension Fracture 27
4.6 Conjugate Fracture 27

4.7 Stress Analysis 28
4.8 Morphology of Fracture 30
4.8.1 Open Fracture; 30
4.8.2 Mineral Filled Fracture; 30
4.8.3 Vuggy Fracture; 30
4.8.4 Deformed Fracture; 30
4.9 Reservoir Characteristic 30
4.9.1 Fracture Density 31
4.9.2 Fracture Porosity 32
4.9.3 Fracture Permeability 32
CHAPTER 05 33
DATA ANALYSIS AND REPRESENTATION 33
5.1 Introduction 33
5.2 Mapping of Fracture 33
5.3 Circular Inventory Method 33
5.4 Rose Diagram 33
5.5 Stereonet 34
NAMMAL GORGE SECTION 34
5.6 Station NO; 01 34
5.7 Station NO; 02 36
5.8 Station NO; 03 38
5.9 Station NO; 04 40
5.10 Station NO; 05 42
5.11 Station NO; 06 44
5.12 Station NO; 07 46
5.13 Station NO; 08 48
5.14 Station NO; 09 50
5.15 Station NO; 10 52
ZALUCH NALA SECTION 55
5.16 Station NO; 01 55
5.17 Station NO; 02 57
5.18 Station NO; 03 59
5.19 Station NO; 04 61
5.20 Station NO; 05 63
5.21 Station NO; 06 64

5.22 Station NO; 07 66
5.23 Station NO; 08 68
5.24 Station NO; 09 70
5.25 Station NO; 10 72
SURGHAR RANGE SECTION 75
5.26 Station NO; 01 75
5.27 Station NO; 02 77
5.28 Station NO; 03 79
5.29 Station NO; 04 81
5.30 Station NO; 05 83
5.31 Station NO; 06 85
5.32 Station NO; 07 87
5.33 Station NO; 08 89
5.34 Station NO; 09 91
5.35 Station NO; 10 93
CHAPTER 06 95
DISCUSION AND CONCLUSIONS 95
6.1 Fracture recorded in Salt Range 95
6.2 Stress analysis 98
6.3 Relationship between Fracture Density (CM^{-1}) and Fracture Porosity (%) 102
6.4 Relationship Between Fracture density (CM^{-1}) and Fracture Permeability (MD) 102
6.5 Relationship between Fracture Porosity and Fracture Permeability 103
6.6 Reservoir potential of each Section 104
6.6.1 Nammal Gorge Section 105
6.6.2 Zaluch Nala Section 107
6.6.3 Surghar Range Section 109
CONCLUSION 111
REFERENCES 112

LIST OF FIGURES

Figure 1. 1 Showing Google Earth Image, Accessibility To The Study Area. The Red Rectangle Represents Location Of The Study Area. 2
Figure 2. 1 Shown tectonic cross section of different features of northern Pakistan after (Lavé and Avouac, 2000). 7
Figure 2. 2 Showes Generalized tectonic map of north Pakistan (After Kazmi and Rana, 1982). 11
Figure 2. 3 The Geological and geographical location of study area, The Red boxes Represent the study area i.e., Nammal Gorge, Zaluch Nala and Surghare Range Section (After Yeats & Hussain, 1987) 13
Figure 3. 1 Generalize stratigraphic column of study area (after Wadood et al.,2021) 23
Figure 3. 2 Field photographs showing A) Intra formational fault in Kingriali formation, Surghar range, B) Surghar fault, Chichali Nala, C) Recumbent fold in Samana suk formation, Zaluch nala, D) Anticline, syncline and small size fault in Mianwali formation, Surghar Range, E) Chevron Fold in Mianwali Formation, Surghar Range, F) S and Z type folds in Shinawari formation, Surghar Range. 25
Figure 4. 1 Showing the flow of water (fluids) along bedding planes and fracture surfaces (Afte 27
Figure 4. 2 Showing Longitudinal (Release), Cross (Extension) and Conjugate Shear (Oblique) fractures with respect to bed and stress direction (After Baitu et al., 2008). 28
Figure 4. 3 Shows the stress orientation in 3D block diagram (After Hunt et al., 2009). 29
Figure 4. 4 Shows the stress orientation in Rose Diagram (After Dasti et al., 2018). Red color . 29
Figure 5. 1 (A) field photograph, (B) Rose diagram of fracture, (C) Plane data of fracture on Stereonet, (D) Poles data of fracture on Stereonet. Number of Release Fractures (Red color) are 02, Conjugate Fractures (Blue color) are 02 whereas Extension Fractures (Black color) are 07. 36
Figure 5. 2 (A) field photograph, (B) Rose diagram of fracture, (C) Plane data of fracture on Stereonet, (D) Poles data of fracture on Stereonet. Number of Release Fractures (Red color) are 03, Conjugate Fractures (Blue color) are 01 whereas Extension Fractures (Black color) are 09. 38
Figure 5. 3 (A) field photograph, (B) Rose diagram of fracture, (C) Plane data of fracture on Stereonet, (D) Poles data of fracture on Stereonet. Number of Release Fractures (Red color) are 06, Conjugate Fractures (Blue color) are 07 whereas Extension Fractures (Black color) are 04. 40
Figure 5. 4 (A) field photograph, (B) Rose diagram of fracture, (C) Plane data of fracture on Stereonet, (D) Poles data of fracture on Stereonet. Number of Release Fractures (Red color) are 08, Conjugate Fractures (Blue color) are 11 whereas Extension Fractures (Black color) are 02. 42
Figure 5. 5 (A) field photograph, (B) Rose diagram of fracture, (C) Plane data of fracture on Stereonet, (D) Poles data of fracture on Stereonet. Number of Conjugate Fractures (Blue color) are 07 and Extension Fractures (Black color) are 04. 44

Figure 5. 6 (A) field photograph, (B) Rose diagram of fracture, (C) Plane data of fracture on Stereonet, (D) Poles data of fracture on Stereonet. Number of Release Conjugate Fractures (Blue color) are 09 and Extension Fractures (Black color) are 03. 46
Figure 5. 7 (A) field photograph, (B) Rose diagram of fracture, (C) Plane data of fracture on Stereonet, (D) Poles data of fracture on Stereonet. Number of Conjugate Fractures (Blue color) are 07 and Extension Fractures (Black color) are 08. 48
Figure 5. 8 (A) field photograph, (B) Rose diagram of fracture, (C) Plane data of fracture on Stereonet, (D) Poles data of fracture on Stereonet. Number of Release Fractures (Red color) are 04, Conjugate Fractures (Blue color) are 06 whereas Extension Fractures (Black color) are 05. 50
Figure 5. 9 (A) field photograph, (B) Rose diagram of fracture, (C) Plane data of fracture on Stereonet, (D) Poles data of fracture on Stereonet. Number of Release Fractures (Red color) are 02, Conjugate Fractures (Blue color) are 07 whereas Extension Fractures (Black color) are 08. 52
Figure 5. 10 (A) field photograph, (B) Rose diagram of fracture, (C) Plane data of fracture on Stereonet, (D) Poles data of fracture on Stereonet. Number of Release Fractures (Red color) are 03, Conjugate Fractures (Blue color) are 07 whereas Extension Fractures (Black color) are 05. 54
Figure 5. 11 (A) field photograph, (B) Rose diagram of fracture, (C) Plane data of fracture on Stereonet, (D) Poles data of fracture on Stereonet. Number of Conjugate Fractures (Blue color) are 06 and Extension Fractures (Black color) are 14. 56
Figure 5. 12 (A) field photograph, (B) Rose diagram of fracture, (C) Plane data of fracture on Stereonet, (D) Poles data of fracture on Stereonet. Number of Release Fractures (Red color) are 03, Conjugate Fractures (Blue color) are 07 whereas Extension Fractures (Black color) are 09. 58
Figure 5. 13 (A) field photograph, (B) Rose diagram of fracture, (C) Plane data of fracture on Stereonet, (D) Poles data of fracture on Stereonet. Number of Conjugate Fractures (Blue color) are 11 and Extension Fractures (Black color) are 05. 60
Figure 5. 14 (A) field photograph, (B) Rose diagram of fracture, (C) Plane data of fracture on Stereonet, (D) Poles data of fracture on Stereonet. Number of Release Fractures (Red color) are 03, Conjugate Fractures (Blue color) are 11 whereas Extension Fractures (Black color) are 08. 62
Figure 5. 15 (A) field photograph, (B) Rose diagram of fracture, (C) Plane data of fracture on Stereonet, (D) Poles data of fracture on Stereonet. Number of Release Fractures (Red color) are 05, Conjugate Fractures (Blue color) are 06 whereas Extension Fractures (Black color) are 06. 64
Figure 5. 16 (A) field photograph, (B) Rose diagram of fracture, (C) Plane data of fracture on Stereonet, (D) Poles data of fracture on Stereonet. Number of Release Fractures (Red color) are 05, Conjugate Fractures (Blue color) are 04 whereas Extension Fractures (Black color) are 15. 66
Figure 5. 17 (A) field photograph, (B) Rose diagram of fracture, (C) Plane data of fracture on Stereonet, (D) Poles data of fracture on Stereonet. Number of Release Fractures (Red color)

are 02, Conjugate Fractures (Blue color) are 04 whereas Extension Fractures (Black color) are 17. 68
Figure 5. 18 (A) field photograph, (B) Rose diagram of fracture, (C) Plane data of fracture on Stereonet, (D) Poles data of fracture on Stereonet. Number of Release Fractures (Red color) are 01, Conjugate Fractures (Blue color) are 02 whereas Extension Fractures (Black color) are 17. 70
Figure 5. 19 (A) field photograph, (B) Rose diagram of fracture, (C) Plane data of fracture on Stereonet, (D) Poles data of fracture on Stereonet. Number of Release Fractures (Red color) are 04, Conjugate Fractures (Blue color) are 10 whereas Extension Fractures (Black color) are 08. 72
Figure 5. 20 (A) field photograph, (B) Rose diagram of fracture, (C) Plane data of fracture on Stereonet, (D) Poles data of fracture on Stereonet. Number of Release Fractures (Red color) are 03, Conjugate Fractures (Blue color) are 15 whereas Extension Fractures (Black color) are 06. 74
Figure 5. 21 (A) field photograph, (B) Rose diagram of fracture, (C) Plane data of fracture on Stereonet, (D) Poles data of fracture on Stereonet. Number of Release Fractures (Red color) are 03, Conjugate Fractures (Blue color) are 06 whereas Extension Fractures (Black color) are 09. 76
Figure 5. 22 (A) field photograph, (B) Rose diagram of fracture, (C) Plane data of fracture on Stereonet, (D) Poles data of fracture on Stereonet. Number of Release Fractures (Red color) are 02, Conjugate Fractures (Blue color) are 08 whereas Extension Fractures (Black color) are 06. 78
Figure 5. 23 (A) field photograph, (B) Rose diagram of fracture, (C) Plane data of fracture on Stereonet, (D) Poles data of fracture on Stereonet. Number of Release Fractures (Red color) are 02, Conjugate Fractures (Blue color) are 07 whereas Extension Fractures (Black color) are 09. 80
Figure 5. 24 (A) field photograph, (B) Rose diagram of fracture, (C) Plane data of fracture on Stereonet, (D) Poles data of fracture on Stereonet. Number of Release Fractures (Red color) are 02, Conjugate Fractures (Blue color) are 8 whereas Extension Fractures (Black color) are10. 82
Figure 5. 25 (A) field photograph, (B) Rose diagram of fracture, (C) Plane data of fracture on Stereonet, (D) Poles data of fracture on Stereonet. Number of Release Fractures (Red color) are 08, Conjugate Fractures (Blue color) are 02 whereas Extension Fractures (Black color) are 14. 84
Figure 5. 26 (A) field photograph, (B) Rose diagram of fracture, (C) Plane data of fracture on Stereonet, (D) Poles data of fracture on Stereonet. Number of Release Fractures (Red color) are 03, Conjugate Fractures (Blue color) are 08 whereas Extension Fractures (Black color) are 07. 86
Figure 5. 27 (A) field photograph, (B) Rose diagram of fracture, (C) Plane data of fracture on Stereonet, (D) Poles data of fracture on Stereonet. Number of Release Fractures (Red color) are 05, Conjugate Fractures (Blue color) are 08 whereas Extension Fractures (Black color) are 05. 88

Figure 5. 28 (A) field photograph, (B) Rose diagram of fracture, (C) Plane data of fracture on Stereonet, (D) Poles data of fracture on Stereonet. Number of Release Fractures (Red color) are 01, Conjugate Fractures (Blue color) are 07 whereas Extension Fractures (Black color) are 10. 90
Figure 5. 29 (A) field photograph, (B) Rose diagram of fracture, (C) Plane data of fracture on Stereonet, (D) Poles data of fracture on Stereonet. Number of Release Fractures (Red color) are 03, Conjugate Fractures (Blue color) are 06 whereas Extension Fractures (Black color) are 09. 92
Figure 5. 30 (A) field photograph, (B) Rose diagram of fracture, (C) Plane data of fracture on Stereonet, (D) Poles data of fracture on Stereonet. Number of Release Fractures (Red color) are 05, Conjugate Fractures (Blue color) are 08 whereas Extension Fractures (Black color) are 08. 94

Figure 6. 1 The calculated maximum stress direction at each station shown on google Earth image. 99
Figure 6. 2 Showing each Station location and their Rose Diagram on Google Earth image. ... 100
Figure 6. 3 Showing each station location and their rose diagram on geological map (from Geological Survey of Pakistan; Ali, 2014). 101
Figure 6. 4 Showing the relationship between Open Fracture Density (CM^{-1}) and Fracture Porosity (%) 102
Figure 6. 5 Showing relationship between Open Fracture Density (CM^{-1}) and Fracture Permeability (MD) 103
Figure 6. 6 Showing relationship between Fracture Porosity (%) and Fracture Permeability (MD) 104
Figure 6. 7 Showing the relationship between Open Fracture Density (CM^{-1}) and Fracture Porosity (%) 106
Figure 6. 8 Showing relationship between Fracture Porosity (%) and Fracture Permeability (MD) 106
Figure 6. 9 Showing the relationship between Open Fracture Density (CM^{-1}) and Fracture Porosity (%) 108
Figure 6. 10 Showing relationship between Fracture Porosity (%) and Fracture Permeability (MD) 108
Figure 6. 11 Showing the relationship between Open Fracture Density (CM^{-1}) and Fracture Porosity (%) 110
Figure 6. 12 Showing relationship between Fracture Porosity (%) and Fracture Permeability (MD). 110

LIST OF TABLES

Table 2. 1 Showes the Tectono- Stratigraphic Regime and Fault System. 6

Table 4. 1 Classification of Natural Fractured Reservoir system (NFR) (compiled from Nelson,31

Table 5. 1. Show fracture data of station 1. 34
Table 5. 2. Show fracture data of station 2. 37
Table 5. 3. Show fracture data of station 3. 39
Table 5. 4. Show fracture data of station 4. 41
Table 5. 5. Show fracture data of station 5. 43
Table 5. 6. Show fracture data of station 6. 45
Table 5. 7. Show fracture data of station 7. 47
Table 5. 8. Show fracture data of station 8. 49
Table 5. 9. Show fracture data of station 9. 51
Table 5. 10. Show fracture data of station 10. 53
Table 5. 11. Show fracture data of station 11. 55
Table 5. 12. Show fracture data of station 12. 57
Table 5. 13. Show fracture data of station 13. 59
Table 5. 14. Show fracture data of station 14. 61
Table 5. 15. Show fracture data of station 15. 63
Table 5. 16. Show fracture data of station 16. 65
Table 5. 17. Show fracture data of station 17. 67
Table 5. 18. Show fracture data of station 18. 69
Table 5. 19. Show fracture data of station 19. 71
Table 5. 20. Show fracture data of station 20. 73
Table 5. 21. Show fracture data of station 21. 75
Table 5. 22. Show fracture data of station 22. 77
Table 5. 23. Show fracture data of station 23. 79
Table 5. 24. Show fracture data of station 24. 81
Table 5. 25. Show fracture data of station 25. 83
Table 5. 26. Show fracture data of station 26. 85
Table 5. 27. Show fracture data of station 27. 87
Table 5. 28. Show fracture data of station 28. 89
Table 5. 29. Show fracture data of station 29. 91
Table 5. 30. Show fracture data of station 30. 93

Table 6. 1 Detail of all fracture recorded at each Section and Sampling station. S.NO = Station number, T.F = Total Fracture, O.F = Open Fracture, F/C.F = Filled or Closed Fracture, R.F = Release Fracture, C.F = Conjugate Fracture, E.F = Extension Fracture, F.D = Fracture Density, F.P (%) = Fracture Porosity Percentage, F. Pe (MD) = Fracture Permeability Millidarcy … 97

Table 6. 2 Qualitative classification of each section according to Nelson, (2001) NFR category based on quantitative data..... 104

Table 6. 3 Qualitative classification of Nmmal Gorge Section according to Nelson, (2001) NFR 105
Table 6. 4 Qualitative classification of Zaluch Nala Section according to Nelson (2001) NFR 107
Table 6. 5 Qualitative classification of Surghar Range Section according to Nelson (2001) NFR classification on the basis of quantitative data. 109

CHAPTER 01
INTRODUCTION

Fractures are geologically discontinuous structures or discrete cracks that form in a rock as a result of stress (Sorkhabi, 2014). Fractures include faults, having shear displacement; joints, having an aperture but lack visual shear displacement, and filled structures such as veins. Fracture can occur on a scale ranging from microns to hundreds of kilometers and have significant effect on crustal process. In recent years tectonic fracture in sedimentary rocks has attained much more attention because they often possess pre-, syn-, or post tectonic history of terrains (Sayab and Jadoon, 2005). The extensive number of fractures present in folded sedimentary rocks has encouraged researchers to make recommendation about the physical relationships between fracture formation and stress distributions related to the folding process (Cosgrove., (1999); Mynatt et al., (2009)). The outcomes of a few recent research studies e.g., Hennings et al. (2000), Jadoon et al. (2003), Bellahsen et al. (2006), Gross and Eyal (2007), Olson, (2007), Baitu et al. (2008), and Mynatt et al., (2009) determine complex correlations between tectonic stress and spatial and temporal changes in local faulting or folding induced stresses and shows that older fractures may control the formation of new fractures. Fractures are commonly associated with folding and have an obvious relationship with folds (Watkins et al., 2018). As a result, it is critical to find out the correlation between fracturing and folding which is usually conducted using stress analysis.

1.1 Location and Accessibility

Salt Range, series of hills and low mountains between the valleys of the Indus and Jhelum rivers, located in the northern part of the Punjab province of Pakistan. It is accessible via M-2 motorway about 160 km from Islamabad. The research work is carried in different sections of Salt Rang l.e. Nammal Gorge, Zaluch Nala, and Surghar Range (Figure 1.1). The name Salt Range derives from widespread deposits of rock salt that form one of the richest salt fields in the world, they are Precambrian in age and can be up to 1,600 feet thick. The range's length from east to west is around 186 miles, while its width in the middle and eastern portions is between 5 to 19 miles. Its average height is 2,200 feet, and its highest elevation, at Sakesar mountain, is 4,992 feet. In addition to the salt deposits, mined from ancient times, the Salt Range contains coal, gypsum, and other minerals.

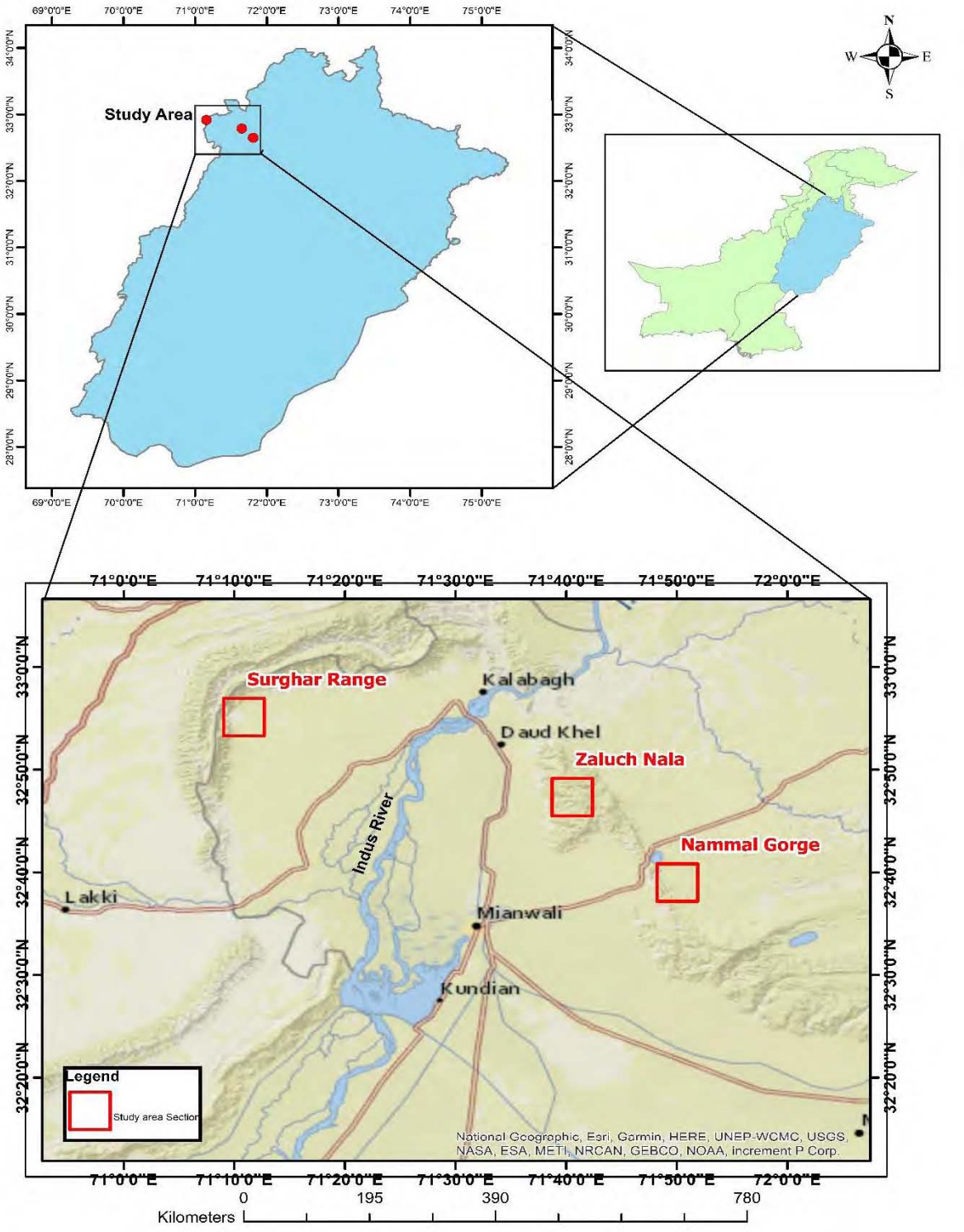

Figure 1. 1 Showing google Earth image, accessibility to the study area. The red rectangle depictures location of the study area.

1.2 Previous Work

The Kingriali Formation is the youngest member of the Triassic-age rocks, which is prominently exposed in several geological sections of the Salt Range and Trans-Indus Ranges (Shah et al., 2010; Qasim et al., 2021). The Kingriali Formation is broadly exposed along the northern and southern margins of the Kohat and Potwar sub-basins, and in lesser Himalayas. The name Kingriali Formation was approved by Stratigraphic Committee of Pakistan before that the Late-Triassic kingriali Formation was known as "Kingriali Dolomite" due to the strength of dolostones and its resistance to weathering and erosion. Detailed stratigraphic investigations of this formation have been performed by various authors, i.e., Gaetani and Garzanti (1991), Valdiya (2016) and Iqbal et al. (2021). 12 microfacies developed within the 130 m thick Kingriali Formation of the Landa Nala Section by Parvez (1992). Malkani and Mahmood (2017) divided the Kingriali Formation into two members, (1) lower member was regarded as the Doya Member and (2) upper unit as the Vanjari Member in the Surghar Range. Alam et al, (2015) carried out the stratigraphic study of the Kingriali Formation at the Paniala area of the Khisor Ranges. Abdulghani et al, (2020) studied the Kingriali Formation revealed in the Kohat sub-basin's sedimentary fabric and diagenetically. The Kingriali Formation was deposited in the supratidal, and peritidal depositional environment, which was influenced by marine water and meteoric water (Abdulghani et al.,2020). The abundant presence of well-preserved palynomorph assemblages, pollens, and many other marine biotas in the upper unit of the Kingriali Formation indicates Rhaetian deposition (Khan et al., 2021).

1.3 Present work

In the current study Fracture analysis of the Kingriali Formation is caried out for the first time to determine the stress analysis responsible for the deformation of the exposed rock and calculating reservoir potential using the Naturally Fracture Reservoir System (NFRS) of classification.

1.4 Aim and Objectives

Main aim of this research is to assess fracture analysis of the Triassic Kingriali Formation in the Salt Range (Nammal Gorge and Zaluch Nala) and Transe Indus Range (Surghar Range) area. The prominent objectives of this research are given below.

1. To identify the different structures (fault, folds, joints, and fracture) of the research area.
2. To calculate the fracture density and attributes data in relation to the stress.

3. To determine the nature (open, filled and closed) and distribution (Release, Conjugate, and Extension) of fractures in the exposed rocks of Kingriali Formation.

4. To calculate the structural deformation (using fracture in rose diagram) in the Kingriali Formation and knowing the tectonic evolution of the research area.

5. To Calculate reservoir potential of Kingriali Formation in study area through Naturally Fracture Reservoir (NFR) system.

1.5 Methodology

The methodology consists of fieldwork and laboratory analysis. The detailed methodology is given in the following sections.

1.5.1 Field Work

Proposed detailed fieldwork was carried out in the study area for data collection including dip strike data of structural features (bedding and fractures,), identification of different sets of fractures folds, and faults. All the geological field features were recorded and photographed for later evaluation, discussion, and reference. All the stations were marked with GPS while field data for fracture analysis was collected using the "circle inventory method".

1.5.2 Laboratory Work

In the lab detail structural analysis was conducted through innovative structural software (e.g., Stereostat/Stereonet or GeoOrient) using fieldwork data. Rose diagrams, great circle plots, pole figures and models of the study area were made for different structural features which were then used for interpretation and writing of final dissertation. Final maps and figures were produced in Corel DRAW and Arc GIS software.

1.6 Significance of the Study

This study provides a better understanding of the structural architecture of the research area i.e., Western Salt Range and Transe Indus Ranges (Surghar Range). It also helps us in determining the relationship of fractures and the orientation of local stresses and the effect of the regional tectonic stress upon them. The reservoir potential of Kingriali Formation was determined by NFR classification. The data obtained will be published in a suitable research journal.

CHAPTER 02
GEOLOGY AND TECTONIC FRAMEWORK

2.1 History of the Indian Plate

All the continents were present from the Early-Triassic to Middle-Jurassic as a supercontinent known as Pangea (Kent et al., 2003). At that time there was a single ocean called Panthalassa that encircled Pangea (Kutschera., 2009). It began to separate after 200 million years and split into the northern Laurasia and southern Gondwana supercontinents between 160-138 million years ago (Scotese., 2001). In later, the Gondwana sub divided into Africa, South America, , India, Antarctica, Australia, Arabia, Madagascar, and New Zealand, while the Laurasia further divided into North America, Europe, and Asia (Golonka, 2012). Following the division of Gondwana, the Indian Plate and Jointed Madagascar, which were both the northern parts of Gondwana, began to move towards the north (around 130 M.Y), where they collided with the Eurasian Plate (40-50 M.Y), which was the southern half of Laurasia (Scotese, 2001; Hinsbergen et al., 2012). The Neo-Tethyan Ocean began to squish towards the north because of the oceanic lithosphere subducting beneath the Eurasian Plate (Chemenda et al., 2000). The Indian Plate was drifting northward when it separated from the Madagascar Plate around 88 M.Y ago as a result of right-lateral strike slip motion (Chatterjee, 2017). The Indian Plate migrated at a rate of up to 8 centimeters per year during 66-90 M.Y, their migration pace climbed to 15-20 cm/year about 65–50 years ago, which is the highest rate recorded in Earth's tectonic history (Hinsbergen et al., 2012; Aitchison et al., 2007). The India Plate travelled the farthest distance (9000 km in 160 M.Y), which is the most of all continental drifts (Chatterjee., 2017). The Shyok-Tsangpo Suture Zone (STSZ) and Indus Tsangpo Suture Zone (ITSZ) are the two north-dipping subduction zones that formed between the Indian Plate and the Eurasian Plate. The STSZ took place south of the Eurasian Plate and north of Neo-Tethys, The Neo-Tethys Ocean is separated into a northern and a southern Neo-Tethys by the southern subduction zone, or ITSZ. (Jain., 2014; Chatterjee., 2017). In the Late Cretaceous (75-100 M.Y), the Kohistan Island Arc (KIA) collided with the Eurasian Plate (Khan et al., 2009). The collision of the Indian Plate and the KIA occurred during the Paleocene-Eocene boundary (about 55 Ma) (Bouilhol., 2013). The sharp decline in the Indian Plate's northward motion towards the Eurasian Plate, which fell from 20 cm/year to 4 cm/year between 50 and 40 years ago, confirms this collision. Because of this collision, the Neo-Tethyan ocean totally dried up and vanished in the Early Eocene (~50 Ma) (Chatterjee., 2017).

2.2 Geology and tectonics of northern part of Pakistan

A collisional border between the Indian Plate and the Eurasian Plate can be found in Pakistan's northernmost region, which has the youngest mountain chains (the Himalaya) This collision happened between 65 and 34 years ago. (Hinsbergen et al., 2012; Aitchison et al., 2007). After the impact, the Indian Plate began to penetrate the Eurasian Plate at a rate of around 5 cm per year; this rate has since slowed to 2 cm per year. These collisions and penetrations resulted in the formation of the Himalayas, which are also to blame for the crustal shortening in the Himalayas. This crustal shortening in turn causes the Indian Plate's faulting and folding system (Neumayer., 2003; Hinsbergen et al., 2012). Five tectono-stratigraphic regimes, separated by a significant fault system, make up the northern part of Pakistan (Ahmad et al, 2004). From north to south their sequence is below (Table 2.1)

S.NO	**Tectono-Stratigraphic regimes and Faults System**	
1	Karakorum Block (Eurasian Plate)	N
2	**……..Main Karakoram Thrust (MKT)……**	
3	Kohistan Island Arc (KIA)	
4	**……..Main Mantle Thrust (MMT)……..**	
5	Northern Deformed Fold and Thrust Belt (NDFTB)	
6	**…….Main Boundary Thrust (MBT)……**	
7	Southern Deformed Fold and Thrust Belt (SDFTB)	
8	**……Salt Range Thrust (SRT) and Trans Indus Range Thrust (TIRT)……**	
9	Punjab Foreland	S

Table 2. 1 The tectono- stratigraphic regime and fault System.

From NDFTB to Punjab Foreland it belongs to Indian Plate. The evolution and context of the Indian Plate are both complicated. Periodic patterns of various tectonic formations appear over the Indian Plate as a result of the plate's complex collisional history. Because of the disparity in relative velocities of the east and west portions of the Indian Plate during the collisional era, the Indian Plate rotated anticlockwise to the Eurasian Plate (Bannert et al., 2012). As a result of this distinction, the Chaman Fault, a left-lateral strike-slip fault that may be up to 1200 km long, separates the western portion of the Indian Plate from the Eurasian Plate (Crupa et al., 2017).

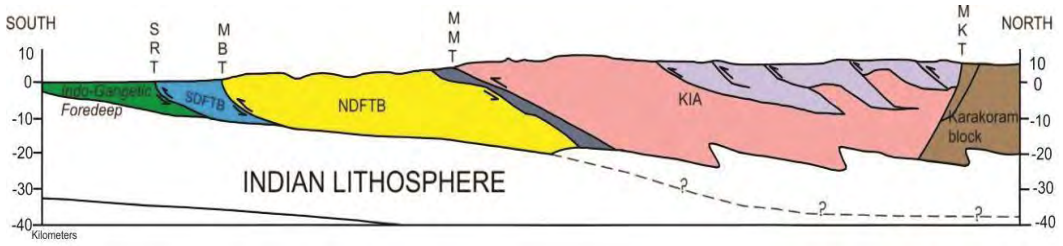

Figure 2. 1 Shown tectonic cross section of different features of northern Pakistan after (Lavé and Avouac, 2000).

Karakoram Block (Eurasian Plate)

The Karakoram Block, which is situated between the Pamirs in the north and KIA in the south, is the southern edge of the Eurasian Plate. With respect to the east, it can be compared to south Tibet's Lhasa Block (Searle and Phillips, 2007). Three broad units have been identified within the Karakoram Block: 1) The Ordovician to Early Cretaceous sedimentary rocks that make up the northern sedimentary belt. 2) The Karakoram Batholith is made up of tonalities, granodiorites, gabbro, diorites, and pre collisional hornblende. 3) The Karakoram Batholith and the Shyoke Suture Zone are separated by the high-grade Southern Karakoram Metamorphic Complex (Borneman et al., 2015). The Karakoram Block comprised of combination of volcanic, meta-sedimentary, sedimentary, and metamorphic rocks.

2.3 Main Karakoram Thrust (MKT)

The Main Karakoram Thrust (MKT) was formed in the Late Cretaceous, which marks the boundary of the collision between the KIA and the Eurasian Plate, is the southern limit of the Karakoram Block (Kayal, 2008; Boreman et al, 2015). KIA is being thrust over by the Eurasian Plate in the MKT zone (Boreman et al, 2015). The mélange sequences in this thrusting system are found throughout Pakistan in various areas. Ophiolites, blueschists, greenschists, metavolcanics, and metasedimentary rocks make up this mélange sequence (Kazmi and Jan, 1997).

2.4 Kohistan Island Arc (KIA)

The KIA have a complicated tectonic history Due to its sandwiched location between two colliding continental plates (Figure 2.1). The KIA was formed in Mesozoic time due to the intra oceanic subduction in Tethyan Ocean (Salam et al., 2019). The KIA is generally trending east-west and divided into Kohistan and Ladakh Island Arcs. From south to north, the KIA is made up of these six units: (1) Jijal Complex, (2) Kamila Amphibolites, (3) Chilas Complex, (4) Kohistan Batholith, (5) Chalt Volcanics, and (6) Yasin Group metasediments. MMT in the south and MKT

in the north define its tectonic boundaries, respectively. Mélange sequences can be seen along each of these thrust faults. The Indus Tsangpo Suture Zone, which is the point at where the Tibetan and Indian plates directly converge, is where the MKT and MMT join (Ahmad, 2003).

2.5 Main Mantle Thrust (MMT)

This collisional boundary between the Indian Plate and KIA was created during the Late Paleocene-Eocene (Salam et al., 2019). The area along which KIA is thrusting over the Indian Plate is the northern limit of the NDFTB (Northern Deform Fold and Thrust Belt). At several locations throughout Pakistan, there are MMT mélange sequences. Ophiolites, greenschists, blueschists, metavolcanic, metagabbro, and metasedimentary rocks make up these mélange sequences (Ahmad and Jehan, 2006) (Kazmi and Jan, 1997). The Proterozoic gneisses and schists of the Nanga Parbat Haramosh mountain, which is up to 15 km thick and formed by the MMT, serve as the re-entrant (Argles, 2000). Generally, MMT dips 25-45° towards north and typically dips 25–45° northward (Malinconico, 1986).

2.6 Northern Deformed Fold and Thrust Belt (NDFTB)

About the 300 km wide Northern Deformed Fold and Trust Belt lies south of MMT. NDFTB is a festoon shape belt containing an intensively deformed sedimentary, meta-sedimentary and igneous rocks. It extends from the Kurram region in the west to the Kashmir Basin in the east, close to the Afghan border. The Main Boundary Thrust forms the southern border of NDFTB.

2.7 Main Boundary Thrust (MBT)

Main Boundary Thrust separate NDFTB from SDFTB (Chaudhry and Ghazanfar, 1993). It demonstrates the further northward movement of the Indian Plate and the southward movement of Himalayan deformation (Thakur et al., 2004). MBT brought the earlier rocks, Mesozoic on top of Miocene rocks (Murree Formation). In the northern edge of the Kalachitta and Hazara ranges, Hazara and Murree Faults are thought to be connected by MBT (Seeber et al., 1979). The MBT zone is made up of several parallel or en-echelon thrust faults that split the northwest Himalayan sequence into two parts, the first part is a deformed sedimentary southern zone called the foreland zone, and the second part is deformed and metamorphosed northern zone called the hinterland zone (Pivnik and Sercombe, 1993).

2.8 Southern Deformed Fold and Thrust Belt (SDFTB)

The Himalayan Mountain range, which stretches from the Ganges Delta (India) to South Waziristan in Pakistan, is rimmed by the SDFTB, an east-west oriented zone of crustal shortening.

It has a significant deposit of fluvial sediments. When synorogenic sediment influx first began in the early-Miocene age, SDFTB behaved as the primary depocenter. It is further divided into 2 tectonic provinces which are separated by the Indus River i.e., Potwar Plateau to the east of the Indus River and the Kohat Plateau to the west of the Indus River. In the north it's bounded by MBT (Hussain and Zhang, 2018). The left-lateral strike-slip Kurram Fault, which separates the Kohat Plateau from North Waziristan, Samana, Darsamand, and Thal on its western side, juxtaposes the extensively deformed Mesozoic rocks with the Eocene-Miocene sediments (Ali, 2010).

2.9 Potwar Plateau

The Potwar Plateau is the eastern side of the SDFTB, with a north-south width of around 150 km, and an internally less deformed fold and thrust belt (Mahmood and Hafeez, 2009). The Hazara and Kalachitta ranges and the SRT form its northern and southern boundaries, respectively. It is separated between the Southern Potwar Deformed Zone, which has less deformation but has a large syncline known as the Soan Syncline, and the NPDZ, which is intensely deformed (Faisal and Dixon, 2015).

2.10 Kohat Plateau

The Indian Plate's tectonic movement northward during the Late Miocene has an impact on the Kohat Plateau. The SDFTB's western region contains this region of deformation. The MBT forms its northern boundary, the Kurram Fault forms its western boundary, and the Surghar Range and Bannu Basin are situated on its southern boundary (Figure 2.1). The Kohat Plateau has several folds, some of which are up to several kilometers long and are in faulted contact with younger strata (Hussain and Zhang, 2018). The northeast-southwest trending folds are physically responsible for controlling the NKFTB (Northern Kohat Fold and Thrust Belt). Most of these folds are tight anticlines with wide synclinal valleys. The NKFTB is also home to vast and substantial anticlines such the Ziarat Anticline, Bazid Khel Anticline, and Panoba Anticline (Ahmad, 2003).

2.11 Salt Range Thrust (SRT) and Trans Indus Range Thrust (TIRT)

The Salt Range Thrust (SRT) and Trans Indus Range Thrust (TIRT) are the youngest of all major Himalayan faults such as MKT, MMT and MBT. The SRT is situated to the east of the Indus River and TIRT is situated to the west of Indus River. These faults sub-horizontal along which various rock types, such as those from different ages, are exposed in various locations. Salt Range contains exposed Precambrian rocks (Salt Range Formation), Khisor Range contains exposed

Cambrian rocks, and Surghar Ranges include exposed Permian rocks (Alam et al., 2005). The SRT and TIRT both are thrusting over Punjab Foreland (Hemphill, 1973).

2.12 Punjab Foreland

A Foreland Fold-Thrust Belt with molasses sediments formed from the mountain front rising is situated at the foothills of the Himalayas. During the Indian plate's ongoing northward movement following the continent-continent collision, molasse sediments from the mountain front rising were distorted, resulting in the Foreland Fold-Thrust Belt that can be found near the foothills of the Himalayas (Green et al., 2008). This structural province is bordered to the north by the Salt Range and Trans Indus Ranges, to the west by the boundary of the Mesozoic and Tertiary fold and thrust belt, and to the southeast by the outcrop of shallow basement of the Indian Shield. This foreland is covered in Quaternary age sediments and serves as the current depocenter for eroded sediments from northern Himalaya (Alam, 2008).

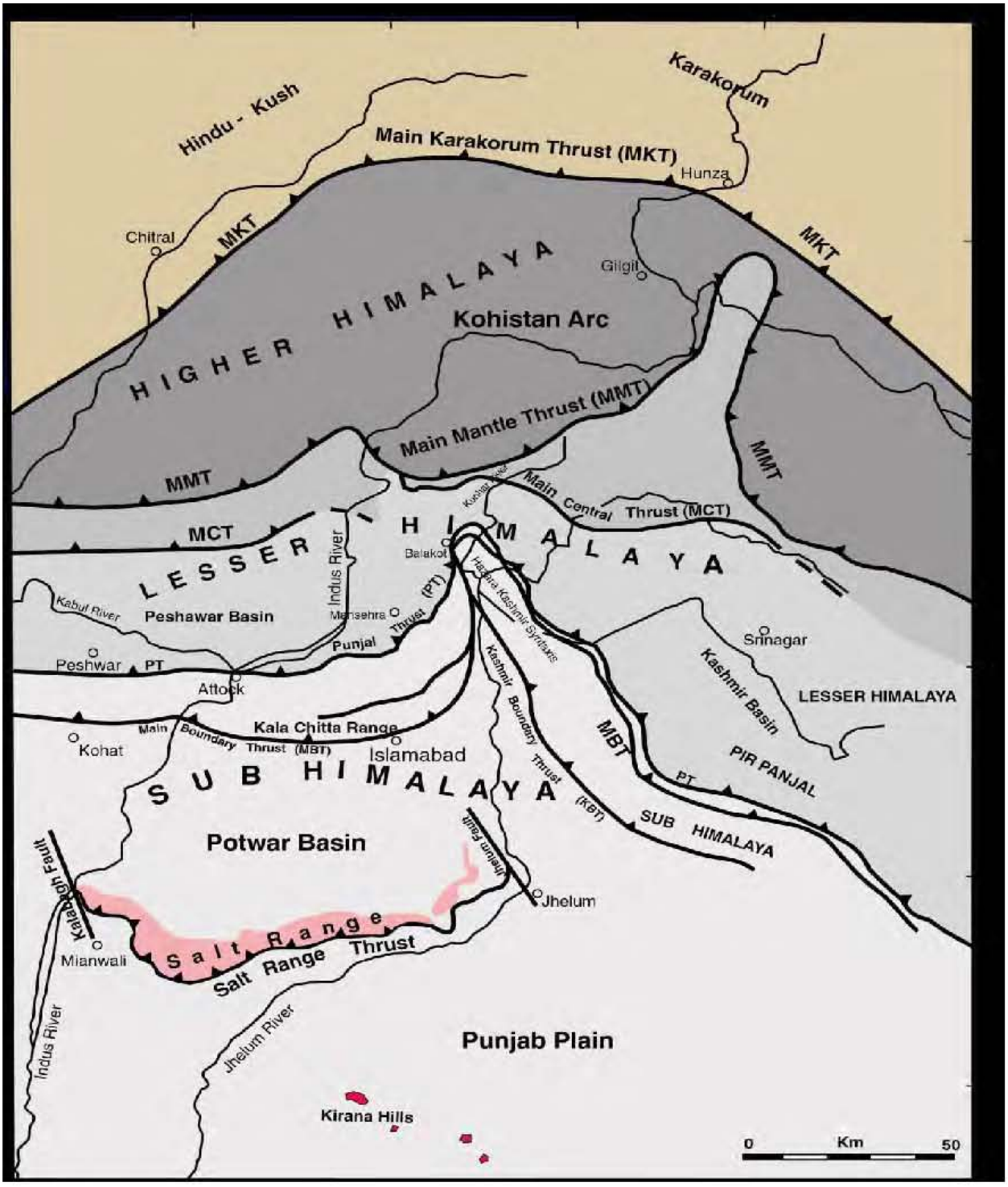

Figure 2. 2 Showes Generalized tectonic map of north Pakistan (After Kazmi and Rana, 1982).

2.13 Tectonic setup of the study Area

The research area is located in Pakistan's sub-Himalayan zone (Fig 2.3), which has seen numerous episodes of compressional and transpressional deformation (Alam, 2008). This thin-skinned deformed zone is bordered in the south by the Salt Range-Trans Indus (SRTI) fault system, and in the north by east-west trending regional intracontinental main boundary thrust (MBT) fault system (Ali, 2010). The southern Himalayan edge is marked by a regional fold and thrust band that stretches from the Ganges delta in India to the Suliman Range in Pakistan in the west (Ali, 2010). The Northern Potwar Deformed Zone (NPDZ), which is characterized by a number of thrust faults and their accompanying fold systems, also exhibits structural complexity in the northern Potwar sub-basin (Leather, 1987). This Himalayan orogeny's external zone is heavily accumulated with fluvial sediment that Pakistani stratigraphy refers to as "molasses sediment." (Alam, 2008). After the Tethyan Sea closed, a sizable volume of clastic sediments were produced by the ongoing orogenic process and deposited in the sub-Himalayan zone between Miocene and Pleistocene age (Alam, 2008). A thick sequence of fluvial-dominated Miocene foredeep sediment and massive margin shelfal marine sediment make up Salt Range, the southern deformed zone of Potwar sub-basin, which has been thrust over the Indo-Gangetic plain along the Salt Range Thrust (SRT) (Lillie et al., 1987). The SRT is a regional scale basal detachment that developed in the Precambrian Salt Range Formation's evaporitic succession and is located on top of a crystalline basement (Indian Sheild Rocks) (Wadia., 1919; Cotter., 1933;). Measured from surface traces as a 120 km long linear tectonic feature, the north-south Kalabagh fault serves as a geological boundary between the potwar and kohat subbasins. (Ali, 2010). The study area is located in the southern deformed fold and thrust belt (SDFTB) (Fig 2.3), which includes the southernmost deformed zones of the kohat and potwar sub-basins. In the kohat sub-basin, the SDFTB includes prominent outcropping frontal ranges such as the Surghar Range and the Khisore-Marwat Range, which are collectively referred to as the Trans Indus Range. The SDFTB in Potwar Sub-basin is made up of the prominent Salt Range.

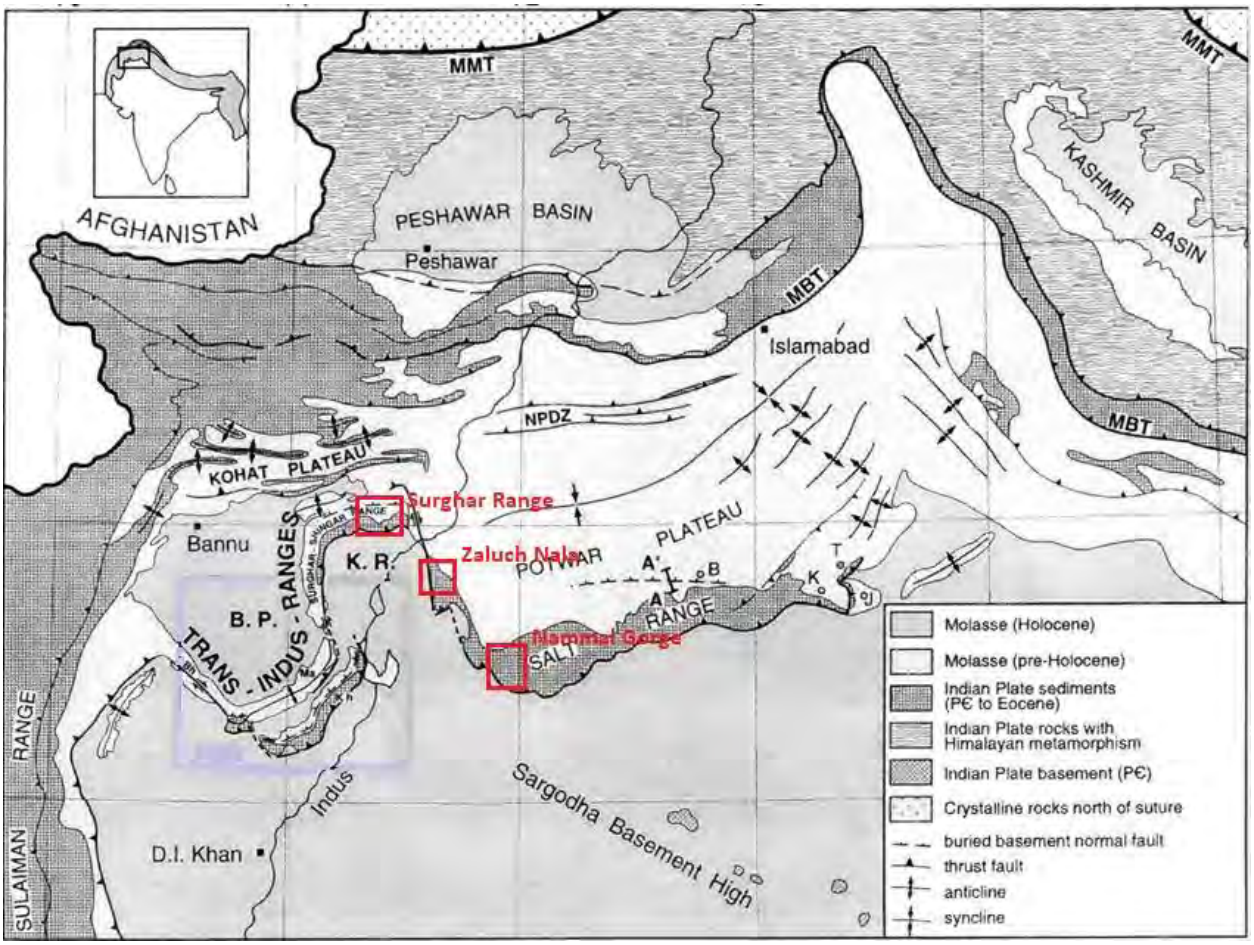

Figure 2. 3 The Geological and geographical location of study area, The Red boxes Represent the study area i.e., Nammal Gorge, Zaluch Nala and Surghare Range Section (After Yeats & Hussain, 1987)

CHAPTER 03
GENERALIZED STRATIGRAPHY AND STRUCTURAL FARMWORK

3.1 Stratigraphy of Nammal Gorge Section

Nammal gorge exposed in the western portion of Salt Range (SR), lies under latitude 32º39'54" N and longitude 71º 48'07" East. Nammal gorge is easily accessible via M2 motorway via Talagang with metaled road. This gorge hosts the sediments from Late Permian at base along with Eocene and Miocene sequences on the top part of the gorge. In Nammal gorge the well-known P-T Boundary (Permo Triassic Boundary) be present which divides the Permian Chiddru Formation from Triassic age Mianwali Formation. The overall stratigraphic succession in the Nammal gorge is described below and shown in figure 3.1.

3.1.1 Wargal Limestone

The Permian age Wargal Limestone are well exposed in Nammal Gorge section. The term "Middle products Limestone (Waagen.,1879), and "Wargal group (Noetling.,1901) are also used to refer this rock formation. The type of section of this Formation lies in the Wargal village of central Salt Range which has been proposed by Teichert (1966). In the research area Wargal Formation of Zaluch Group composed of carbonates with some siliciclastic materials which has been reported mixed with the lithofacies of underlying Amb Formation. the Wargal Limestone have confirmable lower contact with Permian age Amb Formation based on brachiopods and the upper contact is confirmable with the Late Permian age Chidru Formation. Thickness of this Formation in the Nammal Gorge, is 146m whereas it is 183 m thick in Zaluch Nala, 156m thick in Saiyiduwali section, 149m in Paniala arae (Alam et al., 2005; Alam, 2008;Mumtaz et al., 2017)

3.1.2 Chiddru Formation

The Late Permian age Chiddru formation exposed at western Salt Range Nammal gorge, khisor range, and Surghar range (Alam et al., 2005; Alam 2008). Chidru Formation name was proposed by Dunbar (1932), and formalized by Teichert (1966) studied the Formation in different sections. The formation was also known as Chiddru beds (Waagen, 1891) and Chiddru Group (Noetling,1901). In the research area the formation is lithologicaly consist of yellowish grey to dark grey color shale unit, above shale beds sandstone and sandy limestone are present and the topmost part is medium to fine grained white sandstone beds with fossiliferous shale. Chiddru Formation have transitional contact with underlying Wargal Limestone and upper contact marked by a major unconformity (P-T boundary) above which is the Early Triassic age Mianwali

Formation. Thickness of this Formation is 66m in Nammal Gorge, whereas it is 24m thick in Chiddru village, 92m thick in Saiyiduwali section, 68m thick in Paniala section and 44m thick in Surghar Range. (Alam et al., 2005; Alam, 2008)

3.1.3 Mianwali Formation

The Musa Khel group Early Triassic Mianwali Formation is well exposed at western Salt Range, in entire Khisor Range and Surghar Range. The name Mianwali Series was used by (Pascoe, 1959), later it modified to Mianwali Formation (Kummel,1966). This Formation is mainly consists of Limestone, Sandstone, Marl, and some Siltstone and Dolomite. The lower contact of Mianwali Fm is with Late-Permian age Chiddru Formation marked paraconformity and sharp and well define upper contact with Tredian Fm. Thickness of this Formation in Nammal Gorge is 142m whereas it is 130m thick in Lunda Psha Section, 127m in Saiyiduwali , and 118m in Paniala area .(Iqbal et al;. 2014) (Alam et al.,2005; Alam, 2008). Three member members of Mianwali Fm have been recognized by Kummel (1966)

i. Kathwai Member
ii. Mittiwali Member
iii. Narmia Member

3.1.4 Tredian Formation

The Middle-Triassic age Tredian Formation is well exposed at western Salt Range, Surghar Range, and Khisor range. The name Tredian formation was proposed by (Kummel, 1966) before that the formation was known Kingriali sandstones. Tredian Fm comprised of two members (1)the lower “Landa member” which composed of Shale, and various color (reddish, pinkish and greenish) micaceous Sandstone, and (2)the upper Khatkiara member which is contain massive, thick bedded, white sandstone with some inclusions of dolomite in the upper part. The Tredian formation have sharply underlying Mianwali Formation and gradually overlies Kingriali Fm. Thickness of This formation is 76m in Salt Range Zaluch nala section, whereas it is 1660m thick in Tappan Wahan section of the Khisor range 46m thick in Saiyiduwali, and 60m in Paniala area. (Alam et al., 2005;Alam, 2008).

3.1.5 Kingriali Formation

The Late Triassic Kingriali Formation exposed at western Salt Range, Nammal gorge and Zaluch Nala, Surghar Range, and Khisor Range. Firstly, this formation was known by Kingriali Dolomite which later changed into Kingriali Formation (Gee, 1945). The name Kingriali derives from the Khisor range, Kingriali Peaks. Kingriali Formation consist of massive bedded, fine to

coarse grained, grey to brown color Dolomite and some interbedded Marl, greenish Dolomitic Shale and Dolomitic Limestone, in the upper portion of the formation. Kingriali formation have two member, the Lower Doya and Upper Vanjari in Surghar Range (Fatmi et al., 1972). Kingriali Fm has confirmable Lower contact with Tredian Fm while upper disconformable contact with Datta Formation. Thickness of This formation is 67m in Nammal Gorge, 78m thick in Zaluch Nala Section western Salt Range, whereas it is 108m in Surghar Range, and 117m thick in Khisor Range (Ahmad et al.; 2022)

3.1.6 Datta Formation

The Baroch Group Early Jurassic age Datta Formation exposed in Trans Indus Range and Salt Range. Firstly, this Formation was known by "Variegated stage" of Gee, (1945), after replace on Datta Formation (Danilchik and Shah.; 1967). the Formation consist of variegated colored medium to thick bedded Sandstone, Siltstone, Mudstone and Shale with irregularly distributed calcareous Dolomite and fireclay at the lower part of Formation. Datta Formation unconfirmably overlies on Kingriali formation at Salt range and Trans Indus ranges while in Hazara it is unconfirmably overlies on Precambrian Hazara formation. The upper contact is gradational with Middle-Jurassic age Shinawari formation. Thickness of This formation is 150m in Nammal Gorge western Salt Range, whereas it is 230m thick in Punnu nala, 400m thick in Sheikh Badin Hills, 128m thick in Paniala section, and 110m in Landa Psha section. (Alam et al., 2005 and Alam, 2008).

3.1.7 Shinawari Formation

The Middle Jurassic age Shinawari Formation is widely exposed in Salt Range, Khisore and Surghar Range. The Formation consist of Limestone, nodular Marl, calcareous Shale, and some Sandstone. The limestone is thin to medium bedded, grey to brownish colored and fine to coarse grained which contain Oolitic, Ferruginous and sandy beds. The Shale unit is comprised of grey to dark grey color, and calcareous. This Formation have transitional contact with underlying Datta Fm overlying contact with Samana Suk Fm. The Thickness of this Fm is over 400m in Kala Chitta Range, Hazara Kohat, Salt Range and Trans-Indus Ranges, whereas it is 35m thick in Bhoje Nala, 30m thick in Broach Nala, 80m thick in Sheikh Badin Hills, 12m thick in Chak Dalla section (Shah.;1977).

The Samana Suk Formation is Missing in Nammal Gorge While exposed in Zaluch Nala. The Formation is briefly discussed in Stratigraphy of Zaluch Nala.

3.1.8 Chichali Formation

The Surghar Group Jurassic to Early Cretaceous age Chichali Formation Exposed in Kohat, Kala Chitta, Hazara, Chichali Pass and Surghar Ranges. Chichali Formation was first known by Belemnite beds (Spath.; 1939) which later established by (Danilchik, 1961) and refined by (Danilchik and Shah.; 1967). Chichali Fm consist of grey to rusty Brown muddy glauconitic sandstone and dark grey color glauconitic shale. In Salt Range it have Three member, (1) upper member which composed of glauconitic un-fossiliferous sandstone, (2) Middle member with dark green glauconitic sandstone with Belemnites fossils, and (3) lower member which composed of glauconitic shale. Chichali Formation have disconfirmable lower contact with Samana-Suk Fm and gradational upper-contact with Lumshiwal Fm. Thickness of This formation is 55m to 70m in Chichali Pass,15m to 20m thick in western Kohat,12m to 27m thick in Nizampur and Kala Chitta, 33m thick in southern Hazara and 48m thick in Sheikh Badin Hills (Shah,1977).

3.1.9 Hangu Formation

The Early Paleocene age Hangu Formation Exposed in salt Range, Surghar Ranges and Kohat. The formation was firstly known as a Hangu Sandstone (Davies,1930), which is later formalized to Hangu Formation. the Formation is consist of thick bedded grey, white and reddish color, medium grained Sandstone, grey color Shale and some nodular argillaceous limestone. Hangu Formation have unconformable lower contact with Chichali Fm and conformable upper contact with Lockhart Limestone. Thickness of This formation is 45m in Salt Range, 90m thick in Fort Lockhart, 50m thick in Hangu, 150m thick in Kohat, 75m thick in Darsamand, and less than 15m thick in Nizampur Kala Chitta Area (Shah,1977).

3.1.10 Lockhart Limestone

The Late Paleocene age Lockhart Formation exposed in Nammal Gorge Salt Range, Darsamand, Kohat, Kala Chitta and Hazara area. (Shah,1977). The name Kohat Limestone was introduced by (Davies, 1930). The Formation is lithologicaly consist of medium to thick bedded, light grey nodular Limestone and minor grey marl bluish Shale at lower part of the formation. The Lockhart Limestone is conformably overlies and underlies the Hangu and Patala formation respectively. Thickness of This formation is 70m in Nammal Gorge Salt Range, 40m thick in Kohat area, 260m thick in Kala Chitta, 90m to 242m thick in Hazara, and 36m thick in Darsamand.

3.1.11 Patala Formation

The Late Paleocene age Patala Formation exposed throughout Surghar Ranges, Salt Range, Hzara and Kohat-Potwar (Shah,1977). The formation was first known as Patala shale (Davies &

Pinfold 1937), and Nummulitic formation (Waagen and Wynne, 1872). Which later formalized to Patala formation by SCP. The Formation is comprises of thin bedded, greenish color Shale and minor grey color nodular Limestone, Marl, Sandstone, some Coal seems are also existing locally. The Formation has conformably lower contact with Lockhart formation while conformably and transitionally upper contact with Nammal Formation. Thickness of This formation is 90m in Patala Nala 27m in Khewra Gorge Salt Range, 30m to 180m thick in Kohat area, 30m to 75m thick in Surghar Range, 90m to 182m thick in Hazara area, and 60m to 182m thick in Kala Chitta Range (Shah, 1977).

3.1.12 Nammal Formation

The Chherat Group Early Eocene age Nammal Formation is widely exposed in Salt Range and Surghar Ranges. Nammal Formation was firstly known as Nammal Limestone (Gee, 1935) and Nammal Marl (Danilchik and Shah, 1967), Which later formalized to Nammal Formation by SCP. The Nammal Formation consists of olive green Shale, blight grey argillaceous Limestone and grey to bluish Marl. This formation lower contact with Patala Formation, and upper transitional contact with Sakessar Limestone.Thickness of This formation is 100m in Nammal Gorge 40m in Khewra Salt Range, 60m thick in Khairabad, 130m thick in Chichali, and 35m thick Broach Nala Surghar (Shah,1977).

3.1.13 Sakessar Limestone

The Early Eocene age Sakessar Limestone are exposed in Salt Range and Surghar Ranges. The name Sakessar Limestone was proposed by (Gee, 1935). The formation comprises of medium to thick bedded Creem to light grey nodular Limestone with minor Creem color Marl. The formation is throughout highly fossiliferous. Lower contact of this formation is conformable with Nammal Formation and the upper contact in eastern Salt Range conformable with Chorgali Formation, and in Surghar Ranges, and central, western Salt Range the Rawalpindi Group and Siwalik uncomfortably overlies the Sakesar formation. Thickness of This formation is varies from 70m to 150m in Salt Range, whereas it is 220m thick in Chichali, and 300m in other sections of Surghar Ranges (Shah, 1977).

3.2 Stratigraphy of Zaluch Nala Section

Zaluch Nala is the part of western SR situated in Mianwali, lies under 32 47 30 North, 71 37 07 East. Zaluch Nala is easily accessible via metaled road from Mianwali city. This section comprises the sediments from Eocambrian age to Eocene age. The oldest Formation in area is Salt Range Formation which represent the Eocambrian age, Tobra Formation Mark the base of Permian age sequence in the Zaluch Nala, on the top of gorge Eocene age Nammal and Sakessar Formation lies which represent the youngest sequence of the area. The overall stratigraphic succession in the Zaluch Nala is described below and shown in figure 3.1.

3.2.1 Tobra Formation

The Nilawahan Group Early Permian age Tobra formation is exposed in Salt Range and Khisor Ranges. The Formation was firstly known as Salt Range boulder bed (Teichert,1967) and Talchir Boulder Bed (Gee, 1959). Tobra Formation consists of poorly sorted Conglomerate contain pebble to boulder size polished and scratched igneous and metamorphic clasts, and poorly sorted Sandstone. Tobra Formation marks the base of Permian age sequence in Zaluch Nala and have the upper contact with Warchha Sandstone. The Thickness of This formation is 113m in Zaluch Nala western Salt Range, 33m in Eastern Salt Range, 0 to 25m in Central Salt Range, and 68m thick in Khisor Range (Shah,1977).

3.2.2 Warchha Sandstone

The Early-Permian age Warchha Sandstone is widely Exposed in Salt Range and Khisor Ranges. The of name Warchha Sandstone was introduced by (Hussain, 1967). The Formation consist of medium to coarse grained, red to brown color, and medium to thick bedded sandstone, red to maroon colored shale and siltstone with minor carbonates. In study area the formation overlies on Tobra Fm while transitionally Overlain by Sardhai Fm. The Thickness of This formation is 26m to 180m in Salt Range and Khisor Ranges (Shah,1977).

3.2.3 Sardhai Formation

The Early Permian age Sardhai Formation widely exposed in Salt Range and Khisor Range. Name Sardhai Formation was given by (Gee, 1959). The formation consist of bluish to greenish colored clay, light brown color fine grained Sandstone, and some nodular carbonates beds. Sardhai Formation has conformable upper-contact with Amb Fm and transitional lower contact with Warchha Sandstone. The thickness of this formation in type locality Sardhai gorge Eastern Salt Range is 42m; whereas it 65m in western-Salt Range and 50m in Khisor Range (Shah, 1977).

3.2.4 Amb Formation

The Zaluch Group Early Permian age Amb Formation well exposed in Khisor Range andWestern Salt Range. The name Amb Formation was proposed by (Teichert, 1966). The Formation was firstly known as Amb Sandstone bed (Waagen, 1891). The formation consists of thick bedded, medium grained, brownish grey colored Sandstone, medium bedded, grey color, fossiliferous sandy Limestone and grey to dark grey colored Shale. The Amb formation have conformable upper contact with Wargal Formation and transitional lower contact with Sardhai Formation. Thickness of this formation is 80m in type locality Amb village Central Salt Range and 47m thick in Khisor Range (Shah,1977).

The Permian sequence including Wargal Formation, Chidru Formation, and Triassic sequence covering the Mianwali Formation, Tredian and Kingriali Formation, are present in Zaluch Nala with best exposure which has been described in previous section.

3.2.5 Samana Suk Formation

The middle Jurassic age Samana Suk Fm exposed in Salt Range, Trans-Indus Ranges, Hazara, Kohat and Kala Chitta (Shah,1977). The name Samana Suk was introduced by **(**Davies, 1930). The Formation is consist of thin to thick bedded grey color nodular Limestone, few Shale and Marl are also present. Numerous of fossil are present all over the Formation. This Formation has transitional Lower Contact with Shinawari Fm and disconformable upper contact with Chichali Formation. Thickness of This formation is 186m in western salt range, whereas its 366m thick in Bagnotar section Hazara, 129m to 136m thick in Broach Nala of the Surghar Range, and 242m thick in Sheikh Badin Hills (Shah, 1977).

3.2.6 Chichali Formation

Chichali Formation is also exposed in Nammal Gorge which are briefly discussed in Stratigraphy of Nammal Gorge.

3.2.7 Lumshiwal Formation

The Surghar Group Late Cretaceous age Lumshiwal Formation exposed in Salt Range, Kohat, Kala Chitta, Hazara, and Surghar Ranges. The Lumshiwal Formation was firstly known as Lumshiwal Sandstone (Gee, 1945) which later change into Lumshiwal Formation by SCP. The formation consist of thick bedded, reddish, grey to yellow colored, medium grained Sandstone with minor Siltstone and Mudstone, the Belemnite Fossils and Plant remain are also present in formation. The thickness of this formation is 80m to 120m in Lumshiwal Nala, whereas it is 38m

thick in Chichali Pass, 194m thick in western Kohat, 47m thick in Nizampur, 60m in Kala Chitta Range, and 50m thick in southern Hazara (Shah, 1977).

The Paleocene-Eocene sequences are also well-exposed in Zaluch Nala section which has been discussed earlier with the stratigraphy of Nammal Gorge section.

3.3 Surghar Range Section

Surghar Range is the part of Trans Indus Ranges (Kohat Sub Basin) situated to the south of Islamabad at a distance of 235 kilometers. Its easily accessible from Mianwali city via Esa Khel Bannu Road. This gorge host sediment of late Permian Wargal Formation to Pliocene Dhok Pathan Formation. The Permian to Eocene sequence is well exposed in Nammal Gorge and Zaluch Nala which has been discussed earlier in stratigraphy of Nammal Gorge and Zaluch Nala section, the Miocene (Chinji and Nagri Formation) to Pliocene (Dhok Pathan Formation) succession are describe below and shown in figure 3.1.

3.3.1 Chinji Formation

The Siwalik Group Late Miocene age Chinji Formation is well exposed in Kohat Potwar Province and Suliman Ranges. This formation was firstly known by Chinji Zone (Pilgrim, 1913) which later changed into Chinji Formation by SCP. The formation consists of medium grained, cross bedded, ash grey colored soft Sandstone, red colored Clay, and thin bedded intraformational Conglomerate. The formation contains numerous vertebrate fossils. Chinji Formation disconformably overlies Nari Fm while conformably overlain by Nagri FM. Thickness of formation is 750m in type area, whereas it is 1800m thick in Shinghar Range, 300m thick in Rakhi Gaj Nala, 400m in Karkana, 150m thick in Zindapir and 155m thick in Makarwal section (Shah, 1977).

3.3.2 Nagri Formation

The Siwalik Group Late Miocene to Early Pliocene age Nagri Formation is well exposed in Indus Basin and Quetta area. The type locality of formation is the village Nagri Attock district. The name Nagri Formation was introduced by (Lewis, 1937). The formation consists of massive bedded, coarse grained greenish sandstone, sandy to silty Clay, and thick bedded Conglomerate which contain igneous pebble and Eocene Limestone. In Kohat Potwar Province it conformably overlies by Chinji Formation. The thickness of this formation is 700m in Litra Nala, 1100m thick in Sibi, 600m thick in Urak, and 940m thick in Gaj River Kirthar Province (Shah,1977).

3.3.3 Dhok Pathan Formation

The middle Pliocene age Dhok Pathan Formation widespread exposed in Indus Basin and Quetta Region. The name Dhok Pathan was given by (Pilgrim,1913), and Dhok Pathan Formation by (Cotter, 1933). the type locality of the formation is village Dhok Pathan District Attock. The formation consists of thick bedded, moderately Cemented, cross bedded, soft, light grey to Reddish brown colored Sandstone, sandy, Rusty orange Colored Clay, conglomerate and subordinate intercalation of brown Siltstone. This formation have transitional contact with underlying Nagri Fm and disconformable upper contact with Sona Formation. Thickness of this formation is 1330m in Gaud River, 1820m thick in Khair e Murat Range, 1330 to 1500m thick in Suliman Range, 1330m to 2000m thick in Sibi, and 1500m thick in Gaj River Kirthar Province (Shah,1977).

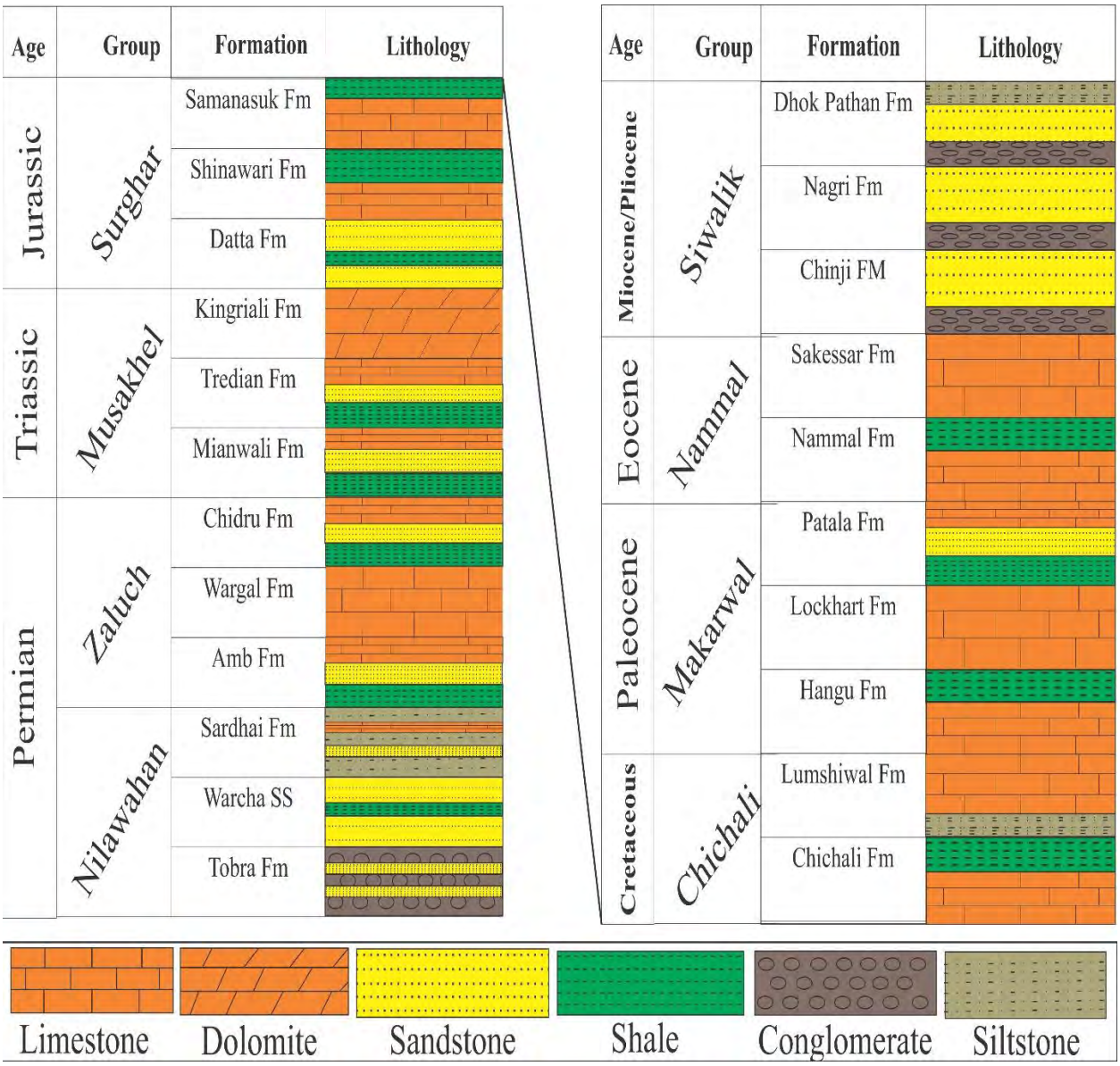

Figure 3. 1 Generalize stratigraphic column of study area (after Wadood et al.,2021)

3.4 Structural Framework

The study area is dominated by thrust tectonic. North-south compressional forces have a major impact on the exposed structures and have caused a variety of folds and faults. East-West trending structures are the dominant features in the studied area. The major structure features observed during the field are discussed below to understand the surface geology of the study area.

3.4.1 Folded and faulted/thrusted Structure

study area is characterized by a series of complex folds and thrust faults. The region has undergone significant tectonic compression, resulting in the folding and faulting of the sedimentary rock layers. The folds are available in different sizes, classes, and types. Faults are available from mesoscopic to macroscopic scale, most of them are reverse/thrust sense of motion and have east-west orientation. These structures have been shaped by the ongoing collision between the Indian Plate and the Eursia Plate. All the observed structures are shown in Figure 3.2.

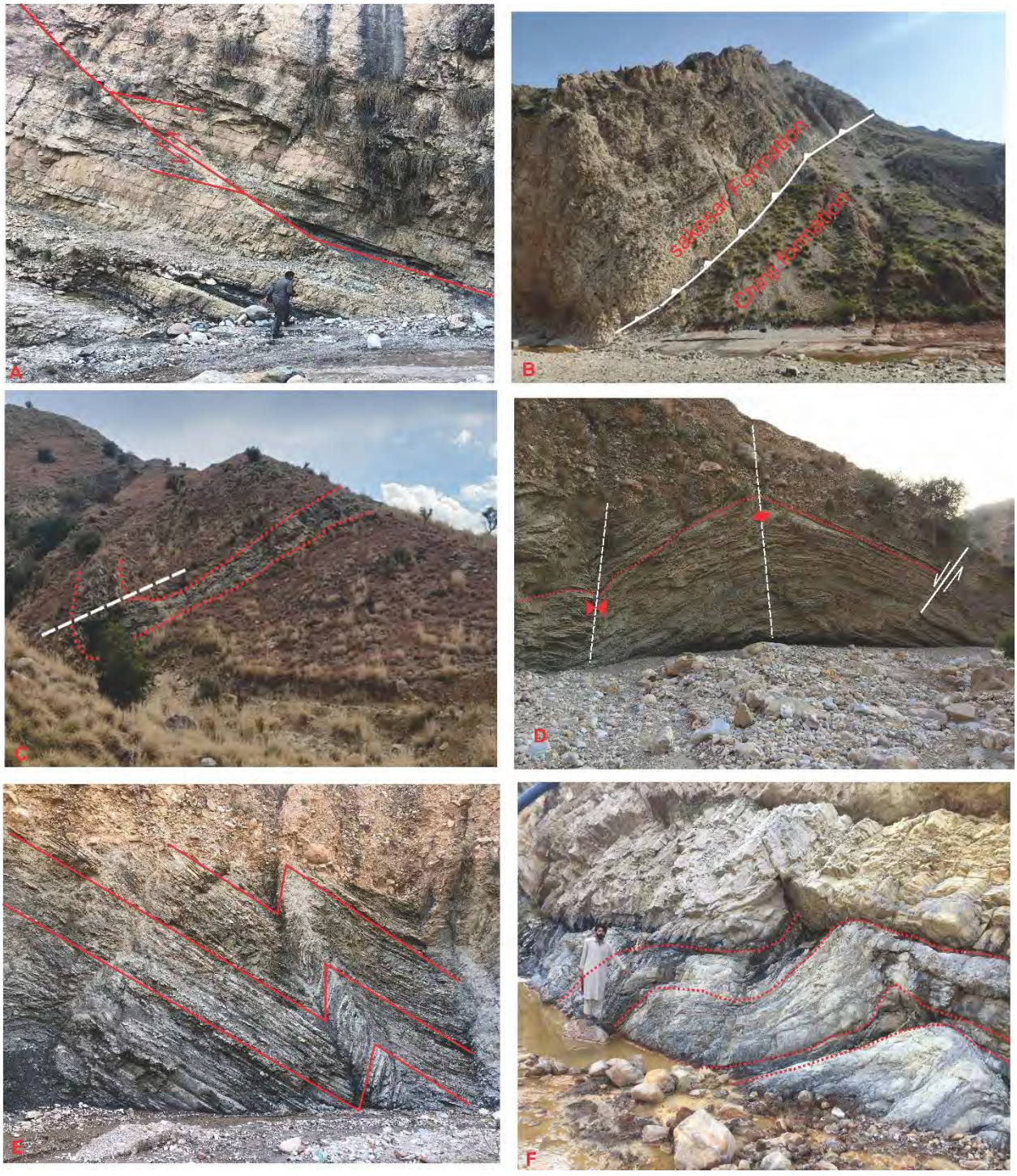

Figure 3. 2 Field photographs showing **A)** Intra formational fault in Kingriali formation, Surghar range, **B)** Surghar fault, Chichali Nala, **C)** Recumbent fold in Samana suk formation, Zaluch nala, **D)** Anticline, syncline and small size fault in Mianwali formation, Surghar Range, **E)** Chevron Fold in Mianwali Formation, Surghar Range, **F)** S and Z type folds in Shinawari formation, Surghar Range.

CHAPTER 04
FRACTURE ANALYSIS

4.1 Fracture

Any crack in a rock is an example of a fracture, which is often used to emphasize the indication that something is broken (Jadoon et al., 2003). There is an unseen movement parallel to the surface of the rock along the smooth surface of fractures. Up to several km may be present along the crack. A zone that has fractures that are closely spaced and related is known as a fracture zone (Singhal and Gupta, 2010).

4.2 Causes of fracture

Every competent rock contains fractures, which increase the porosity and permeability of rocks (Shah and Qadir, 2020). Fractures are the most often occurring produced structures. Due to their close connection to geological history, rock fracture creation is a particularly complex process. Various factors, including Rocks can shrink as a result of magma cooling, tectonic forces, surface movement (landslides and glaciers), and the release of tensions as the overburden rocks are removed owing to erosion.

4.3 Folding and Fracture

Anticlinal folds operate as a hydrocarbon trap that is affected by fracturing and can be used to transport stored fluid into or out of a reservoir (Baitu et al., 2008). Understanding the connection between folding and fracture in this context is crucial and has significant implications for applications for hydrocarbon exploration and extraction are shown in Figures 4.1, and 4.2 (Khan et al., 2007). Folding leads to various fracture types, each with a unique orientation and characteristics is discussed below.

4.4 Release Fracture

This series of fractures, which is geometrically known as a longitudinal fracture, lies parallel to the fold axis (Fig. 4.2) (Baitu et al., 2008). These fractures develop at the point of maximal curvature and are brought on by tension on the folded bed's upper side (Nelson, 2001; Khan et al., 2007; Baitu et al., 2008). Release fracture may arise under tangential longitudinal strain in which the exterior portions of folded competent layers are stretched (Mynatt et al., 2009). Release fractures may have also developed as a result of the release or removal of overburden loads.

4.5 Extension Fracture

Also known as a cross fracture, this type of fracture lies perpendicular to the fold axis (Fig 4.2). These fractures come about as a result of a modest elongation parallel to the fold axis (Baitu et al., 2008; Dasti et al., 2018).

4.6 Conjugate Fracture

These fractures, also known as slip or shear fractures, lie oblique to the fold axis (Fig. 4.2; Jadoon et al., 2005). the orientation of these fractures is parallel to the intermediate stress direction (δ2) (Baitu et al., 2008). Shearing can also lead to the development of slickenside (Jadoon et al., 2003). When compared to longitudinal fractures, these are typically tightening. In comparison to cross fractures and longitudinal fractures, conjugate fractures also have lower hydrogeological conductivity (Singhal and Gupta, 2010).

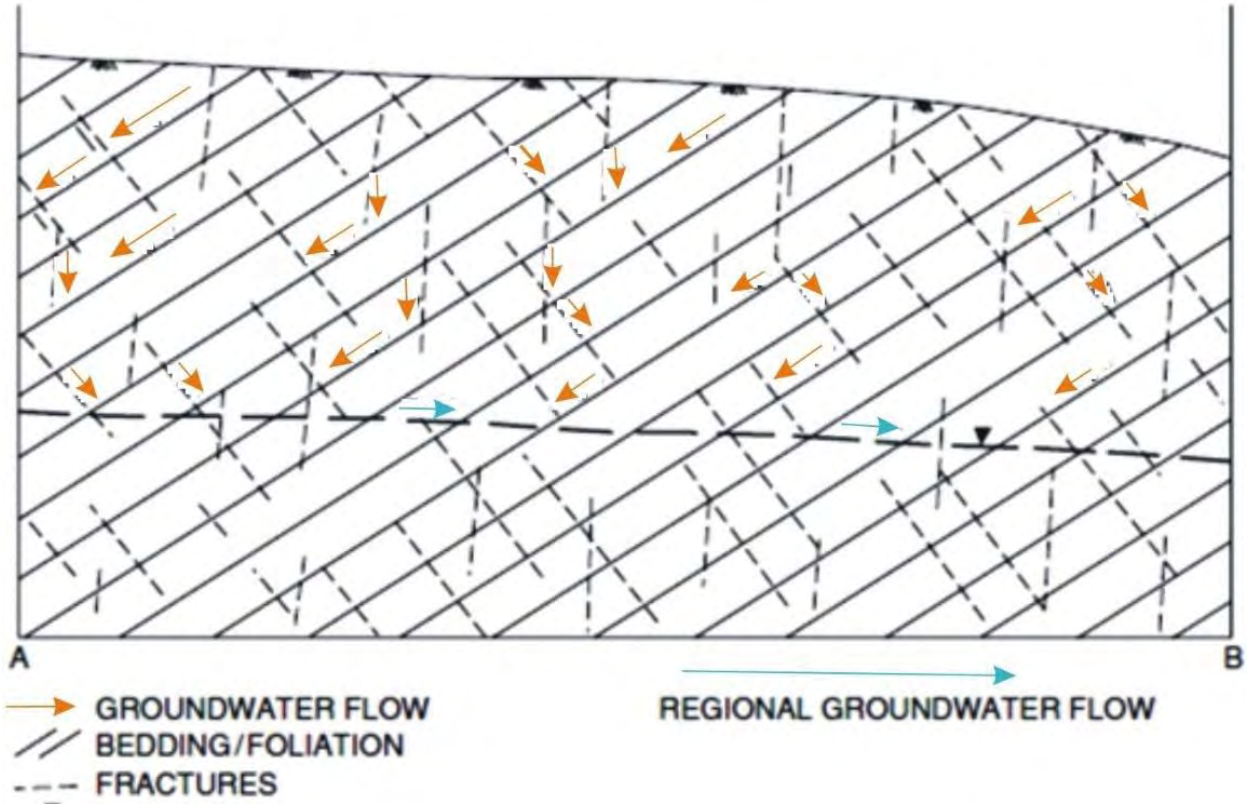

Figure 4. 1 Showing the flow of water (fluids) along bedding planes and fracture surfaces (After Singhal and Gupta, 2010).

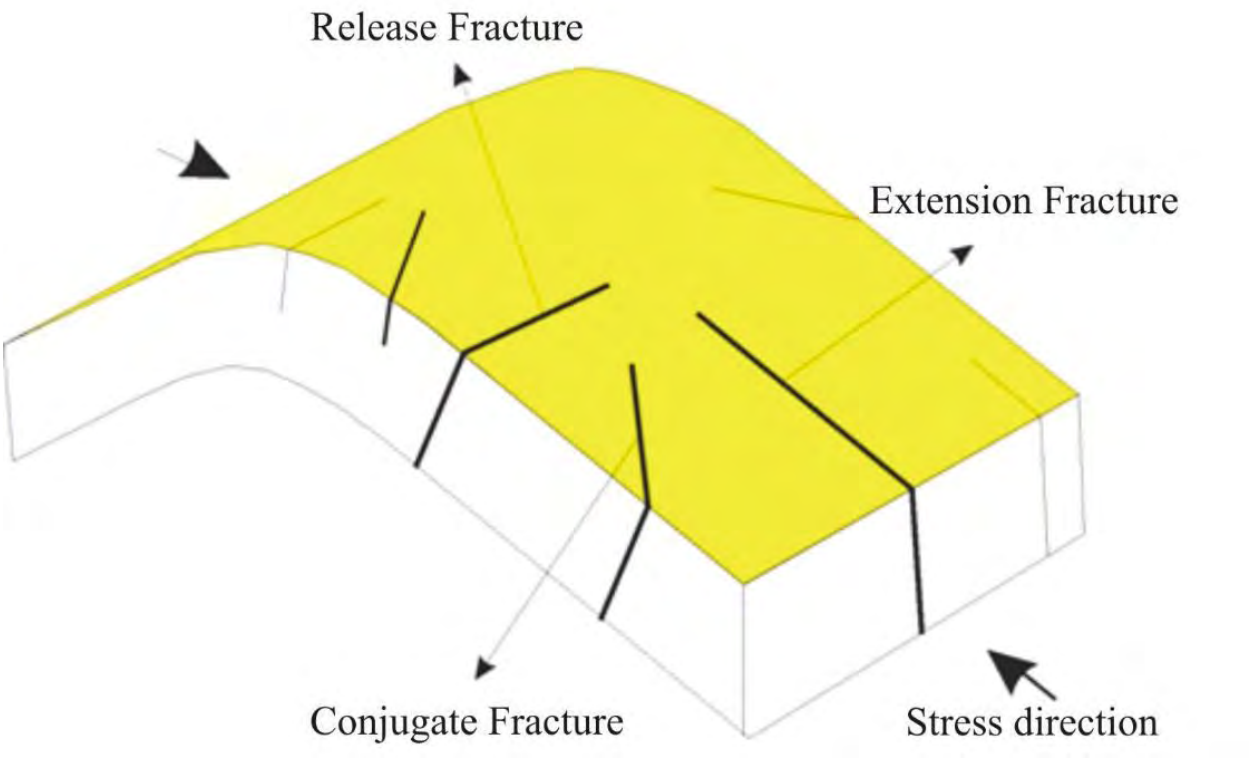

Figure 4. 2 Showing Longitudinal (Release), Cross (Extension) and Conjugate Shear (Oblique) fractures with respect to bed and stress direction (After Baitu et al., 2008).

4.7 Stress Analysis

Natural stresses found in the crust are known as insitu stresses (Figure. 4.3). These occur as a result of the following: a) Gravitational stresses carried on by the overburden's weight b) Crustal tectonic stresses linked with current tectonic forces, such as those brought on by the active collision; c) Residual stresses built up in the rocks as a result of earlier tectonic and conventional stresses. The Rose diagram can be used to display the fracture orientation data. Using the Rose diagram, any orientation data can be readily evaluated (Fig. 4.4). Concentric circles are typically positioned on a grid of radial lines in a Rose diagram. The maximum stress direction (δ1) is parallel to Extensional Fractures and perpendicular to minimum stress direction (δ3) i.e. Release Fractures, while oblique to intermediate stress direction (δ2) i.e. Conjugate Fractures (Baitu et al., 2008). Using fracture data to create rose diagrams that provide stress estimate visually.

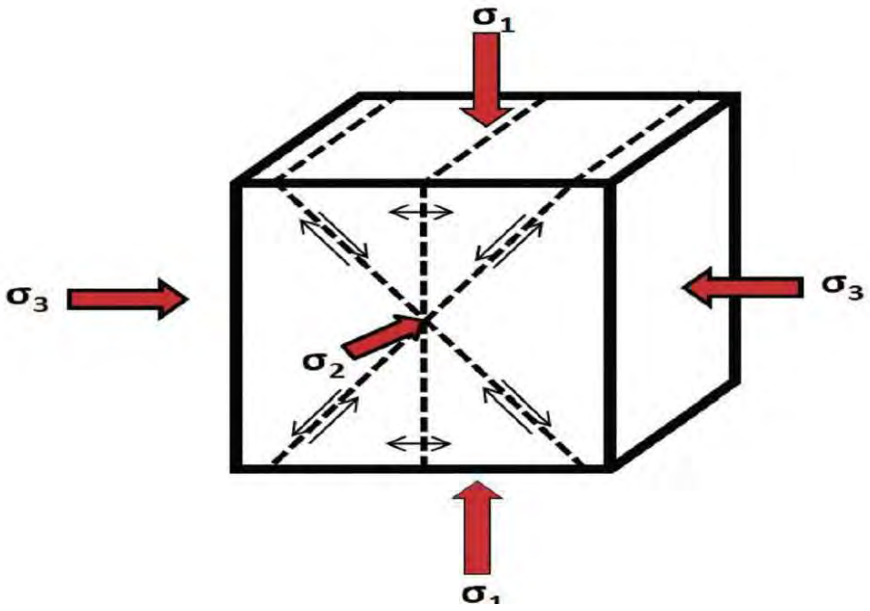

Figure 4. 3 Shows the stress orientation in 3D block diagram (After Hunt et al., 2009).

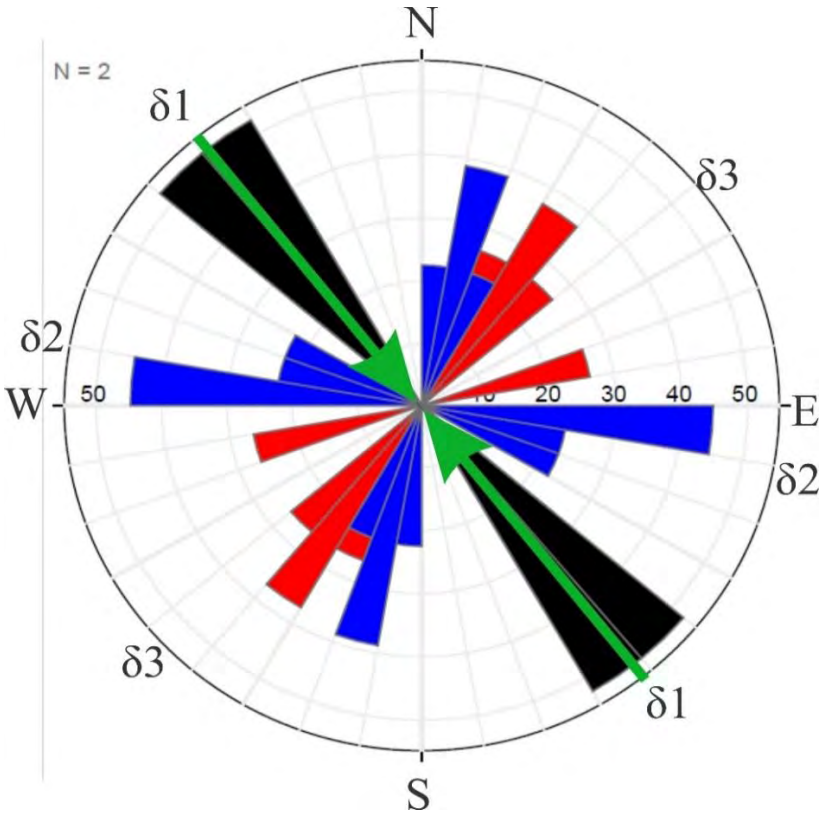

Figure 4. 4 Shows the stress orientation in Rose Diagram (After Dasti et al., 2018). Red color shows Release fractures, blue color indicates Conjugate fractures whereas Black color shows Extension fractures. The Green color arrows pointing towards the center of the rose diagram shows the maximum stress direction.

4.8 Morphology of Fracture

Fractures play a key role in the rock's reservoir properties. Nelson (2001) divided fractures into four categories: open, Mineral filled, Vuggy and deformed fracture.

4.8.1 Open Fracture;

Open fractures are ones that are not filled with tectonic gouge or mineral precipitate. Length, width, and fracture roughness are used to calculate the porosity and permeability of open fractures.

4.8.2 Mineral Filled Fracture;

Fractures that have been partially or entirely filled with a mineral precipitation during a diagnostic procedure are referred to as mineral filled fractures. As a result, by narrowing the fracture, the fracture porosity is decreased.

4.8.3 Vuggy Fracture;

Vuggy fractures are created when the cement or rock matrix along the crack is removed, allowing fluid to pass through and disintegrate the walls. As a result, it significantly increases porosity and permeability.

4.8.4 Deformed Fracture;

Shear stress can manifest as slickenside and gouge-filled deformation bands, both of which can cause deformed fractures. Slickenside is a glassy coating on fracture walls caused by the sliding action of the fracture. As a result, Slickenside lowers the fracture permeability orthogonal to slide fracture surface. Gouge, an incohesive rock, is created when fracture walls slide and grind against one another. It reduces fracture permeability and porosity by totally or partially filling the fracture.

4.9 Reservoir Characteristic

The permeability and porosity of rocks have an impact on the reservoir characteristics because they affect how fluids pass through and are stored. Any reservoir rock's discontinuities are crucial for fluid dynamics and its capacity to store fluid. Joints, shear zones, faults, fractures, and other discontinuities may help or hinder fluid flow, such as a dyke or fault, respectively. In terms of fluid dynamics in rocks, fracture is one of the most significant discontinuities and geological structures that promote fluid storage and movement. As a result, several parameters such as fracture opening, fracture length, fracture width, fracture density, fracture wall roughness, fracture orientation, and fracture continuity directly affect the permeability and porosity of rock (Singhal and Gupta, 2010). Total fracture permeability and porosity for fractured reservoirs includes both effective permeability and porosity as well as fracture permeability and fracture porosity. The effective permeability and porosity are compared with the fracture permeability and

porosity to show how well a reservoir performs (Nelson, 2001). As a result, the reservoir rocks are divided into four classes, namely Type-1, Type-2, Type-3, and Type-4 table.4.1.

S.No	NFR Type	Definition	Porosity value	Permeability value
1	Type-1	Fractures provide essential porosity and permeability	High	High
2	Type-2	Fractures provide essential permeability only.	Intermediate	Intermediate
3	Type-3	Fractures provide a permeability assistance	Low	Low
4	Type-4	Fractures do not provide significant porosity and permeability.	Extremely low or zero.	Extremely low or zero.

Table 4. 1 Classification of Natural Fractured Reservoir system (NFR) (compiled from Nelson, 2001).

The following are the main traits of a reservoir potential for fractured rocks:

1. Fracture density.
2. Fracture porosity.
3. Fracture permeability.

4.9.1 Fracture Density

The fracture density describes how many fractures there are at a specific site. Numerous methods exist for measuring and describing fracture density. i.e., the ratio of the total cumulative length of fractures in a particular volume of rock to the size of the circle or rectangle where the data is being collected. When used in conjunction with the circle inventory method, the fracture density is calculated as the sum of the lengths of all the fractures in the circle divided by its area (Jadoon et al., 2003; Baitu et al., 2008).

Fracture Density (∂) = $(\Sigma L)/\pi r^2$ (Baitu et al., 2008; Dasti et al., 2018)

Where:

ΣL = Cumulative length of fractures.

r = Radius of inventory circle.

4.9.2 Fracture Porosity

In different areas of the research region, the fracture density varies. The lengths, widths, and density of fractures at sample locations all affect porosity. By multiplying the fracture lengths and widths measured inside the inventory circle, the fracture porosity may be calculated. When a fracture's width was varied, we measured it many times before averaging the results. The formula below can be used to calculate the fracture porosity.

$$\text{Fracture Porosity \%} = \left(\frac{1}{A}\right) \sum_{i=1}^{N} (Li \times Wi) \times 100$$

Where:

i = Index to designate each fracture in an inventory circle, its value equal to 1

Li = Length of the i^{th} fracture.

Wi = Width of the i^{th} fracture.

A = Area of the inventory circle.

4.9.3 Fracture Permeability

Permeability is the capacity of a body to permit the passage of fluids. For a fractured reservoir, fracture permeability is crucial, and it has a big impact on the reservoir's performance and quality (Lewis and Dochartaigh, 2006) (Table 4.1). The width of the fractures is mostly related to fracture permeability. The confining pressure increases with depth, which in turn affects the fracture width, so that the fracture width reduces as depth increases (Nelson, 2001). The length, width, and density of the fractures are measured at the sample station to determine the perimeters for fracture permeability in the inventory circle technique. The following equation can be used to determine the fracture permeability (Muskat, 1949).

$$K = (3.5 \times 10^{8})\left(\frac{1}{A}\right) \sum_{i=1}^{N} (Li \times Wi^{3})$$

Where:

K = Permeability in Darcy, 1 Darcy is equal to approximately 10^{-12} m^2

i = Index to designate each fracture in an inventory circle, its value equal to 1.

Wi = Width of the i^{th} fracture.

Li = Length of the i^{th} fracture.

A = Area of the inventory circle.

3.5×10^{8} = Factor to convert cm^2 to Darcy.

CHAPTER 05
DATA ANALYSIS AND REPRESENTATION

5.1 Introduction

This chapter includes a compilation of fracture data along with mathematical calculations of various parameters. Each station's fracture data were plotted independently, along with field pictures. Additionally, each fracture's strike, dip, type, length, width, and morphology are listed. The petrophysical properties i.e., density, porosity, and permeability of the mapped fractures were calculated using the fracture data. Rose diagrams were constructed for each station, and the directions of maximum stress were determined, in order to compute the tectonic stress direction responsible for the deformation in the Salt Range. All the information served as a base for a descriptive investigation of the region's tectonic development and Fracture.

5.2 Mapping of Fracture

The mapping of fractures involved various steps. First the data is collected in the field therefore field data were collected from Kingriali Formation in different part of salt Range including Nammal Gorge, Zaluch Nala and Surghar Range. The innovative circle inventory method was used for collecting fracture data in the field.

5.3 Circular Inventory Method

For fracture data collection the convenient circle inventory method was used. A total of 30 sampling stations were selected which represented different parts of the Salt Range including Nammal Gorge, Zaluch Nala, and Surghar Range. This technique involves drawing a circle on the surface where the fractures are located that has a known and predefined radius (Davis et al., 2011). In our situation it was always a bedding plane. To use this method, all the fractures in this circle must be measured. The lengths, widths, and orientations of each fracture inside the circle were measured. On the bedding plane, circles with a radius of 25 cm were drawn using paint spray and measuring tape. Using the Brunton Compass, the strike and dip of each fracture were measured and measuring tape were used to measure fracture length and width. Each fracture was marked after measurement to prevent repetition. The length and width of each fracture are accurately measured within the inventory circle during the field.

5.4 Rose Diagram

The fracture orientation data is given on a Rose Diagram for fracture analysis. (Baitu et al., 2008). The Rose diagram gives a quick visual estimate of the direction of stress (Dasti et al., 2018).

A typical Rose diagram is built on a grid, with concentric circles superimposed over a series of radial lines and placed every 10° degrees in a geographic quadrant (Marshak Mitra, 1988). In the Rose diagram, the length of the petals reveals the proportion of fractures in a given direction i.e., in (figure 5.1). The presence of more petals in a certain direction corresponds to more fractures in that direction, and vice versa. In the rose diagram release fractures are shown by red color, Conjugate fractures by blue color, and Extensional fractures by black color. The rose diagram, field photos and all the detailed fracture data of each station is shown in section 5.1.

5.5 Stereonet

Stereonet is used to map the orientation of planes and lines, which is made up of great and small circles that are perpendicular to one another. Great circles pass through the sphere center. From upper pole to lower pole, the longitudinal lines on the globe are great circle lines. Except for the equator, the small circles do not pass from the sphere's center. The small circles represent globe's latitude lines. The position is determined by using the great and small circles.

NAMMAL GORGE SECTION

5.6 Station NO; 01

Area; Western Salt Range

Location; Nammal Gorge

Altitude; 9924

GPS Location; N32°39'00", E071°48'31"

Bed Strike; S69°W

Bed Dip; 52°NW

Bed Thickness; Massive Bed

Fracture Set; 04

Table 5. 1. Show fracture data of station 1.

S.NO	Strike	Dip	Length (CM)	Width (CM)	Open/Filled or Closed	Filled with	Remarks or Termination	Type
1	N25°W	46°NE	50	2	Open		Continuous	Extension
2	N19°W	57°NE	17	1	Open		Both	Extension
3	N26°W	58°NE	40	0.5	Open		One	Extension
4	N07°W	81°SE	50	3	Open		Continuous	Extension
5	S15°W	84°NW	20	1	Open		One	Conjugate
6	N08°W	82°NE	13	0.5	Open		One	Extension
7	N83°W	23°NE	44	0.5	Open		Continuous	Release
8	S64°E	40°SW	21	0.5	Open		Both	Extension
9	N22°W	40°NE	22	0.5	Open		One	Extension
10	S69°E	38°SW	22	0.2	Open		Both	Conjugate
11	N52°E	26°SE	15	0.3	Open		Both	Release

Calculation;

A. Fracture Density $(\partial) = (\Sigma L)/\pi\, r^2$

   FD= 314/3.14 $(25)^2$

   FD= 314/1962.5

   FD= 0.16 cm^1 (As all fracture are open, therefore this is both the open and total fracture density)

B. Fracture Porosity % = $\left(\frac{1}{A}\right)\sum_{i=1}^{N}(Li \times Wi) \times 100$

   FP= (1/1962.5) (365.9) x 100

   FP= 18.64 %

C. Fracture Permeability (K) = $(3.5 \times 10^8)(\frac{1}{A})\sum_{i=1}^{N}(Li \times Wi^3)$

   K= (3.5 $\times 10^8$) (1/1962.5) x 1805.08

   K= 321.92 $\times 10^6$ Darcy

D. Maximum Stress Direction; N23°W

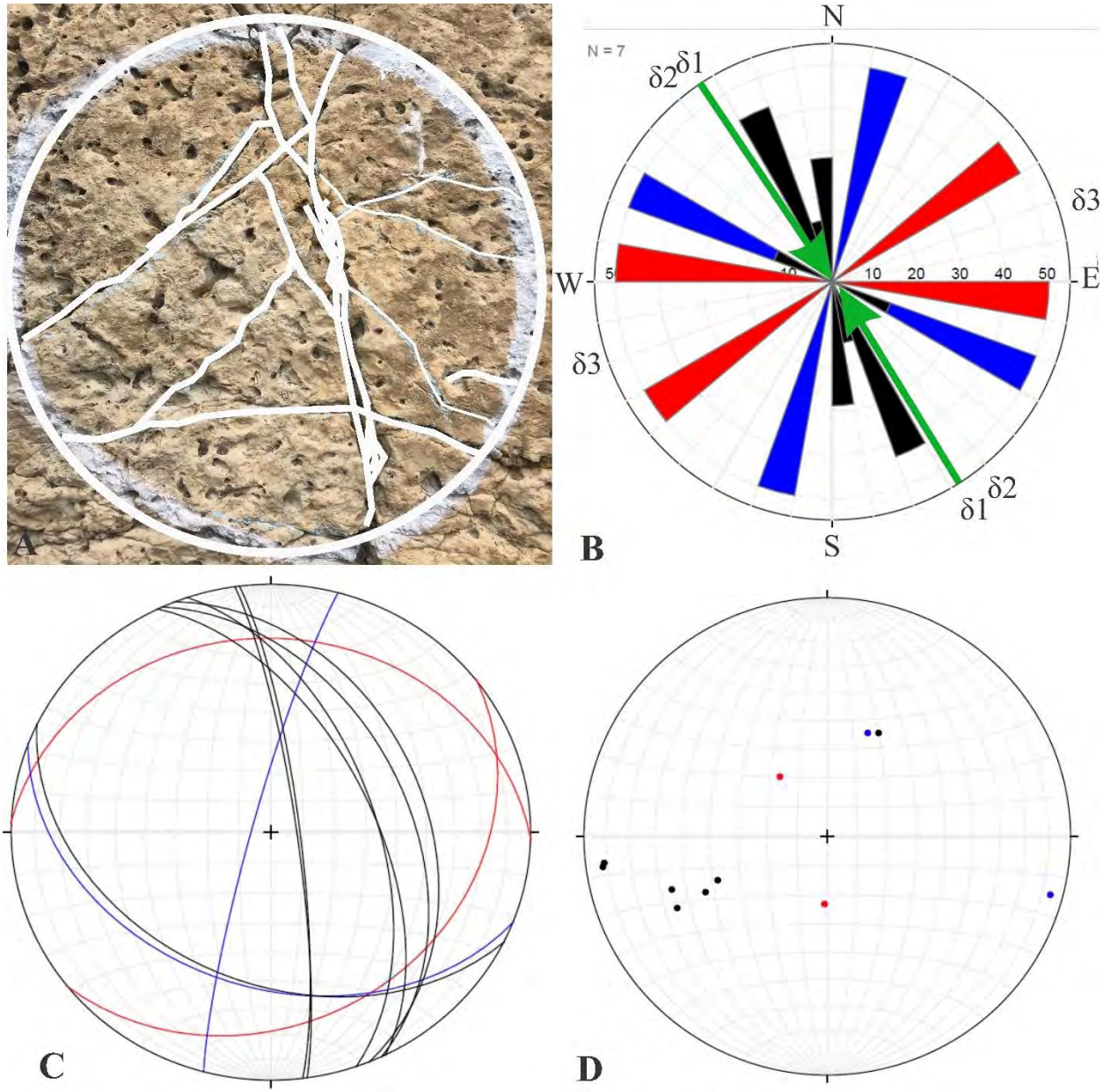

Figure 5. 1 (A) field photograph, (B) Rose diagram of fracture, (C) Plane data of fracture on Stereonet, (D) Poles data of fracture on Stereonet. Number of Release Fractures (Red color) are 02, Conjugate Fractures (Blue color) are 02 whereas Extension Fractures (Black color) are 07.

5.7 Station NO; 02

Area; Western Salt Range

Location; Nammal Gorge

Altitude; 1011

GPS Location; N32°39'38" E071°47'55"

Bed Strike; S72°W

Bed Dip; 47°NW

Bed Thickness; Massive Bed

Fracture Set; 03

Table 5. 2. Show fracture data of station 2.

S.NO	Strike	Dip	Length (CM)	Width (CM)	Open/Filled or Closed	Filled with	Remarks or Termination	Type
1	S87°E	28°SW	43	2	Open		Continuous	Release
2	N70°E	23°SE	50	1.5	Open		Continuous	Release
3	N10°E	09°SE	48	1.5	Open		Continuous	Extension
4	S65°E	52°SW	26	1	Open		One	Conjugate
5	S01°W	79°NW	11	1	Open		Continuous	Extension
6	N03°W	63°NE	09	0.5	Open		Both	Extension
7	N03°W	77°NE	12	0.2	Open		Both	Extension
8	N32°W	49°NE	14	0.5	Open		Both	Extension
9	N48°E	05°SE	16	0.5	Open		One	Release
10	N45°W	43°NE	23	0.2	Open		One	Extension
11	S11°W	77°NW	19	0.5	Open		One	Extension
12	N10°W	44°NE	20	0.2	Open		One	Extension
13	N16°W	49°NE	15	0.2	Open		One	Extension

Calculation;

A. Fracture Density $(\partial) = (\Sigma L)/\pi\, r^2$

   FD= 306/3.14 $(25)^2$

   FD= 306/1962.5

   FD= 0.155 cm^1 (As all fracture are open, therefore this is both the open and total fracture density)

B. Fracture Porosity % = $\left(\frac{1}{A}\right) \sum_{i=1}^{N} (Li \times Wi) \times 100$

   FP= (1/1962.5) (313) x 100

   FP= 15.94 %

C. Fracture Permeability (K) = $(3.5 \times 10^8)\left(\frac{1}{A}\right) \sum_{i=1}^{N} (Li \times Wi^3)$

   K= (3.5×10^8) (1/1962.5) x 719.07

   K= 128.24 $\times 10^6$

D. Maximum Stress Direction; N09ºW

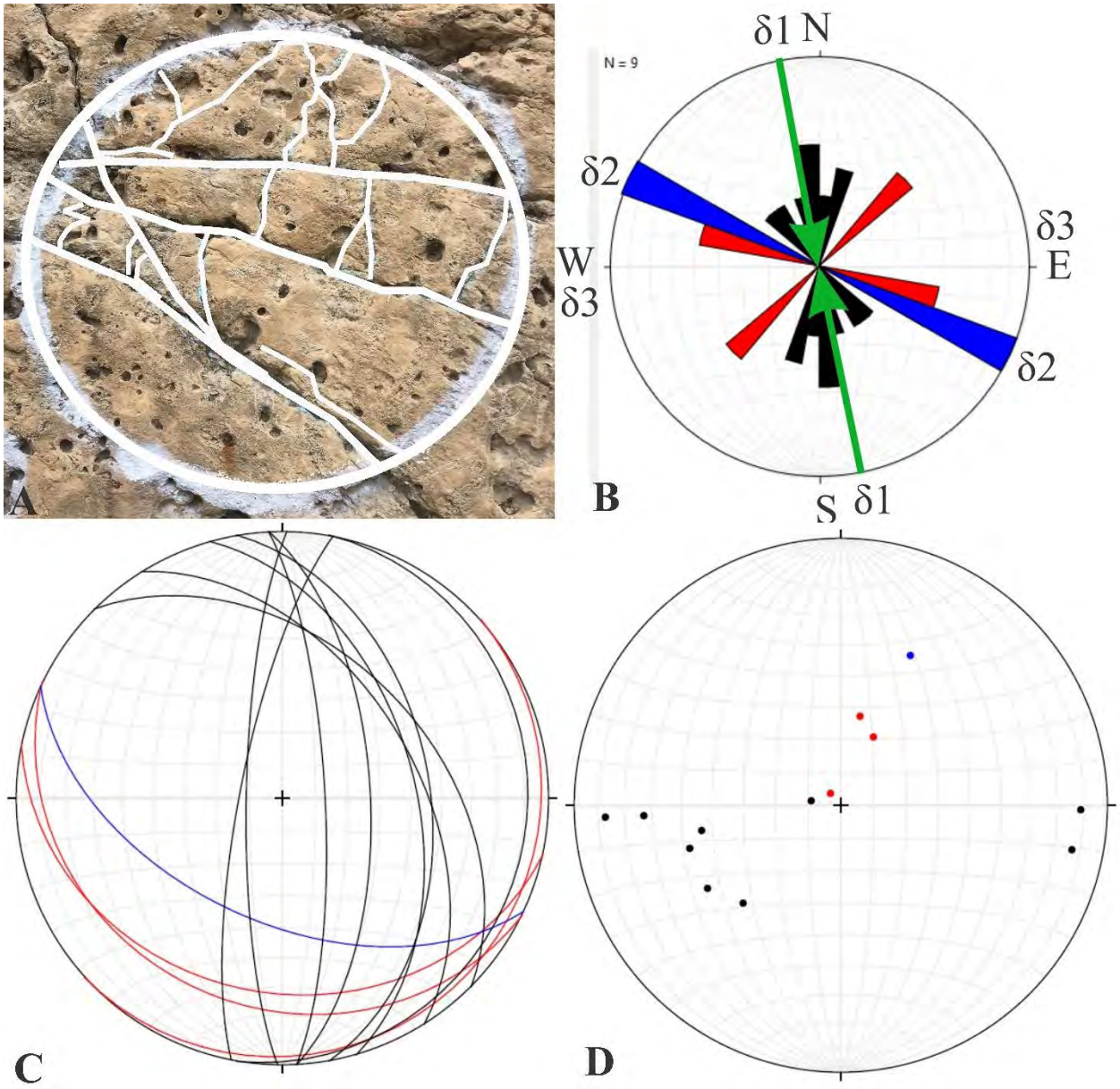

Figure 5. 2 (A) field photograph, (B) Rose diagram of fracture, (C) Plane data of fracture on Stereonet, (D) Poles data of fracture on Stereonet. Number of Release Fractures (Red color) are 03, Conjugate Fractures (Blue color) are 01 whereas Extension Fractures (Black color) are 09.

5.8 Station NO; 03

Area; Western Salt Range

Location; Nammal Gorge

Altitude; 1001

GPS Location; 32°39'73"N, 071°47'82"E

Bed Strike; S68°W

Bed Dip; 48°NW

Bed Thickness; Massive Bed

Fracture Set; 03

Table 5. 3. Show fracture data of station 3.

S.NO	Strike	Dip	Length (CM)	Width (CM)	Open/Filled or Closed	Filled with	Remarks or Termination	Type
1	S52°E	57°SW	46	2	Open		Continuous	Conjugate
2	S73°E	62°SW	14	0.5	Open		One	Release
3	N06°E	36°SE	41	0.5	Open		One	Extension
4	S87°E	44°SW	39	1	Open		Continuous	Release
5	S49°E	89°SW	30	0.5	Open		One	Conjugate
6	N62°W	76°NE	45	0.5	Open		One	Conjugate
7	S70°E	65°SW	15	0.4	Open		One	Conjugate
8	S64°E	58°SW	20	0.5	Open		Both	Conjugate
9	N33°W	20°NE	14	0.1	Open		One	Extension
10	S01°W	49°NW	10	0.2	Open		Both	Extension
11	S74°E	56°SW	12	0.2	Open		Both	Release
12	S82°E	66°SW	17	0.1	Open		Both	Release
13	S70°E	59°SW	20	0.5	Open		Both	Conjugate
14	S40°E	82°SW	13	0.3	Open		One	Extension
15	S68°E	55°SW	13	0.2	Open		One	Conjugate
16	N62°E	82°SE	11	0.2	Open		One	Release
17	S80°E	67°SW	15	0.5	Open		One	Release

Calculation;

A. Fracture Density $(\partial) = (\Sigma L)/\pi\, r^2$

   FD= 375/3.14 $(25)^2$

   FD= 375/1962.5

   FD= 0.191 cm^1 (As all fracture are open, therefore this is both the open and total fracture density)

B. Fracture Porosity % = $\left(\frac{1}{A}\right) \sum_{i=1}^{N} (Li \times Wi) \times 100$

   FP= (1/1962.5) (245.7) x 100

   FP= 12.51 %

C. Fracture Permeability (K) = $(3.5 \times 10^8)(\frac{1}{A}) \sum_{i=1}^{N} (Li \times Wi^3)$

   K= (3.5×10^8) (1/1962.5) x 434.99

   K= 77.57×10^6

D. Maximum Stress Direction; N18ºW

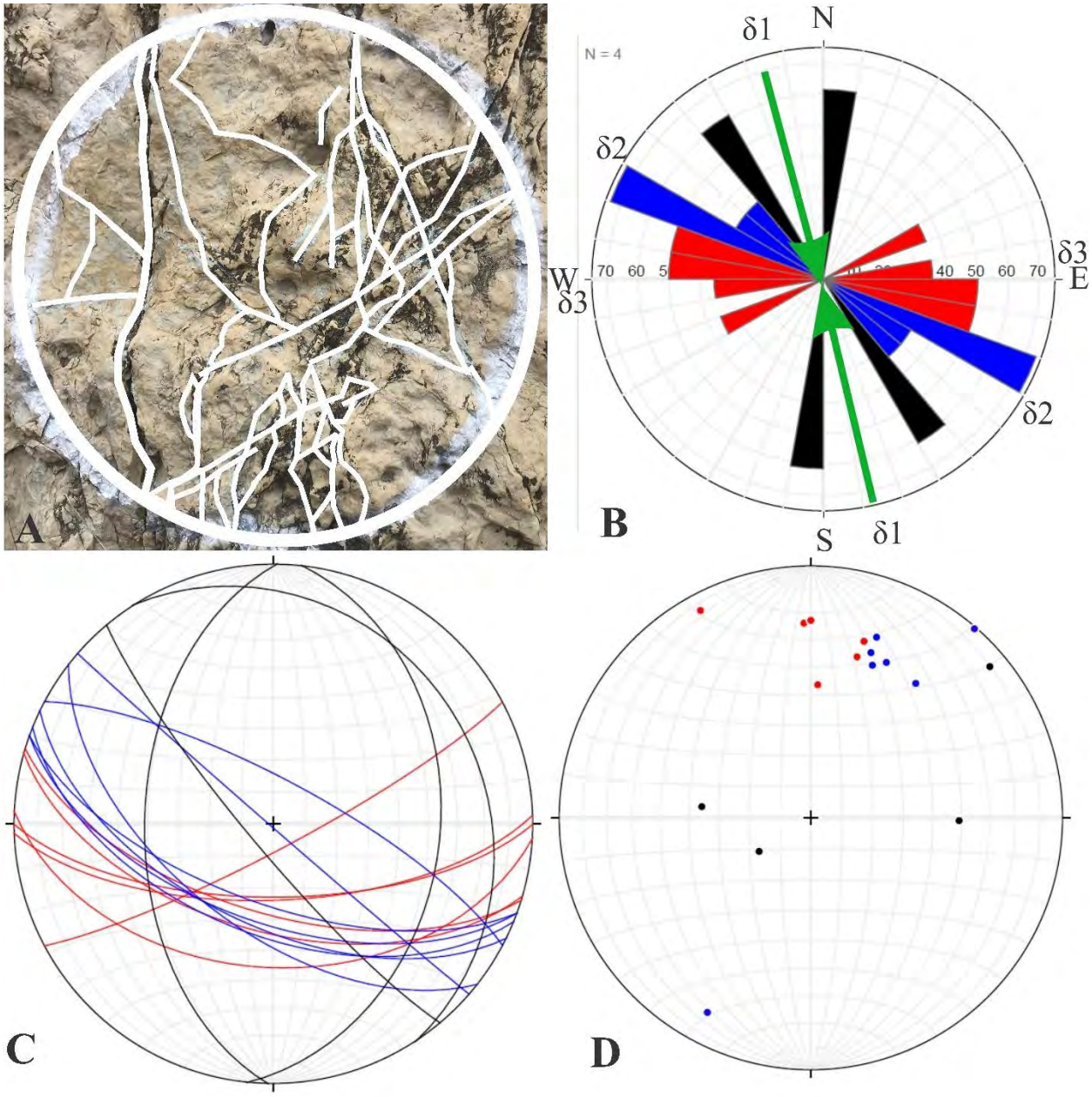

Figure 5. 3 (A) field photograph, (B) Rose diagram of fracture, (C) Plane data of fracture on Stereonet, (D) Poles data of fracture on Stereonet. Number of Release Fractures (Red color) are 06, Conjugate Fractures (Blue color) are 07 whereas Extension Fractures (Black color) are 04.

5.9 Station NO; 04

Area; Western Salt Range

Location; Nammal Gorge

Altitude; 1002

GPS Location; 32°39'39"N, 071°47'56"E

Bed Strike; S61ºW

Bed Dip; 56°NW

Bed Thickness; Massive Bed Fracture Set; 04

Table 5. 4. Show fracture data of station 4.

S.NO	Strike	Dip	Length (CM)	Width (CM)	Open/Filled or Closed	Filled with	Remarks or Termination	Type
1	S70°E	66°SW	48	1.5	Open		Continuous	Conjugate
2	S79°E	58°SW	20	0.5	Open		One	Conjugate
3	S84°E	58°SW	44	2.5	Open		Continuous	Conjugate
4	N10°E	46°SE	23	0.5	Open		Continuous	Conjugate
5	N16°E	35°SE	23	0.5	Open		One	Conjugate
6	S10°W	25°NW	27	0.2	Open		One	Conjugate
7	N38°E	31°SE	26	0.1	Open		One	Release
8	N39°E	32°SE	11	0.1	Open		One	Release
9	N49°E	12°SE	19	0.5	Open		Continuous	Release
10	N01°E	24°SE	27	0.2	Open		One	Conjugate
11	N36°E	13°SE	31	0.1	Open		One	Release
12	N31°E	18°SE	36	0.1	Open		One	Release
13	S86°E	23°SW	26	0.1	Open		Both	Conjugate
14	N77°E	25°SE	27	0.2	Open		Both	Release
15	N20°E	27°SE	10	0.1	Open		Both	Conjugate
16	N48°E	19°SE	13	0.1	Open		Both	Release
17	S88°E	37°SW	10	O.1	Open		Both	Conjugate
18	S87°E	10°SW	11	0.1	Open		One	Conjugate
19	N28°E	02°SE	16	0.1	Open		One	Release
20	N13°W	43°NE	38	1	Open		One	Extension
21	S47°E	70°SW	13	0.2	Open		Both	Extension

Calculation;

A. Fracture Density $(\partial) = (\Sigma L)/\pi\, r^2$

   FD= 499/3.14 $(25)^2$

   FD= 499/1962.5

   FD= 0.25 cm^1 (As all fracture are open, therefore this is both the open and total fracture density)

B. Fracture Porosity % = $\left(\frac{1}{A}\right) \sum_{i=1}^{N} (Li \times Wi) \times 100$

   FP= (1/1962.5) (300.3) x 100

   FP= 15.30 %

C. Fracture Permeability (K) = (3.5×10^8) (1/A) Σi=1 $(Li \times Wi^3)$

   K= (3.5×10^8) (1/1962.5) x 1016.68

   K= 181.13 $\times 10^6$

D. Maximum Stress Direction; N39ºW

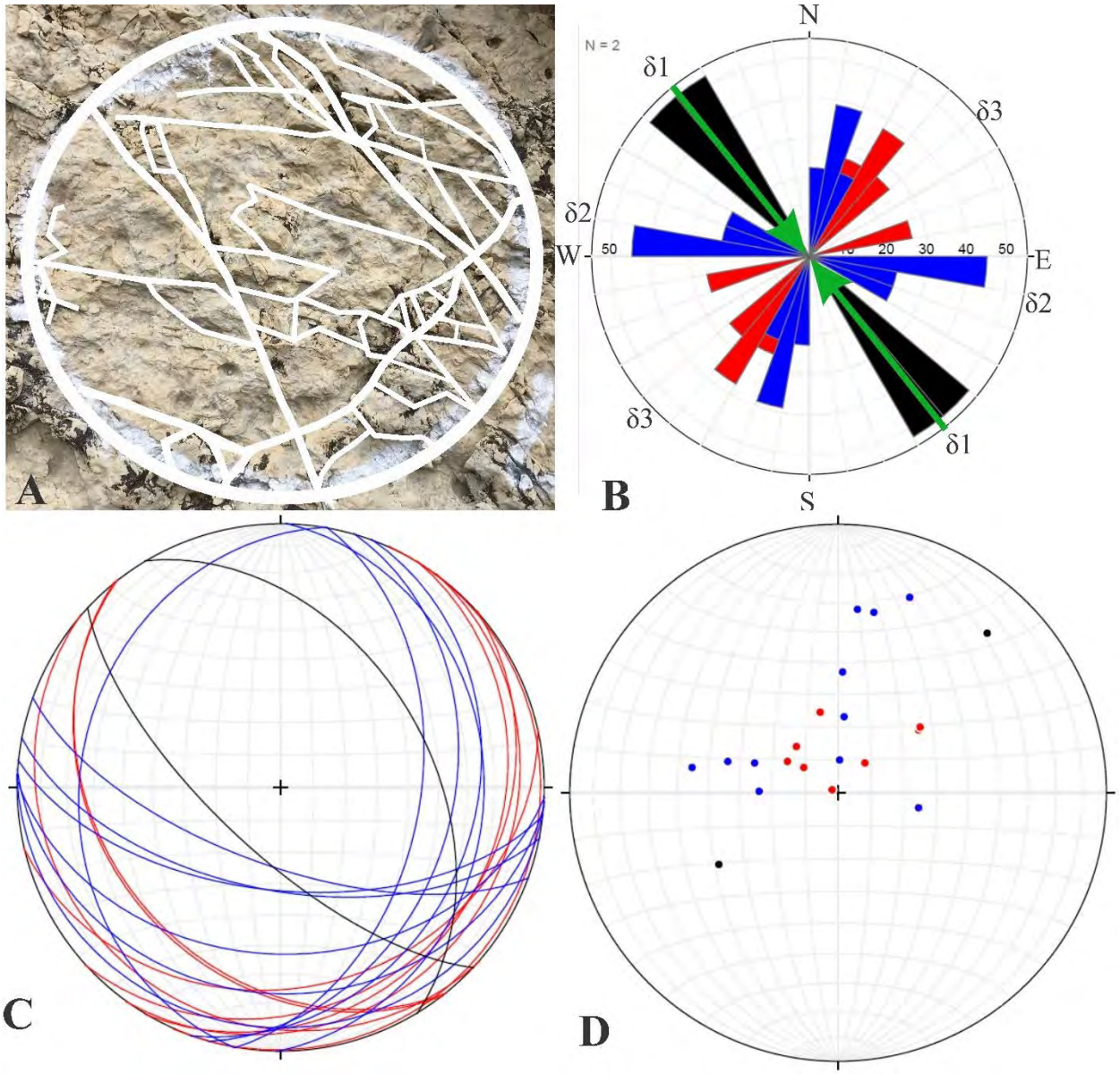

Figure 5. 4 (A) field photograph, (B) Rose diagram of fracture, (C) Plane data of fracture on Stereonet, (D) Poles data of fracture on Stereonet. Number of Release Fractures (Red color) are 08, Conjugate Fractures (Blue color) are 11 whereas Extension Fractures (Black color) are 02.

5.10 Station NO; 05

Area; Western Salt Range

Location; Nammal gorge

Altitude; 1003

GPS Location; 32°39'97"N, 071°47'54.23"E

Bed Strike; S°68W

Bed Dip; 45°NW

Bed Thickness; Massive Bed

Fracture Set; 03

Table 5. 5. Show fracture data of station 5.

S.NO	Strike	Dip	Length (CM)	Width (CM)	Open/Filled or Closed	Filled with	Remarks or Termination	Type
1	S60°E	50°SW	26	1	Open		Continuous	Extension
2	S72°E	61°SW	40	0.6	Open		One	Conjugate
3	S66°E	53°SW	26	0	Closed		Both	Conjugate
4	S68°E	38°SW	48	1	Open		Continuous	Conjugate
5	S77°E	57°SW	23	0.6	Open		Both	Conjugate
6	S88°E	47°SW	14	0.5	Open		Both	Conjugate
7	N02°E	47°SE	38	0.5	Open		One	Conjugate
8	S85°E	52°SW	21	0.5	Open		Both	Conjugate
9	N04°W	17°NE	37	0.4	Open		One	Extension
10	N33°W	25°NE	50	1	Open		Continuous	Extension
11	N19°W	35°NE	10	0	Closed		One	Extension

Calculation;

A. Fracture Density $(\partial) = (\Sigma L)/\pi\, r^2$

   FD= 333/3.14 $(25)^2$

   FD= 333/1962.5

   FD= 0.16 cm^1

   Open Fracture Density= 297/1962.5

   FD= 0.15 cm^1

B. Fracture Porosity % = $\left(\frac{1}{A}\right)\sum_{i=1}^{N}(Li \times Wi) \times 100$

   FP= (1/1962.5) (213.1) x 100

   FP= 10.85 %

C. Fracture Permeability (K) = $(3.5 \times 10^8)(\frac{1}{A})\sum_{i=1}^{N}(Li \times Wi^3)$

   K= (3.5×10^8) (1/1962.5) x 149.10

   K= 26.59 $\times 10^6$

D. Maximum Stress Direction; N29ºW

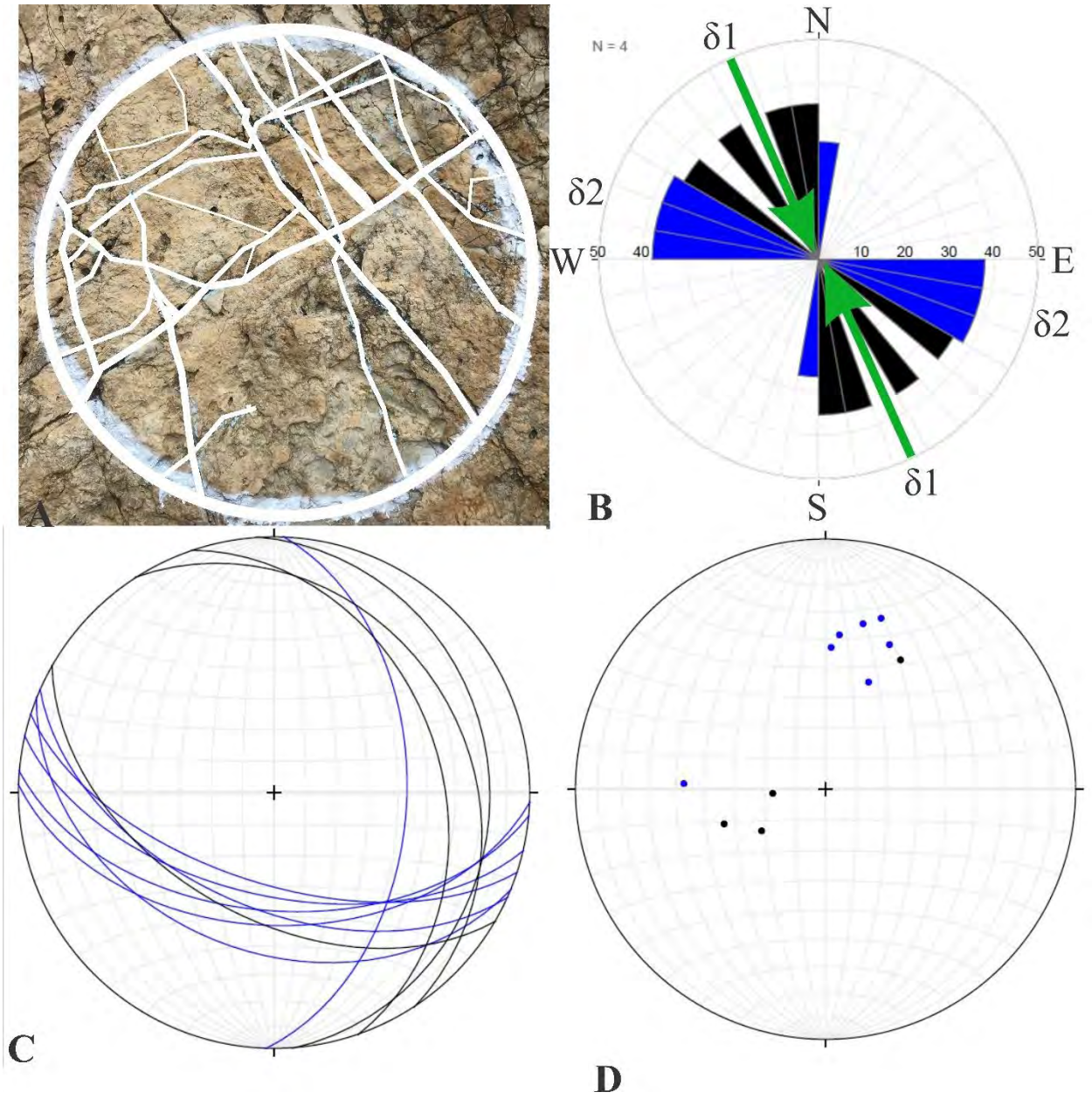

Figure 5. 5 (A) field photograph, (B) Rose diagram of fracture, (C) Plane data of fracture on Stereonet, (D) Poles data of fracture on Stereonet. Number of Conjugate Fractures (Blue color) are 07 and Extension Fractures (Black color) are 04.

5.11 Station NO; 06

Area; Western Salt Range

Location; Nammal gorge

Altitude; 1004

GPS Location; 32°39'99"N, 071°47'87"E

Bed Strike; S66°W

Bed Dip; 50°NW

Bed Thickness; Massive Bed

Fracture Set; 02

Table 5. 6. Show fracture data of station 6.

S.NO	Strike	Dip	Length (CM)	Width (CM)	Open/Filled or Closed	Filled with	Remarks or Termination	Type
1	S72°E	26°SW	19	1	Open		Continuous	Conjugate
2	S65°E	31°SW	16	1	Open		Continuous	Conjugate
3	S55°E	39°SW	21	0.5	Open		Continuous	Conjugate
4	N05°E	30°SE	50	1	Open		Continuous	Extension
5	S78°E	28°SW	48	1.5	Open		Continuous	Conjugate
6	S60°E	42°SW	14	0.1	Open		Both	Conjugate
7	S65°E	46°SW	15	0.7	Open		One	Conjugate
8	S22°E	48°SW	15	0.2	Open		One	Extension
9	N63°W	88°SE	35	1	Open		One	Extension
10	N66°W	80°SE	06	0.2	Open		One	Conjugate
11	S60°E	47°SW	20	0.1	Open		One	Conjugate
12	S63°E	46°SW	20	0.1	Open		One	Conjugate

Calculation;

A. Fracture Density $(\partial) = (\Sigma L)/\pi\, r^2$

   FD= 279/3.14 $(25)^2$

   FD= 279/1962.5

   FD= 0.142 cm^1 (As all fracture are open, therefore this is both the open and total fracture density)

B. Fracture Porosity % = $\left(\frac{1}{A}\right)\sum_{i=1}^{N}(Li \times Wi) \times 100$

   FP= (1/1962.5) (441.2) x 100

   FP= 22.48 %

C. Fracture Permeability (K) = $(3.5 \times 10^8)(\frac{1}{A})\sum_{i=1}^{N}(Li \times Wi^3)$

   K= (3.5×10^8) (1/1962.5) x 615.94

   K= 109.85 $\times 10^6$

D. Maximum Stress Direction; N12ºW

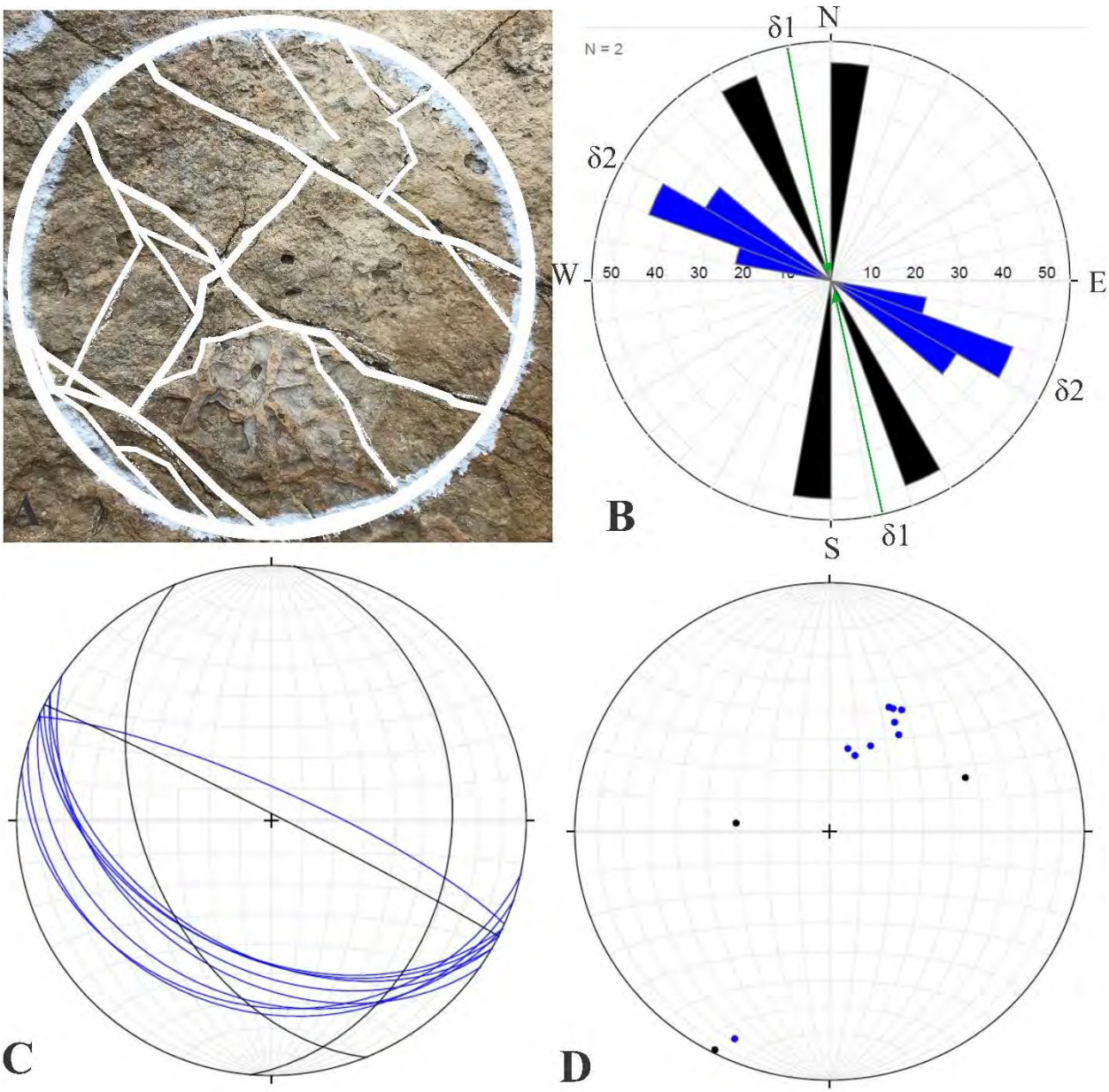

Figure 5. 6 (A) field photograph, (B) Rose diagram of fracture, (C) Plane data of fracture on Stereonet, (D) Poles data of fracture on Stereonet. Number of Release Conjugate Fractures (Blue color) are 09 and Extension Fractures (Black color) are 03.

5.12 Station NO; 07

Area; Western Salt Range

Location; Nammal Gorge

Altitude; 1005

GPS Location; 32°39'37.9"N, 071°47'53.21"E

Bed Strike; S55°W

Bed Dip; 51°NW

Bed Thickness; Massive Bed

Fracture Set; 03

Table 5. 7. Show fracture data of station 7.

S.NO	Strike	Dip	Length (CM)	Width (CM)	Open/Filled or Closed	Filled with	Remarks or Termination	Type
1	S63°E	64°SW	27	0.2	Open		One	Extension
2	S80°E	42°SW	12	0.3	Open		One	Conjugate
3	S86°E	44°SW	15	0.2	Open		One	Conjugate
4	NO5°E	38°SE	13	0	Closed		Both	Conjugate
5	S84°E	48°SW	27	0.5	Open		One	Conjugate
6	S78°E	49°SW	41	0.5	Open		One	Conjugate
7	S72°E	66°SW	50	0.2	Open		Continuous	Conjugate
8	S69°E	48°SW	47	0.2	Open		Continuous	Conjugate
9	S65°E	44°SW	32	0.3	Open		Continuous	Extension
10	N35°W	30°NE	50	03	Open		Continuous	Extension
11	N18°W	44°NE	15	0.1	Open		One	Extension
12	N17°W	43°NE	13	0.3	Open		One	Extension
13	N33°W	43°NE	13	0.2	Open		One	Extension
14	N13°W	39°NE	13	0.2	Open		One	Extension
15	N06°W	34°NE	07	0	Closed		One	Extension

Calculation;

A. Fracture Density $(\partial) = (\Sigma L)/\pi\, r^2$

   FD= 375/3.14 $(25)^2$

   FD=375/1962.5

   FD= 0.19 cm^1

   Open Fracture Density= 355/1962.5

   FD= 0.18 cm^1

B. Fracture Porosity % = $\left(\frac{1}{A}\right) \sum_{i=1}^{N} (Li \times Wi) \times 100$

   FP= (1/1962.5) (2325) x 100

   FP= 11.97%

C. Fracture Permeability (K) = $(3.5 \times 10^8)(\frac{1}{A}) \sum_{i=1}^{N} (Li \times Wi^3)$

   K= (3.5 $\times 10^8$) (1/1962.5) x 1338.12

   K= 238.64 $\times 10^6$

D. Maximum Stress Direction; N33°W

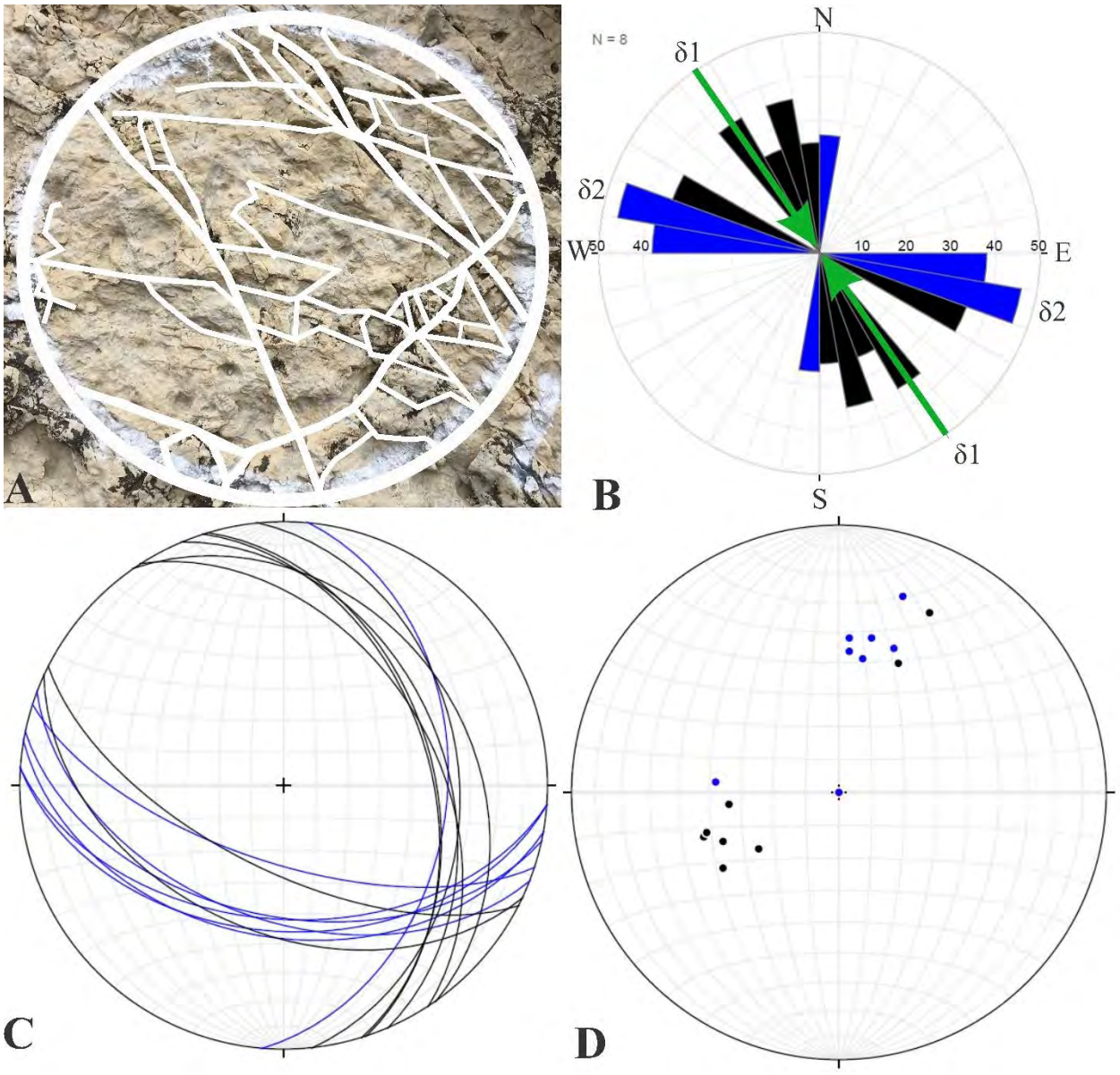

Figure 5. 7 (A) field photograph, (B) Rose diagram of fracture, (C) Plane data of fracture on Stereonet, (D) Poles data of fracture on Stereonet. Number of Conjugate Fractures (Blue color) are 07 and Extension Fractures (Black color) are 08.

5.13 Station NO; 08

Area; Western Salt Range

Location; Nammal Gorge

Altitude; 1001

GPS Location; 32°39'39"N, 071°47'56"E

Bed Strike; S83°W

Bed Dip; 55°NW

Bed Thickness; Massive Bed

Fracture Set; 03

Table 5. 8. Show fracture data of station 8.

S.NO	Strike	Dip	Length (CM)	Width (CM)	Open/Filled or Closed	Filled with	Remarks or Termination	Type
1	S53°E	65°SW	11	1.5	Open		Continuous	Conjugate
2	S57°E	74°SW	37	1.5	Open		Continuous	Conjugate
3	S70°E	85°SW	42	02	Open		Continuous	Release
4	S64°E	85 SW	46	02	Open		Continuous	Conjugate
5	S49°E	87°SW	48	1.5	Open		Continuous	Conjugate
6	S65°E	76°SW	10	01	Open		One	Conjugate
7	S63°E	63°SW	22	0.2	Open		Both	Conjugate
8	S76°E	57°SW	43	0.3	Open		One	Release
9	S55°E	69°SW	33	0.2	Open		One	Conjugate
10	S77°E	68°SW	17	0.2	Open		Both	Release
11	S76°E	70°SW	12	0.2	Open		One	Release
12	N05°E	42°SE	20	02	Open		One	Extension
13	N27°W	55°NE	08	0.1	Open		Both	Extension
14	N10°W	73°NE	11	0.1	Open		Both	Extension
15	N23°W	22°NE	48	01	Open		Continuous	Extension

Calculation;

A. Fracture Density $(\partial) = (\Sigma L)/\pi\, r^2$

   FD= 408/3.14 $(25)^2$

   FD= 408/1962.5

   FD= 0.20 cm^1 (As all fracture are open, therefore this is both the open and total fracture density)

B. Fracture Porosity % = $\left(\frac{1}{A}\right)\sum_{i=1}^{N}(Li \times Wi) \times 100$

   FP= (1/1962.5) (449.6) x 100

   FP= 22.91 %

C. Fracture Permeability (K) = $(3.5 \times 10^8)\left(\frac{1}{A}\right)\sum_{i=1}^{N}(Li \times Wi^3)$

   K= (3.5 $\times 10^8$) (1/1962.5) x 1247.37

   K= 222.46 $\times 10^6$

D. Maximum Stress Direction; N14ºW

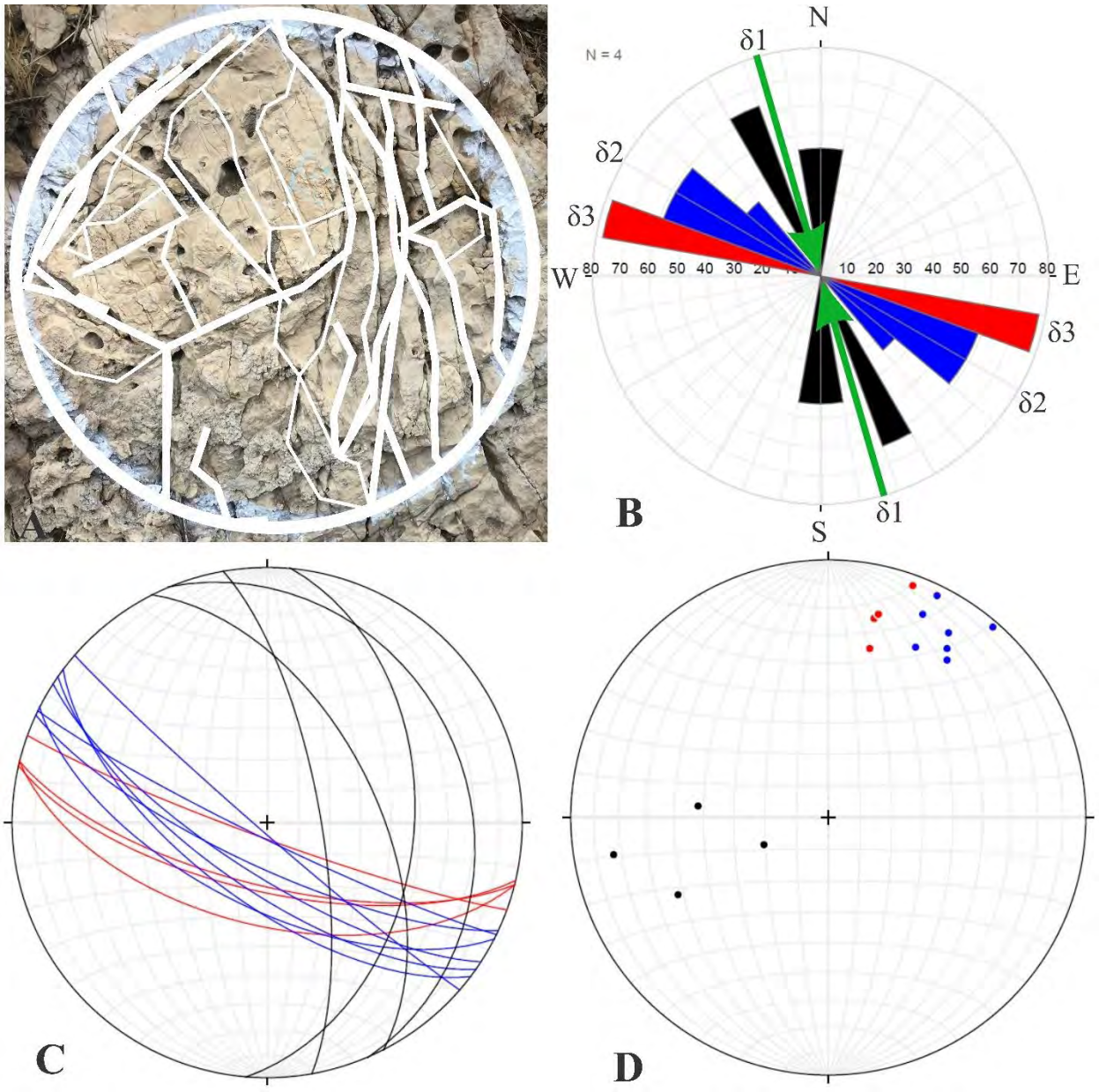

Figure 5. 8 (A) field photograph, (B) Rose diagram of fracture, (C) Plane data of fracture on Stereonet, (D) Poles data of fracture on Stereonet. Number of Release Fractures (Red color) are 04, Conjugate Fractures (Blue color) are 06 whereas Extension Fractures (Black color) are 05.

5.14 Station NO; 09

Area; Western Salt Range

Location; Nammal Gorge

Altitude; 1001

GPS Location; 32° 39'341"N, 071°47'52"E

Bed Strike; S73°W

Bed Dip; 49°NW

Bed Thickness; Massive Bed

Fracture Set; 04

Table 5. 9. Show fracture data of station 9.

S.NO	Strike	Dip	Length (CM)	Width (CM)	Open/Filled or Closed	Filled with	Remarks or Termination	Type
1	N24°W	33°NE	32	0.1	Open		Continuous	Extension
2	N15°W	50°NE	10	0.2	Open		Both	Extension
3	S27°W	63°NW	50	0.5	Filled	Calcite	Continuous	Conjugate
4	S16°W	47°NW	12	0.2	Open		One	Conjugate
5	S26°W	67°NW	35	1.5	Filled	Calcite	Continuous	Conjugate
6	S72°E	42°SW	31	0.2	Open		Continuous	Conjugate
7	N17°W	28°NE	38	0.2	Open		Continuous	Extension
8	N09°W	37°NE	17	0.1	Open		Both	Extension
9	N18°W	23°NE	16	0.1	Open		One	Extension
10	N18°W	27°NE	15	0.3	Open		One	Extension
11	N38°E	09°SE	50	0.5	Filled	Calcite	Continuous	Conjugate
12	S47°W	50°NW	10	0.1	Open		One	Extension
13	S88°E	18°SW	12	0.1	Open		One	Release
14	N10°W	22°NE	23	0.2	Open		One	Extension
15	S65°E	44°SW	33	0.1	Open		One	Conjugate
16	S48°E	52°SW	10	0.1	Open		One	Conjugate
17	S82°E	19°SW	15	0.1	Open		One	Release

Calculation;

A. Fracture Density $(\partial) = (\Sigma L)/\pi\, r^2$

   FD= 409/3.14 $(25)^2$

   FD= 409/1962.5

   FD= 0.20 cm^1

   Open Fracture Density= 274/1962.5

   FD= 0.13cm^1

B. Fracture Porosity % = $\left(\frac{1}{A}\right) \sum_{i=1}^{N} (Li \times Wi) \times 100$

   FP= (1/1962.5) (144.3) x 100

   FP= 7.35 %

C. Fracture Permeability (K) = $(3.5 \times 10^8)\left(\frac{1}{A}\right) \sum_{i=1}^{N} (Li \times Wi^3)$

   K= (3.5 $\times 10^8$) (1/1962.5)

   K= 40.62 $\times 10^6$ Darcy

D. Maximum Stress Direction; N13°W

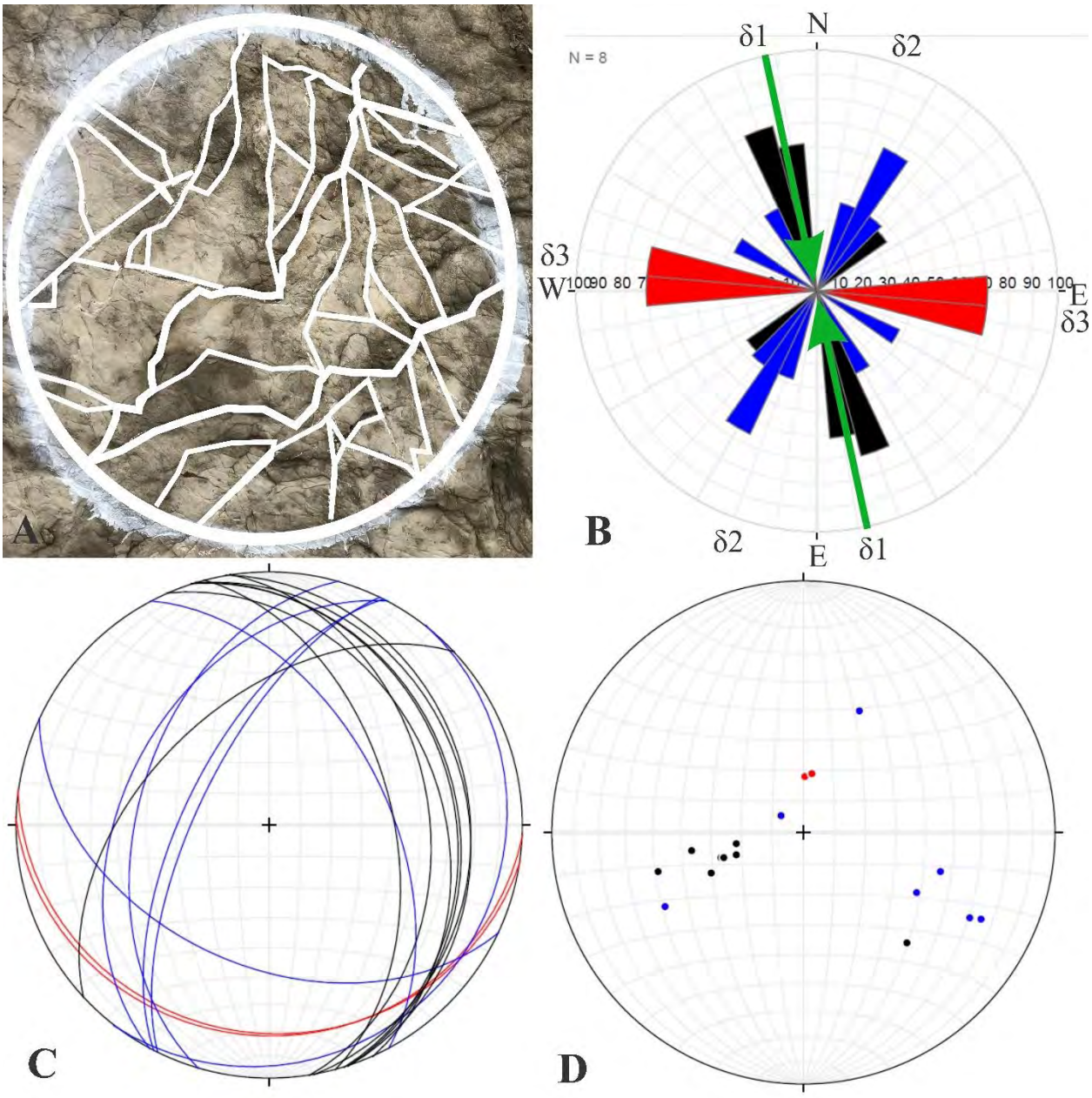

Figure 5. 9 (A) field photograph, (B) Rose diagram of fracture, (C) Plane data of fracture on Stereonet, (D) Poles data of fracture on Stereonet. Number of Release Fractures (Red color) are 02, Conjugate Fractures (Blue color) are 07 whereas Extension Fractures (Black color) are 08.

5.15 Station NO; 10

Area; Western Salt Range

Location; Nammal gorge

Altitude; 1002

GPS Location; 32°39'52"N, 071°47'61"E

Bed Strike; S76°W

Bed Dip; 53°NW

Bed Thickness; Massive Bed Fracture Set; 04

Table 5. 10. Show fracture data of station 10.

S.NO	Strike	Dip	Length (CM)	Width (CM)	Open/Filled or Closed	Filled with	Remarks or Termination	Type
1	S62°E	38°SW	31	02	Filled	Calcite	Continuous	Conjugate
2	S45°E	68°SW	29	0.1	Open		One	Extension
3	S52°E	57°SW	33	0.1	Open		One	Conjugate
4	N10°W	39°NE	17	0.1	Open		One	Extension
5	S01°W	59°NW	32	0.1	Open		One	Extension
6	S37°W	68°NW	21	0.1	Open		One	Conjugate
7	S14°W	35°NW	20	0.1	Open		Both	Extension
8	S68°E	37°SW	39	0.1	Open		Continuous	Conjugate
9	S75°E	58°SW	24	0.1	Open		One	Release
10	N14°E	28°SE	41	0.2	Open		Continuous	Extension
11	N70°E	13°SE	37	0.5	Open		One	Release
12	N76°W	20°NE	50	0.5	Open		Continuous	Release
13	N42°E	18°SE	26	0.1	Open		One	Conjugate
14	N25°E	23°SE	21	0.1	Open		One	Conjugate
15	S25°W	47°NW	10	0.5	Open		One	Conjugate

Calculation;

A. Fracture Density $(\partial) = (\Sigma L)/\pi\, r^2$

   FD= 431/3.14 $(25)^2$

   FD= 431/1962.5

   FD= 0.21 cm^1

   Open Fracture Density= 400/1962.5

   FD= 0.20 cm^1

B. Fracture Porosity % = $\left(\frac{1}{A}\right) \sum_{i=1}^{N} (Li \times Wi) \times 100$

   FP= (1/1962.5) (144.9) x 100

   FP= 7.38 %

C. Fracture Permeability (K) = $(3.5 \times 10^8)(\frac{1}{A}) \sum_{i=1}^{N} (Li \times Wi^3)$

   K= (3.5×10^8) (1/1962.5) x 260.71

   K= 46.49 $\times 10^6$

D. Maximum Stress Direction; N03°W

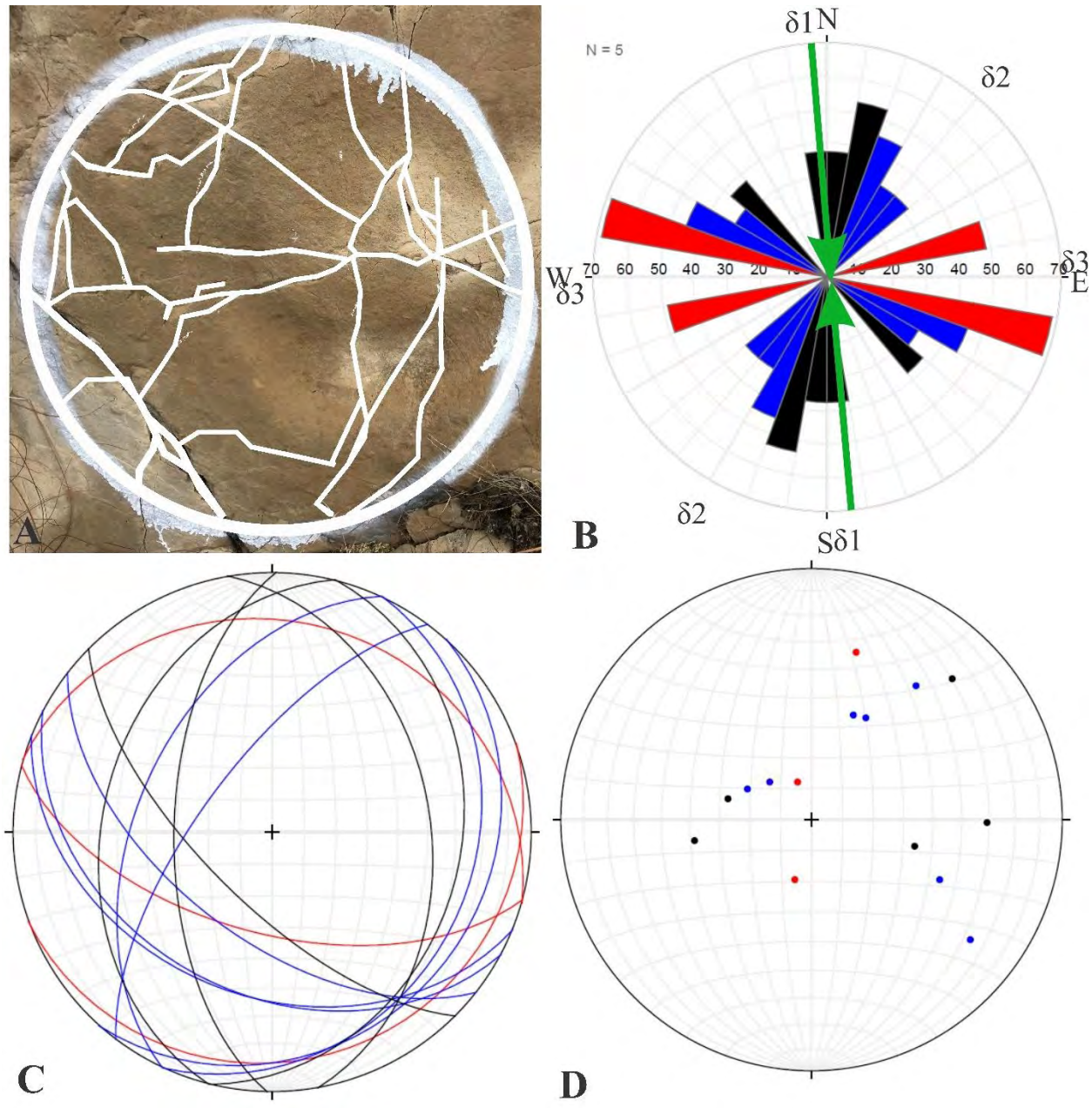

Figure 5. 10 (A) field photograph, (B) Rose diagram of fracture, (C) Plane data of fracture on Stereonet, (D) Poles data of fracture on Stereonet. Number of Release Fractures (Red color) are 03, Conjugate Fractures (Blue color) are 07 whereas Extension Fractures (Black color) are 05.

ZALUCH NALA SECTION

5.16 Station NO; 01

Area; Western Salt Range Location; Zaluch Nala

Altitude; 1188 GPS Location;32°47'19.98"N, 71°39'02.11"E

Bed Strike; S66°W Bed Dip; 70°NW

Bed Thickness; Massive Bed Fracture Set; 03

Table 5. 11. Show fracture data of station 11.

S.NO	Strike	Dip	Length (CM)	Width (CM)	Open/Filled or Closed	Filled with	Remarks or Termination	Type
1	N19°W	13°NE	38	0.5	Open		Continuous	Extension
2	N31°W	17°NE	36	0.3	Open		One	Extension
3	S10°W	07°NW	50	02	Open		Continuous	Conjugate
4	S20°W	03°NW	09	0.1	Open		Both	Conjugate
5	S66°E	75°SW	24	1.5	Open		One	Conjugate
6	N52°W	71°NE	12	0.2	Open		One	Extension
7	N42°W	80°NE	13	0.2	Open		One	Extension
8	N51°W	79°NE	08	0.1	Open		Both	Extension
9	N49°W	82°NE	50	0.7	Open		Continuous	Extension
10	N46°W	85°NE	07	0.2	Open		Both	Extension
11	N62°W	77°NE	49	0.5	Open		Continuous	Conjugate
12	N18°W	32°NE	11	0.2	Open		One	Extension
13	S47°E	89°SW	17	0.1	Open		Both	Extension
14	N44°W	76°NE	27	0.5	Open		One	Extension
15	S41°E	55°SW	17	0.4	Open		One	Extension
16	S49°E	78°SW	24	0.5	Open		One	Extension
17	S48°E	56°SW	23	0.5	Open		One	Extension
18	N53°W	81°NE	31	0.5	Open		One	Extension
19	S60°E	11°SW	07	0.2	Open		Both	Conjugate
20	S59°E	57°SW	36	0.5	Open		Continuous	Conjugate

Calculation;

A. Fracture Density $(\partial) = (\Sigma L)/\pi\, r^2$

FD= 489/3.14 $(25)^2$

FD= 489/1962.5

FD= 0.249 cm^1 (As all fracture are open, therefore this is both the open and total fracture density)

B. Fracture Porosity % = $\left(\frac{1}{A}\right) \sum_{i=1}^{N} (Li \times Wi) \times 100$

FP= (1/1962.5) (316) x 100

FP= 16.10 %

C. Fracture Permeability (K) = $(3.5 \times 10^8)(\frac{1}{A}) \sum_{i=1}^{N}(Li \times Wi^3)$

K= (3.5×10^8) (1/1962.5) x 529.02

K= 94.34 $\times 10^6$

D. Maximum Stress Direction; N27°W

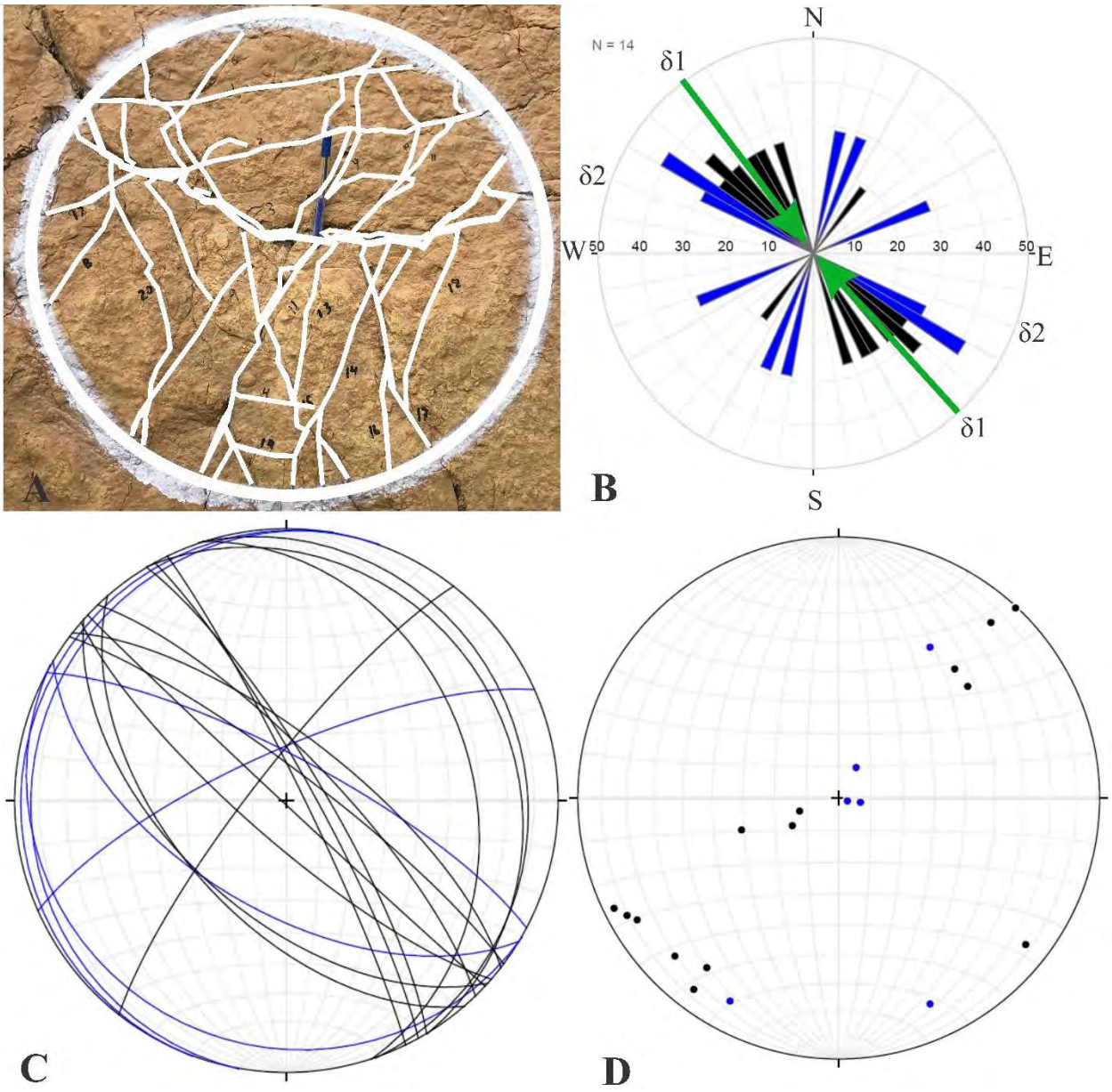

Figure 5. 11 (A) field photograph, (B) Rose diagram of fracture, (C) Plane data of fracture on Stereonet, (D) Poles data of fracture on Stereonet. Number of Conjugate Fractures (Blue color) are 06 and Extension Fractures (Black color) are 14.

5.17 Station NO; 02

Area; Western Salt Range Location; Zaluch Nala

Altitude; 1197 GPS Location; 32°47'20.25"N, 71°39'02.9"E

Bed Strike; S76°W Bed Dip; 87°NW

Bed Thickness; Massive Bed Fracture Set; 04

Table 5. 12. Show fracture data of station 12.

S.NO	Strike	Dip	Length (CM)	Width (CM)	Open/Filled or Closed	Filled with	Remarks or Termination	Type
1	N25°W	08°NE	15	0.3	Open		One	Conjugate
2	N40°E	15°SE	24	0.5	Open		One	Conjugate
3	S65°E	62°SW	50	01	Open		Continuous	Conjugate
4	S65°E	46°SW	08	0.5	Open		One	Conjugate
5	N42°W	27°NE	07	0.5	Open		One	Extension
6	N32°W	77°NE	16	0.6	Open		One	Extension
7	S57°E	75°SW	30	0.2	Open		One	Conjugate
8	N42°W	84°NE	28	0.5	Open		One	Extension
9	S45°E	89°SW	27	0.4	Open		One	Extension
10	N05°E	19°SE	06	0.5	Open		Both	Extension
11	S69°E	15°SW	39	01	Open		One	Release
12	N90°E	12°SE	17	0.4	Open		One	Release
13	S62°E	72°SW	33	0.5	Open		Continuous	Conjugate
14	N86°E	11°SE	07	0.7	Open		One	Release
15	N39°W	84°NE	24	0.6	Open		One	Extension
16	S66°E	47°SW	24	0.5	Open		One	Conjugate
17	N21°W	16°NE	29	0.5	Open		One	Extension
18	N43°W	26°NE	15	0.4	Open		One	Extension
19	N30°W	22°NE	19	0.5	Open		Both	Extension

Calculation;

A. Fracture Density $(\partial) = (\Sigma L)/\pi\, r^2$

   FD= 418/3.14 $(25)^2$

   FD= 418/1962.5

   FD= 0.212 cm^1 (As all fracture are open, therefore this is both the open and total fracture density)

B. Fracture Porosity % = $\left(\frac{1}{A}\right) \sum_{i=1}^{N} (Li \times Wi) \times 100$

   FP= (1/1962.5) (241) x 100

   FP= 12.28 %

C. Fracture Permeability (K) = $(3.5 \times 10^8)(\frac{1}{A}) \sum_{i=1}^{N}(Li \times Wi^3)$

K= (3.5×10^8) (1/1962.5) x 126.71

K= 22.59 $\times 10^6$

D. Maximum Stress Direction; N24°W

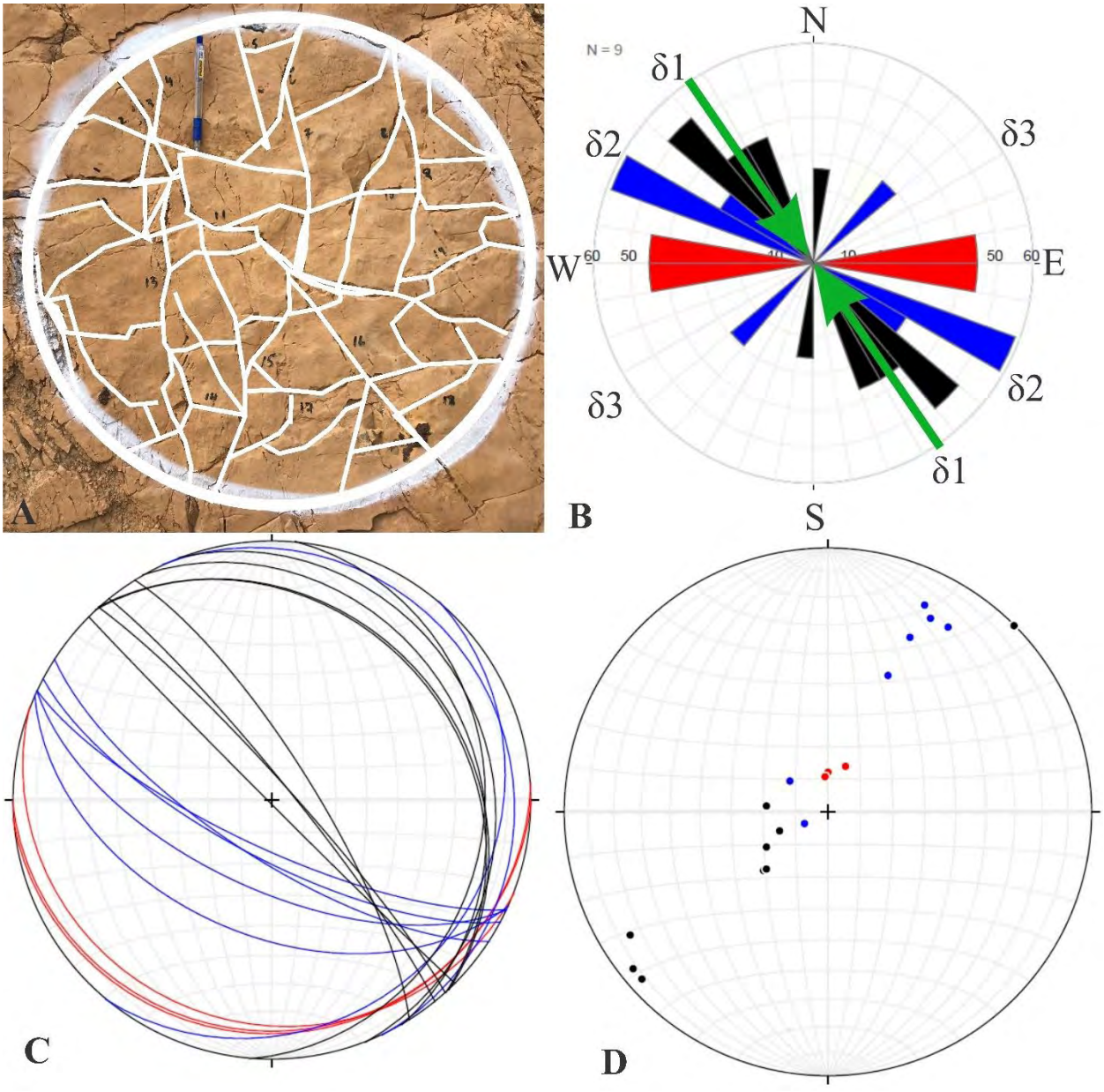

Figure 5. 12 (A) field photograph, (B) Rose diagram of fracture, (C) Plane data of fracture on Stereonet, (D) Poles data of fracture on Stereonet. Number of Release Fractures (Red color) are 03, Conjugate Fractures (Blue color) are 07 whereas Extension Fractures (Black color) are 09.

5.18 Station NO; 03

Area; Western Salt Range

Location; Zaluch Nala

Altitude; 1230

GPS Location; 32°47'19.82"N, 71°39'01.40"E

Bed Strike; S76°W

Bed Dip; 63°NW

Bed Thickness; Massive Bed

Fracture Set; 02

Table 5. 13. Show fracture data of station 13.

S.NO	Strike	Dip	Length (CM)	Width (CM)	Open/Filled or Closed	Filled with	Remarks or Termination	Type
1	S04°W	08°NW	33	0.7	Open		Continuous	Extension
2	N01°W	09°NE	39	0.6	Open		Continuous	Extension
3	S09°W	08°NW	31	0.5	Open		One	Extension
4	N51°W	11°NE	50	0.9	Open		Continuous	Conjugate
5	N66°W	10°NE	37	01	Open		Continuous	Conjugate
6	S58°E	72°SW	20	0.2	Open		Both	Conjugate
7	S53°E	88°SW	29	01	Open		One	Conjugate
8	S72°E	70°SW	28	1.5	Open		One	Conjugate
9	S67°E	70°SW	08	1.5	Open		One	Conjugate
10	S73°E	65°SW	26	0.2	Open		One	Conjugate
11	N23°W	84°NE	40	01	Open		Continuous	Extension
12	S65°E	74°SW	05	0.6	Open		One	Conjugate
13	N20°W	14°NE	05	0	Closed		One	Extension
14	S61°E	70°SW	06	0.7	Open		Both	Conjugate
15	S69°E	57°SW	12	0	Closed		Both	Conjugate
16	S52°E	75°SW	05	0.2	Open		Both	Conjugate

Calculation;

A. Fracture Density $(\partial) = (\Sigma L)/\pi\, r^2$

   FD= 374/3.14 $(25)^2$

   FD= 374/1962.5

   FD= 0.190 cm^1

   Open Fracture Density= 357/1962.5

   FD= 0.181

B. Fracture Porosity % = $\left(\frac{1}{A}\right)\sum_{i=1}^{N}(Li \times Wi) \times 100$

   FP= (1/1962.5) (284.4) x 100

   FP= 14.49 %

C. Fracture Permeability (K) = $(3.5 \times 10^8)\left(\frac{1}{A}\right)\sum_{i=1}^{N}(Li \times Wi^3)$

K= (3.5 ×10^8) (1/1962.5) x 268.75

K= 47.92 ×10^6 Darcy

D. Maximum Stress Direction; N07ºW

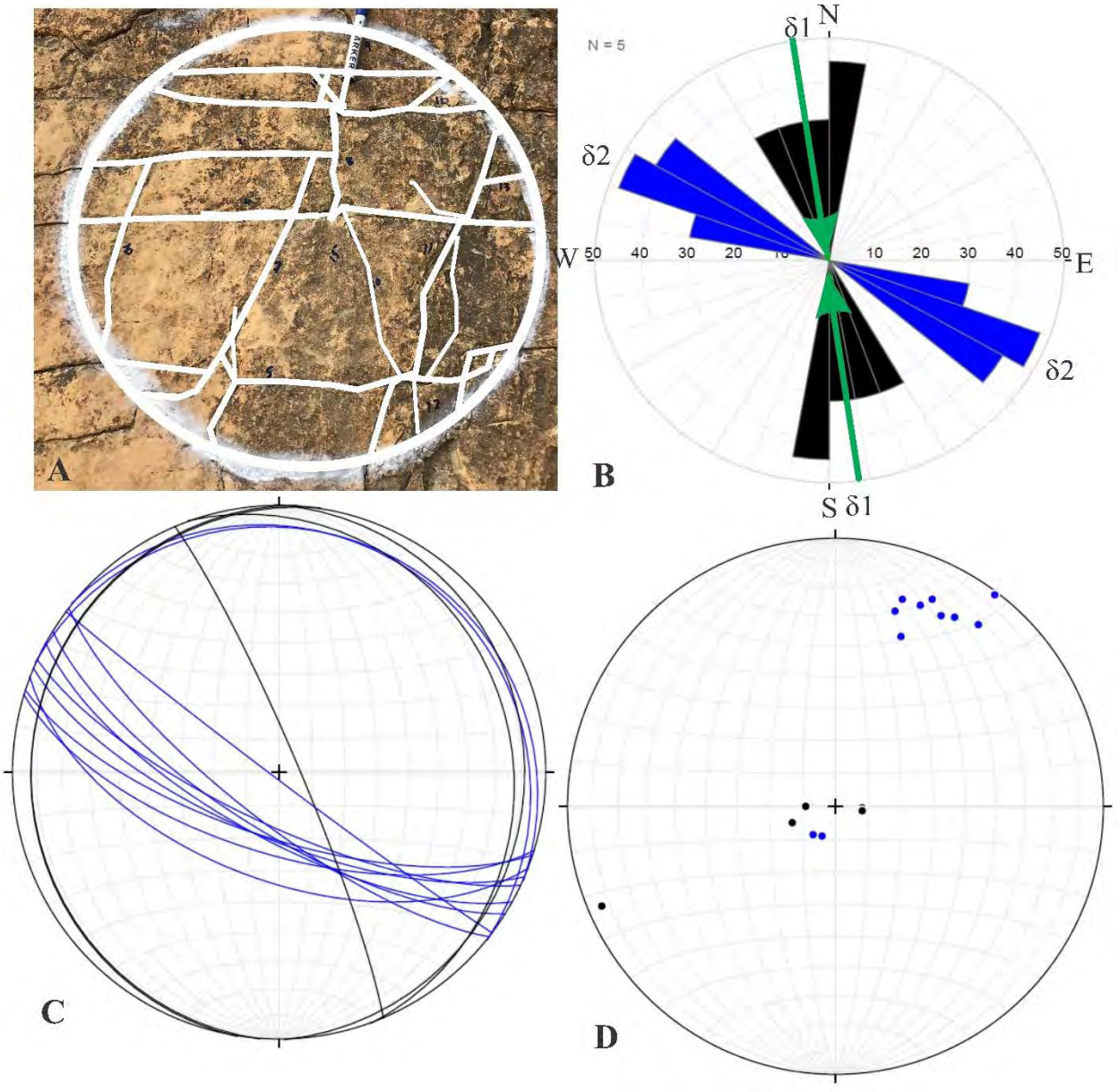

Figure 5. 13 (A) field photograph, (B) Rose diagram of fracture, (C) Plane data of fracture on Stereonet, (D) Poles data of fracture on Stereonet. Number of Conjugate Fractures (Blue color) are 11 and Extension Fractures (Black color) are 05.

5.19 Station NO; 04

Area; Western Salt Range

Location; Zaluch Nala

Altitude; 1272

GPS Location; 32°47'25.80"N, 71°39'03.23"E

Bed Strike; S79°W

Bed Dip; 54°NW

Bed Thickness; Massive Bed

Fracture Set; 04

Table 5. 14. Show fracture data of station 14.

S.NO	Strike	Dip	Length (CM)	Width (CM)	Open/Filled or Closed	Filled with	Remarks or Termination	Type
1	S76°E	56°SW	07	0.1	Open		One	Conjugate
2	N42°W	79°NE	20	0.5	Open		One	Release
3	S71°E	69°SW	28	0.3	Open		One	Conjugate
4	S59°E	29°SW	10	0.3	Open		One	Conjugate
5	S78°E	17°SW	18	0.2	Open		Continuous	Conjugate
6	N34°W	18°NE	22	0.3	Open		One	Extension
7	S40°W	05°NW	10	0.5	Open		Both	Extension
8	N14°E	05°SE	30	1.5	Open		One	Conjugate
9	N02°W	56°NE	24	0.3	Open		One	Extension
10	N05°W	55°NE	12	0	Closed		One	Extension
11	N05°W	43°NE	08	0	Closed		One	Extension
12	S73°E	40°SW	08	0.2	Open		Both	Conjugate
13	N32°E	05°SE	50	0.5	Open		Continuous	Conjugate
14	S55°W	29°NW	06	0.5	Open		Both	Release
15	N11°W	49°NE	16	01	Open		One	Extension
16	N09°W	44°NE	11	0.8	Open		Both	Extension
17	S76°E	51°SW	09	0	Closed		One	Conjugate
18	S69°E	76°SW	45	0.2	Open		Both	Conjugate
19	S33°W	06°NW	45	0.8	Open		Continuous	Conjugate
20	S53°E	04°SW	36	0.6	Open		Continuous	Conjugate
21	N02°W	46°NE	12	0.4	Open		Both	Extension
22	S86°E	57°SW	06	0.3	Open		One	Release

Calculation;

A. Fracture Density $(\partial) = (\Sigma L)/\pi\, r^2$

FD= 433/3.14 $(25)^2$

FD= 433/1962.5

FD= 0.220 cm^1

Open Fracture Density= 404/1962.5

FD= 0.20 cm^1

B. Fracture Porosity % = $\left(\frac{1}{A}\right) \sum_{i=1}^{N} (Li \times Wi) \times 100$

FP= (1/1962.5) (217.1) x 100

FP= 11.06 %

C. Fracture Permeability (K) = $(3.5 \times 10^8)(\frac{1}{A}) \sum_{i=1}^{N} (Li \times Wi^3)$

K= (3.5 $\times 10^8$) (1/1962.5) x 162.67

K= 29.02 $\times 10^6$ Darcy

D. Maximum Stress Direction; N05ºW

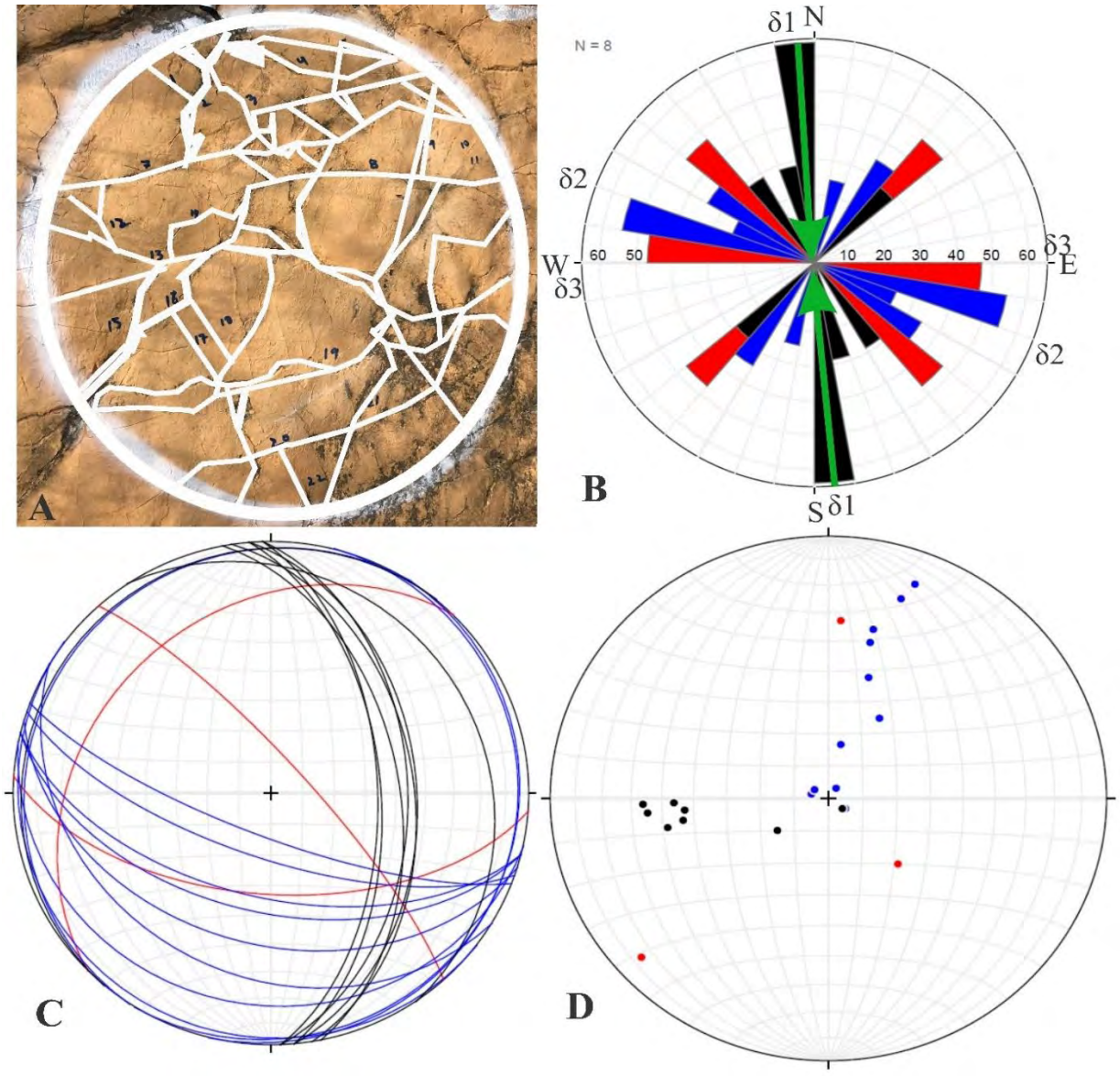

Figure 5. 14 (A) field photograph, (B) Rose diagram of fracture, (C) Plane data of fracture on Stereonet, (D) Poles data of fracture on Stereonet. Number of Release Fractures (Red color) are 03, Conjugate Fractures (Blue color) are 11 whereas Extension Fractures (Black color) are 08.

5.20 Station NO; 05

Area; Western Salt Range Location; Zaluch Nala

Altitude; 1269 GPS Location; 32°47'25.39"N, 71°39'03.50"E

Bed Strike; S80°W Bed Dip; 65°NW

Bed Thickness; Massive Bed Fracture Set; 04

Table 5. 15. Show fracture data of station 15.

S.NO	Strike	Dip	Length (CM)	Width (CM)	Open/Filled or Closed	Filled with	Remarks or Termination	Type
1	N39°E	13°SE	37	02	Open		Continuous	Conjugate
2	N76°E	06°SE	41	1.5	Open		One	Release
3	S15°W	08°NW	37	1.5	Open		One	Extension
4	N35°E	20°SE	16	00	Closed		Both	Conjugate
5	N15°W	54°NE	43	0.3	Open		Continuous	Extension
6	N23°W	50°NE	35	0.1	Open		Both	Extension
7	N05°W	56°NE	49	0.5	Open		Continuous	Extension
8	S03°W	54°NW	38	02	Open		Continuous	Extension
9	N83°E	07°SE	10	02	Open		One	Release
10	S25°W	69°NW	12	0.5	Open		One	Conjugate
11	S70°E	27°SW	30	0.2	Open		One	Conjugate
12	N04°E	24°SE	21	0.5	Open		Both	Extension
13	S80°E	37°SW	13	0.1	Open		Both	Release
14	S69°E[2]	58°SW	11	0.3	Open		Both	Conjugate
15	S79°E	65°SW	12	0.3	Open		Both	Release
16	S75°E	77°SW	09	0.5	Open		One	Release
17	S60°E	54°SW	15	00	Closed		One	Conjugate

Calculation;

A. Fracture Density $(\partial) = (\Sigma L)/\pi\, r^2$

FD= 429/3.14 $(25)^2$

FD= 429/1962.5

FD= 0.218 cm^1

Open Fracture Density= 398/1962.5

FD= 0.20 cm^1

B. Fracture Porosity % = $\left(\frac{1}{A}\right)\sum_{i=1}^{N}(Li \times Wi) \times 100$

FP= (1/1962.5) (363.1) x 100

FP= 18.06 %

C. Fracture Permeability (K) = $(3.5 \times 10^8)(\frac{1}{A})\sum_{i=1}^{N}(Li \times Wi^3)$

K= (3.5 ×10^8) (1/1962.5) x 957.127

K= 170.69 ×10^6 Darcy

D. Maximum Stress Direction; N04ºW

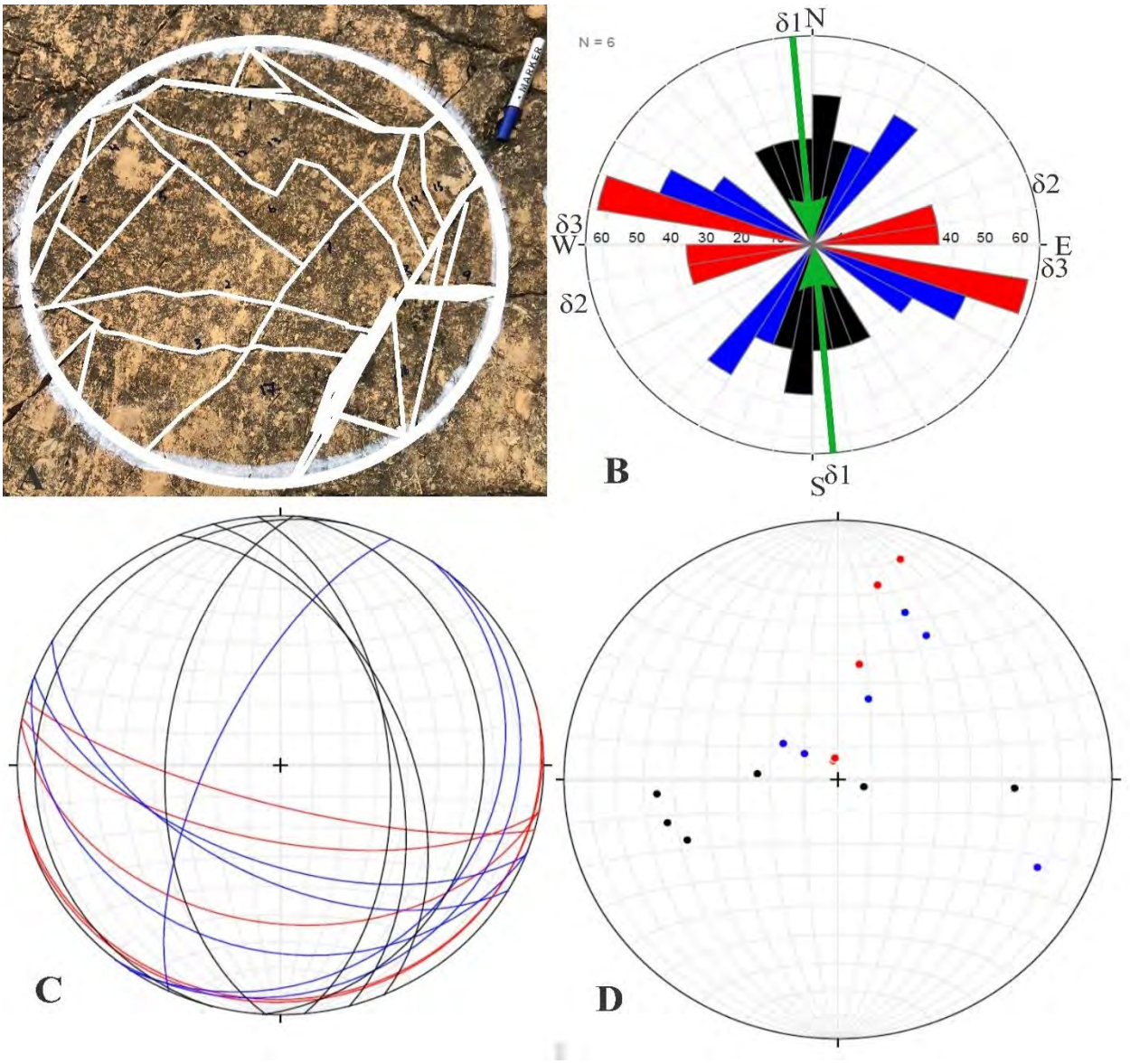

Figure 5. 15 (A) field photograph, (B) Rose diagram of fracture, (C) Plane data of fracture on Stereonet, (D) Poles data of fracture on Stereonet. Number of Release Fractures (Red color) are 05, Conjugate Fractures (Blue color) are 06 whereas Extension Fractures (Black color) are 06.

5.21 Station NO; 06

Area; Western Salt Range Location; Zaluch Nala

Altitude; 1261 GPS Location; 32°47'25.11"N, 71°39'03.58"E

Bed Strike; N69°E Bed Dip; 68°SE

Bed Thickness; Massive Bed Fracture Set; 04

Table 5. 16. Show fracture data of station 16.

S.NO	Strike	Dip	Length (CM)	Width (CM)	Open/Filled or Closed	Filled with	Remarks or Termination	Type
1	N37°W	56°NE	19	1.5	Open		One	Extension
2	N28°W	66°NE	25	02	Open		One	Extension
3	S52°E	89°SW	07	1.5	Open		One	Conjugate
4	S37°E	78°SW	07	00	Closed		One	Extension
5	N44°W	74°NE	16	0.1	Open		One	Extension
6	N47°W	74°NE	40	2.5	Open		Continuous	Extension
7	N57°W	75°NE	11	02	Open		One	Conjugate
8	S88°E	45°SW	10	0.5	Open		One	Release
9	S85°E	48°SW	15	0.2	Open		One	Release
10	N02°E	59°SE	21	01	Open		One	Extension
11	N03°E	57°SE	30	0.8	Open		One	Extension
12	N76°W	05°NE	07	0.3	Open		Both	Conjugate
13	N43°W	64°NE	33	01	Open		One	Extension
14	N38°W	24°NE	27	0.2	Open		One	Extension
15	N47°W	65°NE	20	0.2	Open		One	Extension
16	N38°W	55°NE	15	00	Closed		One	Extension
17	N07°W	05°NE	51	01	Open		Continuous	Extension
18	N07°W	43°NE	41	0.3	Open		One	Extension
19	N40°W	08°NE	17	0.2	Open		Continuous	Extension
20	S83°E	64°SW	10	0.1	Closed		Continuous	Release
21	S83°E	56°SW	15	0.1	Open		Both	Release
22	S83°E	56°SW	15	0.1	Open		Both	Release
23	N03°W	35°NE	28	0.2	Open		Both	Extension
24	N20°E	36°SE	12	0.5	Open		Both	Conjugate

Calculation;

A. Fracture Density $(\partial) = (\Sigma L)/\pi\, r^2$

   FD= 492/3.14 $(25)^2$

   FD= 492/1962.5

   FD= 0.250 cm^1

   Open Fracture Density= 360/1962.5

   FD= 0.234 cm^1

B. Fracture Porosity % = $\left(\frac{1}{A}\right) \sum_{i=1}^{N} (Li \times Wi) \times 100$

   FP= (1/1962.5) (392.4) x 100

   FP= 19.99 %

C. Fracture Permeability (K) = $(3.5 \times 10^8)(\frac{1}{A}) \sum_{i=1}^{N}(Li \times Wi^3)$

K= (3.5×10^8) (1/1962.5) x 1066.193

K= 190.14 $\times 10^6$ Darcy

D. Maximum Stress Direction; N29ºW

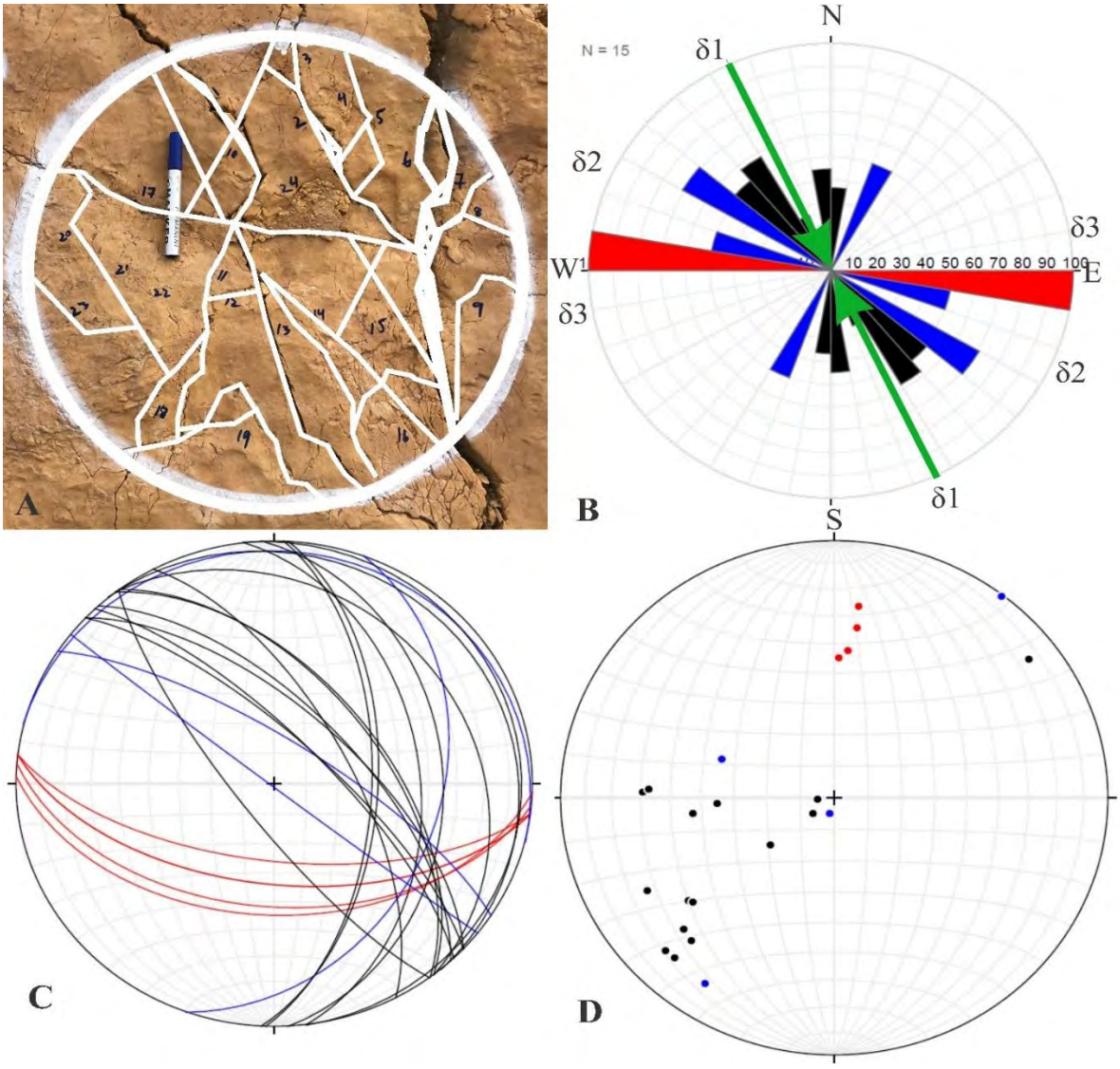

Figure 5. 16 (A) field photograph, (B) Rose diagram of fracture, (C) Plane data of fracture on Stereonet, (D) Poles data of fracture on Stereonet. Number of Release Fractures (Red color) are 05, Conjugate Fractures (Blue color) are 04 whereas Extension Fractures (Black color) are 15.

5.22 Station NO; 07

Area; Western Salt Range Location; Zaluch Nala

Altitude; 1173 GPS Location; 32°47'21.49"N, 71°39'07.56"E

Bed Strike; N58°E Bed Dip; 72°SE

Bed Thickness; Massive Bed Fracture Set; 04

Table 5. 17. Show fracture data of station 17.

S.NO	Strike	Dip	Length (CM)	Width (CM)	Open/Filled or Closed	Filled with	Remarks or Termination	Type
1	S04°W	06°NW	17	02	Open		One	Conjugate
2	N17°W	46°NE	49	02	Open		Continuous	Extension
3	S34°E	59°SW	32	0.8	Open		Continuous	Extension
4	S22°E	06°SW	36	01	Open		Continuous	Extension
5	S59°W	08°NW	25	0.2	Open		Continuous	Release
6	N78°W	72°NE	30	0.3	Open		Continuous	Conjugate
7	N35°W	72°NE	17	0.2	Open		One	Extension
8	N32°W	76°NE	08	0.2	Open		One	Extension
9	N32°W	66°NE	19	0.2	Open		One	Extension
10	N31°W	61°NE	09	0.2	Open		One	Extension
11	S60°W	36°NW	18	0.3	Open		One	Extension
12	N26°W	54°NE	20	0.2	Open		Both	Extension
13	S05°W	05°NW	17	0.3	Open		Both	Conjugate
14	N44°W	83°NE	10	0.2	Open		Both	Extension
15	S74°E	45°SW	27	0.7	Open		Both	Conjugate
16	N23W	43°NE	27	0.5	Open		Both	Extension
17	S67°W	57°NW	20	0.2	Open		Both	Release
18	N20°W	56°NE	31	0.2	Open		One	Extension
19	N20°W	64°NE	29	0.1	Open		Both	Extension
20	S58°E	10°SW	11	0.5	Open		One	Extension
21	N36°W	64°NE	23	0.2	Open		Continuous	Extension
22	N33°W	48°NE	18	0.8	Open		Continuous	Extension
23	N19°W	53°NE	41	01	Open		Continuous	Extension

Calculation;

A. Fracture Density $(\partial) = (\Sigma L)/\pi\, r^2$

FD= 534/3.14 $(25)^2$

FD= 534/1962.5

FD= 0.272 cm^1 (As all fracture are open, therefore this is both the open and total fracture density)

B. Fracture Porosity % = $\left(\frac{1}{A}\right)\sum_{i=1}^{N}(Li \times Wi) \times 100$

FP= (1/1962.5) (345.7) x 100

FP= 17.61 %

C. Fracture Permeability (K) = $(3.5 \times 10^8)\left(\frac{1}{A}\right)\sum_{i=1}^{N}(Li \times Wi^3)$

K= (3.5×10^8) (1/1962.5) x 647.851

K= 115.54 ×10^6 Darcy

D. Maximum Stress Direction; N29ºW

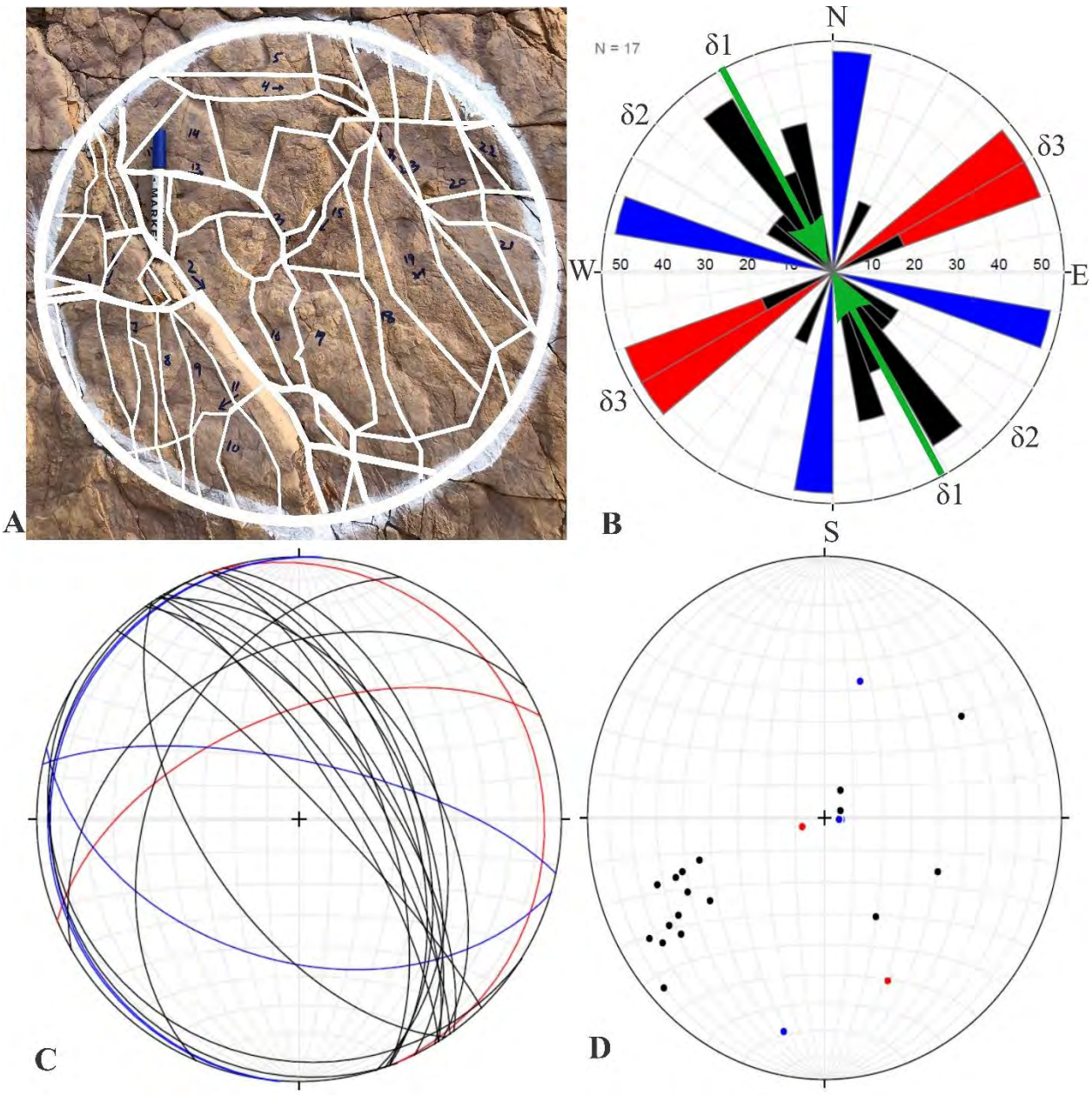

Figure 5. 17 (A) field photograph, (B) Rose diagram of fracture, (C) Plane data of fracture on Stereonet, (D) Poles data of fracture on Stereonet. Number of Release Fractures (Red color) are 02, Conjugate Fractures (Blue color) are 04 whereas Extension Fractures (Black color) are 17.

5.23 Station NO; 08

Area; Western Salt Range

Location; Zaluch Nala

Altitude; 1184

GPS Location; 32°47'21.36"N, 71°39'08.18"E

Bed Strike; N83°E Bed Dip; 65°SE

Bed Thickness; Massive Bed Fracture Set; 03

Table 5. 18. Show fracture data of station 18.

S.NO	Strike	Dip	Length (CM)	Width (CM)	Open/Filled or Closed	Filled with	Remarks or Termination	Type
1	N15°E	43°SE	17	0.5	Open		One	Extension
2	N42°W	03°NE	12	0.2	Open		One	Conjugate
3	N32°W	18°NE	08	0.7	Open		One	Extension
4	N04°W	47°NE	50	1.5	Open		Continuous	Extension
5	S22°W	10°NW	14	0.3	Open		Both	Extension
6	N18°E	38°SE	18	0.2	Open		One	Extension
7	S23°W	21°NW	14	01	Open		Continuous	Extension
8	N01°W	56°NE	24	0.5	Open		One	Extension
9	S04°W	37°NW	11	00	Closed		One	Extension
10	S16°W	43°NW	13	0.1	Filled	Calcite	One	Extension
11	S13°W	50°NW	11	0.2	Open		Both	Extension
12	N14°E	49°SE	22	1.5	Open		One	Extension
13	N07°W	62°NE	06	0.7	Open		Both	Extension
14	S87°E	45°SW	50	2.5	Open		Continuous	Release
15	S50°E	04°SW	10	1.5	Open		One	Conjugate
16	N02°E	28°SE	17	0.8	Open		One	Extension
17	N16°W	55°NE	23	0.3	Open		One	Extension
18	N16°W	60°NE	14	0.3	Open		One	Extension
19	N02°W	48°NE	11	0.2	Open		One	Extension
20	S09°W	53°NW	21	0.1	Filled	Calcite	Both	Extension

Calculation;

A. Fracture Density $(\partial) = (\Sigma L)/\pi\, r^2$

FD= 366/3.14 $(25)^2$

FD= 366/1962.5

FD= 0.186 cm^1

Open Fracture Density= 360/1962.5

FD= 0.163 cm^1

B. Fracture Porosity % = $\left(\frac{1}{A}\right) \sum_{i=1}^{N} (Li \times Wi) \times 100$

FP= (1/1962.5) (335) x 100

FP= 17.07 %

C. Fracture Permeability (K) = $(3.5 \times 10^8)\left(\frac{1}{A}\right) \sum_{i=1}^{N} (Li \times Wi^3)$

K= (3.5×10^8) (1/1962.5) x 1092.458

K= 194.83 $\times 10^6$ Darcy

D. Maximum Stress Direction; N03ºE

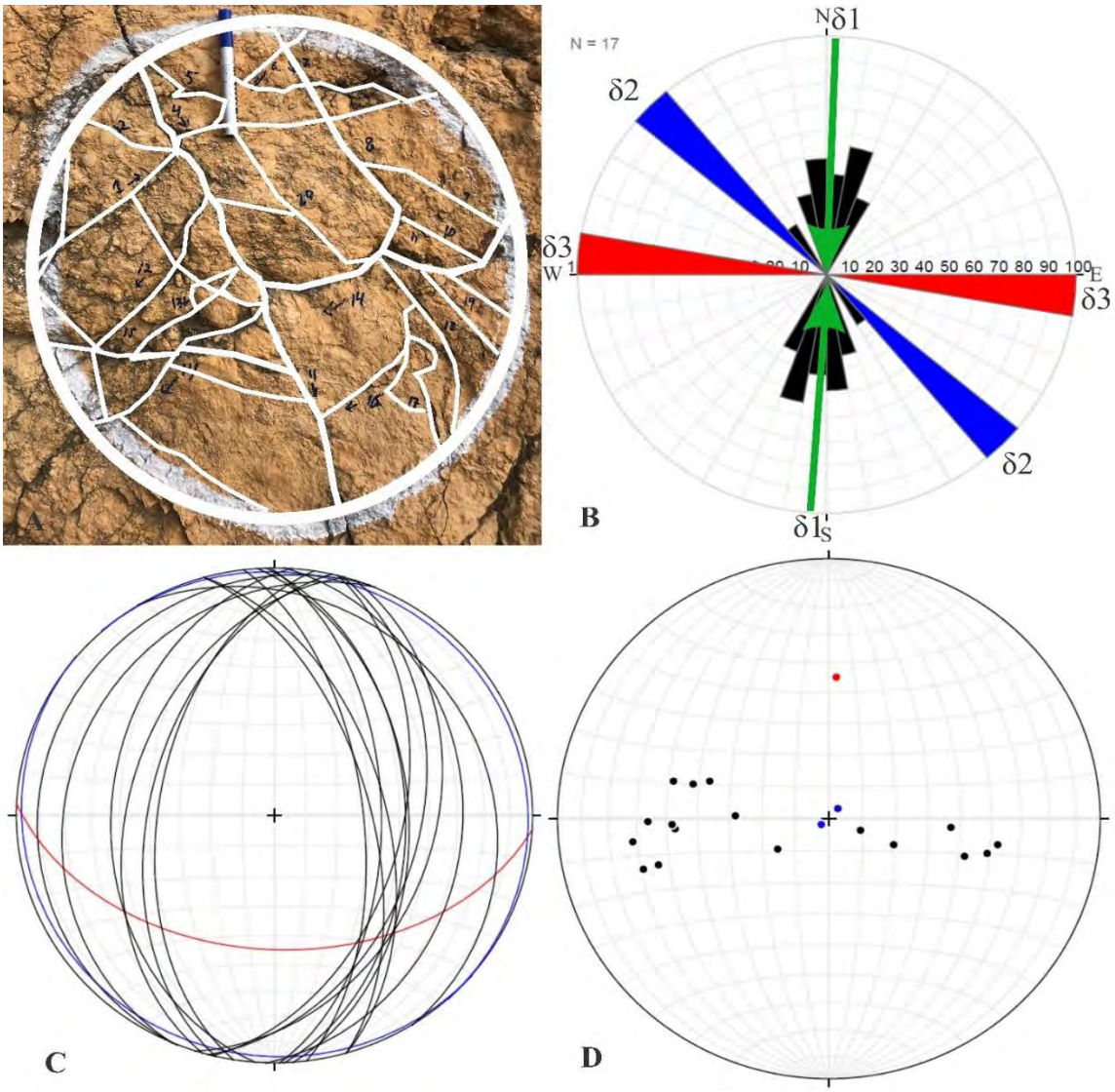

Figure 5. 18 (A) field photograph, (B) Rose diagram of fracture, (C) Plane data of fracture on Stereonet, (D) Poles data of fracture on Stereonet. Number of Release Fractures (Red color) are 01, Conjugate Fractures (Blue color) are 02 whereas Extension Fractures (Black color) are 17.

5.24 Station NO; 09

Area; Western Salt Range

Location; Zaluch Nala

Altitude; 1206

GPS Location; 32°47'21.30"N, 71°39'08.77"E

Bed Strike; N59°E

Bed Dip; 42°SE

Bed Thickness; Massive Bed

Fracture Set; 04

Table 5. 19. Show fracture data of station 19.

S.NO	Strike	Dip	Length (CM)	Width (CM)	Open/Filled or Closed	Filled with	Remarks or Termination	Type
1	S46°W	13°NW	52	02	Open		Continuous	Release
2	S59°W	14°NW	48	1.5	Open		Continuous	Release
3	S13°W	30°NW	47	01	Open		Continuous	Conjugate
4	S05°W	47°NW	19	01	Open		Both	Conjugate
5	S50°E	42°SW	15	0.5	Open		Both	Extension
6	S63°E	46°SW	10	0.2	Open		One	Conjugate
7	S57°E	47°SW	18	0.1	Open		One	Extension
8	S56°E	40°SW	18	0.2	Open		Both	Extension
9	S63°E	73°SW	09	0.5	Open		Both	Conjugate
10	S51°E	34°SW	26	01	Open		One	Extension
11	S63°E	37°SW	09	0.2	Open		Both	Conjugate
12	S41°W	16°NW	18	01	Open		Continuous	Release
13	S67°E	53°SW	14	1.2	Open		One	Conjugate
14	S52°E	34°SW	15	01	Open		One	Extension
15	S76°E	73°SW	11	0.5	Open		One	Conjugate
16	S67°E	62°SW	10	0.7	Open		Both	Conjugate
17	S55°E	41°SW	38	01	Open		Continuous	Extension
18	S04°W	13°NW	12	01	Open		Both	Conjugate
19	S66°E	47°SW	22	0.2	Open		One	Conjugate
20	S31°W	25°NW	10	0.1	Open		Both	Release
21	S53°E	44°SW	17	0.2	Open		One	Extension
22	S60°E	39°SW	09	0.1	Open		Both	Extension

Calculation;

A. Fracture Density $(\partial) = (\Sigma L)/\pi\, r^2$

   FD= 447/3.14 $(25)^2$

   FD= 447/1962.5

   FD= 0.227 cm^1 (As all fracture are open, therefore this is both the open and total fracture density)

B. Fracture Porosity % = $\left(\frac{1}{A}\right)\sum_{i=1}^{N}(Li \times Wi) \times 100$

   FP= (1/1962.5) (411.2) x 100

   FP= 20.95 %

C. Fracture Permeability (K) = $(3.5 \times 10^8)(\frac{1}{A})\sum_{i=1}^{N}(Li \times Wi^3)$

   K= (3.5×10^8) (1/1962.5) x 785.642

   K= 140.11 $\times 10^6$ Darcy

D. Maximum Stress Direction; S55ºE

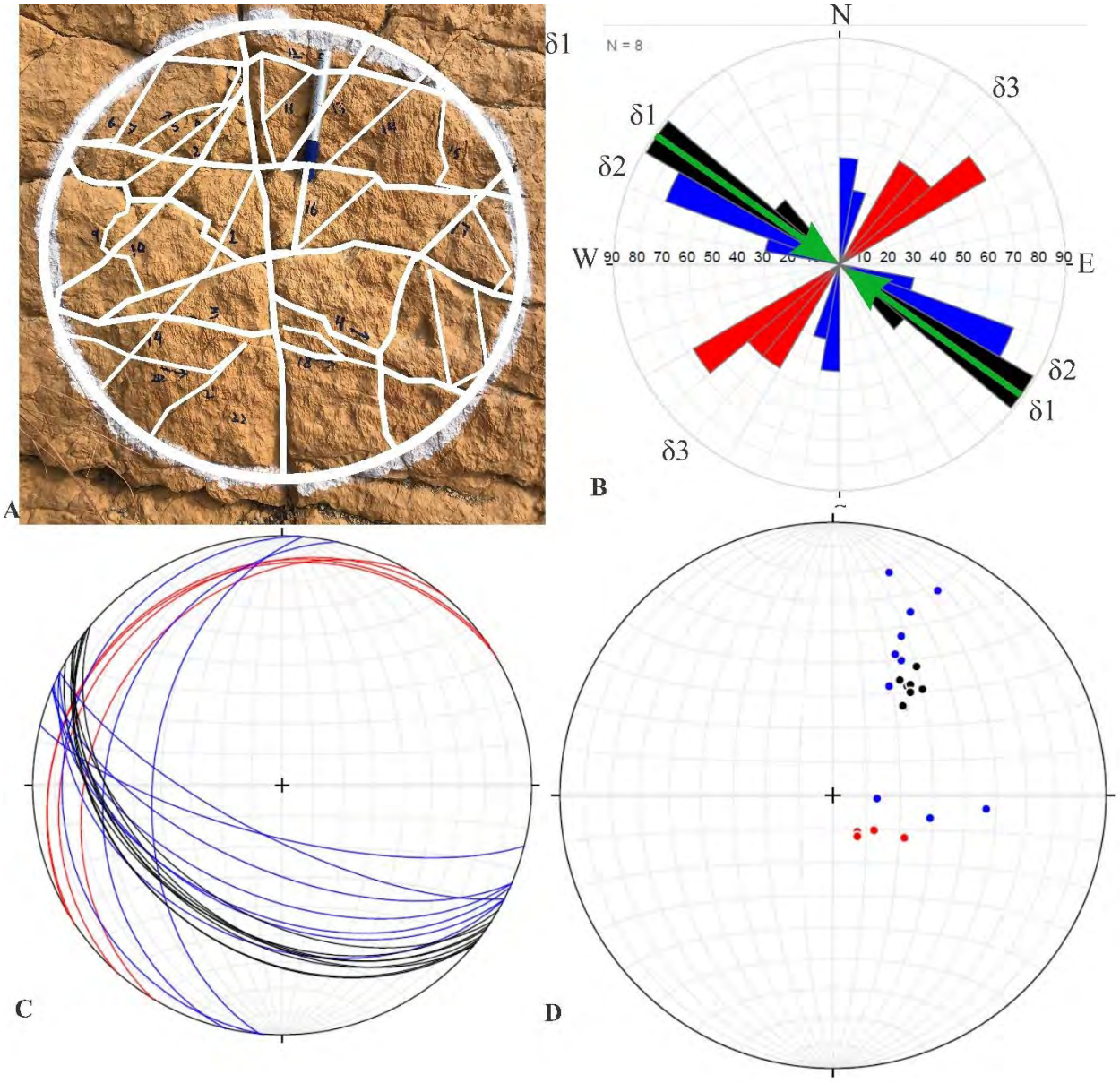

Figure 5. 19 (A) field photograph, (B) Rose diagram of fracture, (C) Plane data of fracture on Stereonet, (D) Poles data of fracture on Stereonet. Number of Release Fractures (Red color) are 04, Conjugate Fractures (Blue color) are 10 whereas Extension Fractures (Black color) are 08.

5.25 Station NO; 10

Area; Western Salt Range	Location; Zaluch Nala
Altitude; 1208	GPS Location; 32°47'20.93"N, 71°39'09.15"E
Bed Strike; N66°E	Bed Dip; 54°SE
Bed Thickness; Massive Bed	Fracture Set; 04

Table 5. 20. Show fracture data of station 20.

S.NO	Strike	Dip	Length (CM)	Width (CM)	Open/Filled or Closed	Filled with	Remarks or Termination	Type
1	S09°W	10°NW	50	02	Open		Continuous	Conjugate
2	S05°W	07°NW	35	02	Open		Continuous	Extension
3	S05°W	07°NW	14	02	Open		Continuous	Extension
4	S77°E	42°SW	50	1.5	Open		Continuous	Conjugate
5	S73°E	47°SW	21	0.5	Open		Both	Conjugate
6	N04°E	49°SE	27	0.5	Open		Both	Extension
7	N08°E	66°SE	13	0.2	Open		Both	Conjugate
8	N01°E	31°SE	21	0.2	Open		Both	Extension
9	N90°E	37°SE	28	0.2	Open		Both	Release
10	S80°E	58°SW	14	0.2	Open		Both	Conjugate
11	S82°E	54°SW	23	0.2	Open		Both	Conjugate
12	S75°E	65°SW	19	0.3	Open		Both	Conjugate
13	S63°E	40°SW	29	1.2	Open		Both	Conjugate
14	S18°W	43°NW	19	0.1	Filled	Calcite	One	Conjugate
15	S78°E	44°SW	19	0.2	Open		One	Conjugate
16	S74°E	41°SW	19	0.1	Filled	Calcite	One	Conjugate
17	N27°W	53°NE	13	0.2	Open		Both	Extension
18	S78°E	45°SW	22	0.1	Filled	Calcite	Continuous	Conjugate
19	S79°E	44°SW	21	0.2	Open		One	Conjugate
20	N17°W	45°NE	21	0.1	Filled	Calcite	One	Extension
21	S57°E	58°SW	19	0.2	Open		One	Conjugate
22	S43°W	22°NW	13	0.2	Open		One	Release
23	S15°W	81°NW	10	0.2	Open		One	Conjugate
24	S85°E	57°SW	09	0.2	Open		One	Release

Calculation;

A. Fracture Density $(\partial) = (\Sigma L)/\pi\, r^2$

   FD= 529/3.14 $(25)^2$

   FD= 529/1962.5

   FD= 0.269 cm^1

   Open Fracture Density= 448/1962.5

   FD= 0.228 cm^1

B. Fracture Porosity % = $\left(\frac{1}{A}\right) \sum_{i=1}^{N} (Li \times Wi) \times 100$

   FP= (1/1962.5) (386.2) x 100

   FP= 19.67 %

C. Fracture Permeability (K) = $(3.5 \times 10^8)(\frac{1}{A}) \sum_{i=1}^{N} (Li \times Wi^3)$

K= (3.5 ×10^8) (1/1962.5) x 1023.697

K= 182.57 ×10^6 Darcy

D. Maximum Stress Direction; N05ºW

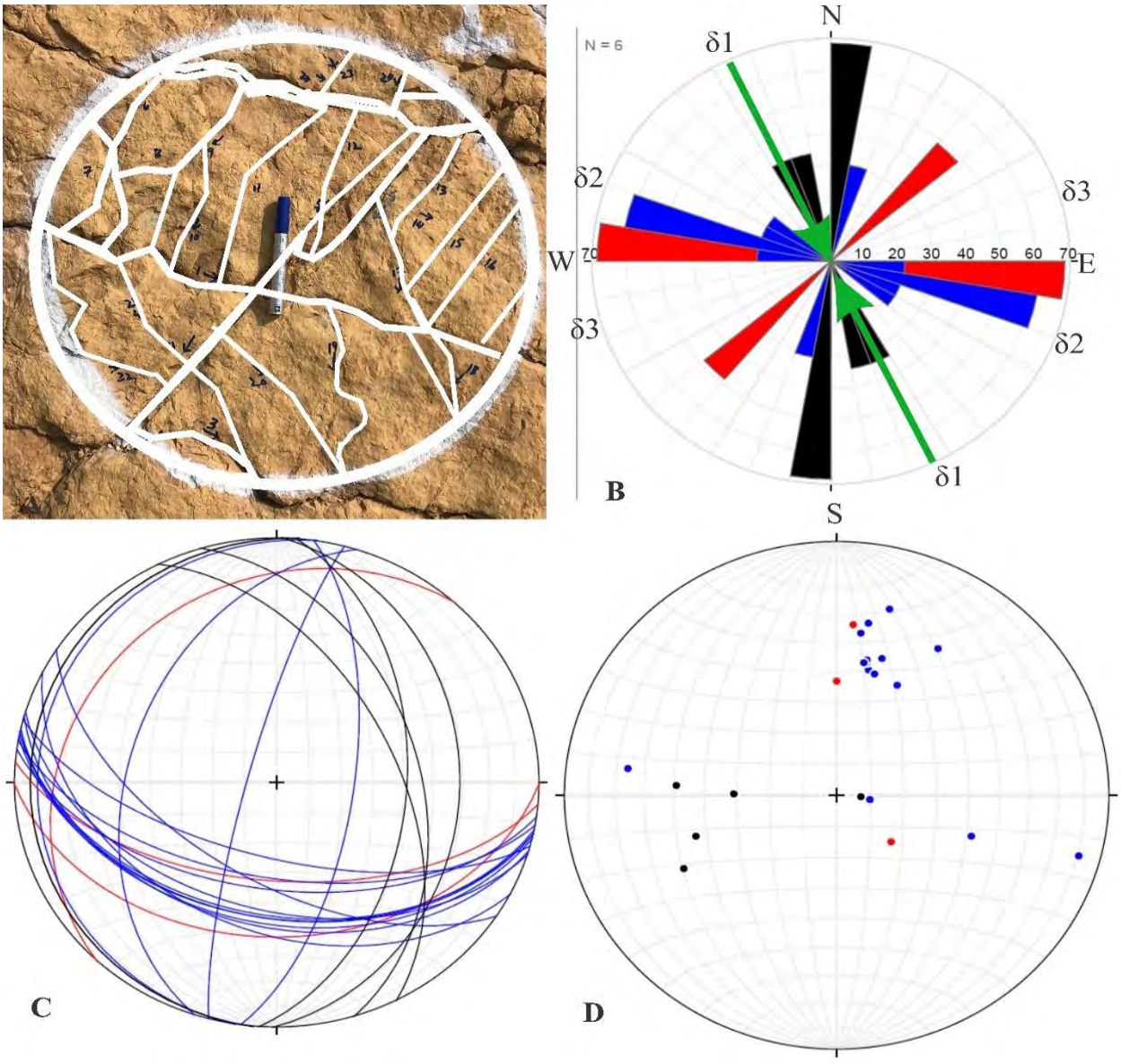

Figure 5. 20 (A) field photograph, (B) Rose diagram of fracture, (C) Plane data of fracture on Stereonet, (D) Poles data of fracture on Stereonet. Number of Release Fractures (Red color) are 03, Conjugate Fractures (Blue color) are 15 whereas Extension Fractures (Black color) are 06.

SURGHAR RANGE SECTION

5.26 Station NO; 01

Area; Surghar Range

Location; Mala Khel

Altitude; 1219

GPS Location; 32°55'07.77N", 71°09'22.41"E

Bed Strike; N83°W

Bed Dip; 43°NE

Bed Thickness; Massive Bed

Fracture Set; 03

Table 5. 21. Show fracture data of station 21.

S.NO	Strike	Dip	Length (CM)	Width (CM)	Open/Filled or Closed	Filled with	Remarks or Termination	Type
1	S30°W	30°NW	23	0.2	Open		Continuous	Conjugate
2	S20°W	23°NW	17	0.8	Open		One	Extension
3	S50°W	17°NW	13	01	Open		One	Conjugate
4	S13°W	48°NW	50	0.8	Open		Continuous	Extension
5	S10°W	42°NW	50	0.8	Open		Continuous	Extension
6	S11°W	37°NW	17	0.3	Open		One	Extension
7	S15°W	34°NW	12	0.4	Open		Both	Extension
8	N90°E	60°SE	23	0.5	Open		One	Release
9	S60°E	55°SW	29	01	Open		One	Release
10	N27°E	82°SE	13	0.5	Open		One	Extension
11	S41°W	37°NW	07	0.2	Open		Both	Conjugate
12	S44°W	40°NW	11	0.1	Open		Both	Conjugate
13	S79°E	70°SW	21	0.5	Open		One	Release
14	S63°E	57°SW	08	0.5	Open		Both	Conjugate
15	S17°W	57°NW	10	0.2	Open		One	Extension
16	S06°W	60°NW	20	0.1	Open		Both	Extension
17	N15°W	65°NE	11	0.2	Open		Both	Extension
18	N35°W	72°NE	13	0.2	Open		Both	Conjugate

Calculation;

A. Fracture Density $(\partial) = (\Sigma L)/\pi\, r^2$

   FD= 348/3.14 $(25)^2$

   FD= 348/1962.5

   FD= 0.177 cm^1 (As all fracture are open, therefore this is both the open and total fracture density)

B. Fracture Porosity % = $\left(\frac{1}{A}\right) \sum_{i=1}^{N} (Li \times Wi) \times 100$

   FP= (1/1962.5) (193.9) x 100

   FP= 9.88 %

C. Fracture Permeability (K) = $(3.5 \times 10^8)(\frac{1}{A}) \sum_{i=1}^{N}(Li \times Wi^3)$

K= (3.5×10^8) (1/1962.5) x 114.758

K= 20.46×10^6

D. Maximum Stress Direction; N11ºE

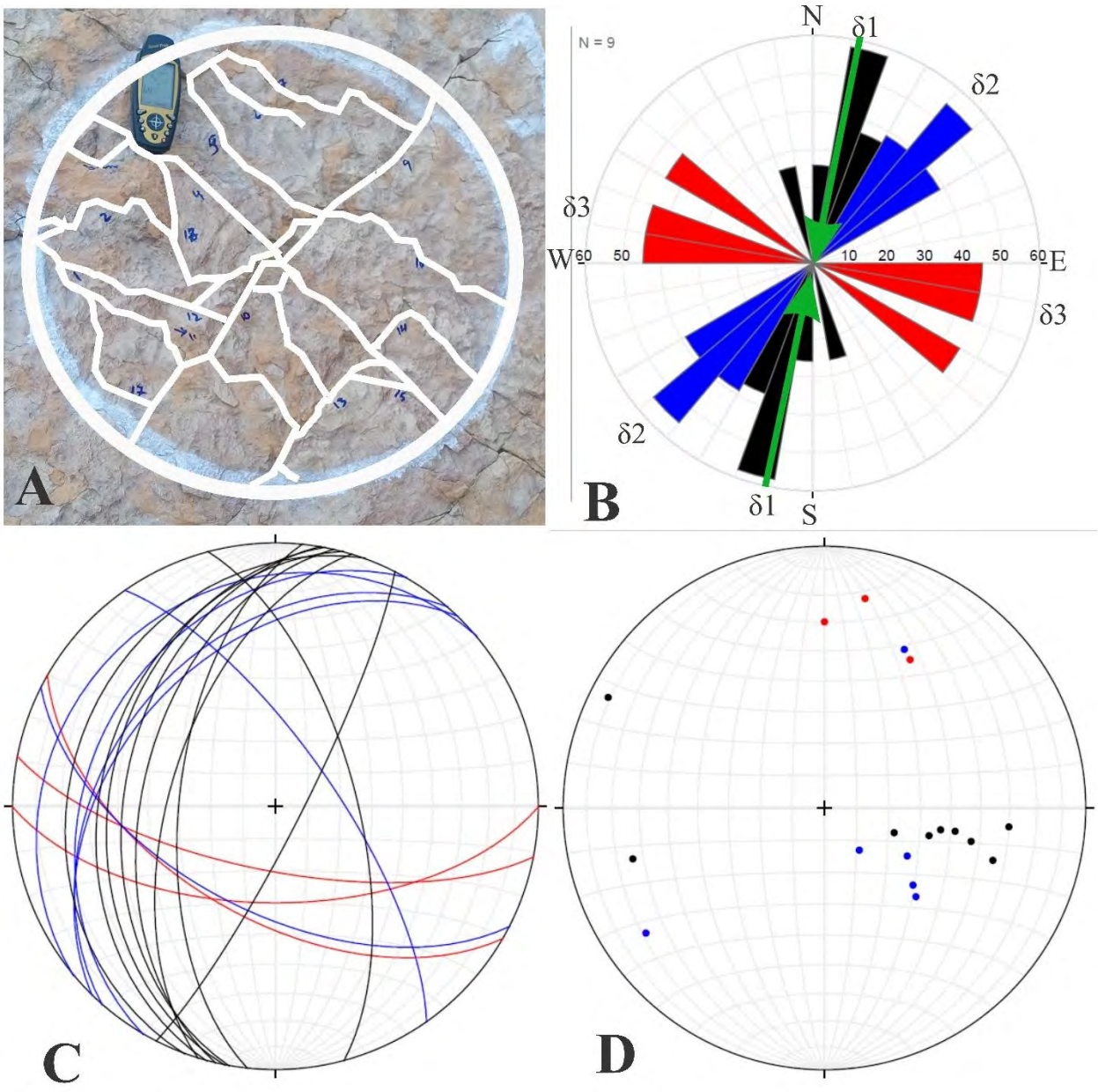

Figure 5. 21 (A) field photograph, (B) Rose diagram of fracture, (C) Plane data of fracture on Stereonet, (D) Poles data of fracture on Stereonet. Number of Release Fractures (Red color) are 03, Conjugate Fractures (Blue color) are 06 whereas Extension Fractures (Black color) are 09.

5.27 Station NO; 02

Area; Surghar Range

Location; Mala Khel

Altitude; 1211

GPS Location; 32°55'06.39"N, 71°09'21.62"E

Bed Strike; N80°W

Bed Dip; 51°NE

Bed Thickness; Massive Bed

Fracture Set; 04

Table 5. 22. Show fracture data of station 22.

S.NO	Strike	Dip	Length (CM)	Width (CM)	Open/Filled or Closed	Filled with	Remarks or Termination	Type
1	S34°E	60°SW	22	0.5	Open		One	Conjugate
2	S35°E	11°SW	22	0.3	Open		One	Conjugate
3	N19°W	77°NE	37	0.8	Open		Continuous	Extension
4	S69°W	54°NW	22	0.5	Open		One	Conjugate
5	S67°E	29°SW	12	0.2	Open		One	Extension
6	S69°W	45°NW	11	0.7	Open		Both	Conjugate
7	S09°W	60°NW	10	0.5	Open		One	Extension
8	S13°W	60°NW	50	0.2	Open		Continuous	Extension
9	S78°E	51°SW	11	0.2	Open		One	Release
10	S16°E	23°SW	23	0.1	Filled	Calcite	One	Extension
11	N30°W	75°NE	49	1.5	Open		Continuous	Conjugate
12	S02°E	27°SW	15	01	Open		Both	Extension
13	N80°E	69°SE	12	01	Open		Both	Release
14	S46°W	25°NW	16	0.2	Open		One	Conjugate
15	S62°W	32°NW	18	0.2	Open		One	Conjugate
16	S52°W	50°NW	19	0.1	Filled	Calcite	Continuous	Conjugate

Calculation;

A. Fracture Density $(\partial) = (\Sigma L)/\pi\, r^2$

   FD= 349/3.14 $(25)^2$

   FD= 349/1962.5

   FD= 0.177 cm^1

   Open Fracture Density= 307/1962.5

   FD= 0.156 cm^1

B. Fracture Porosity % = $\left(\frac{1}{A}\right) \sum_{i=1}^{N} (Li \times Wi) \times 100$

   FP= (1/1962.5) (197) x 100

   FP= 10.03 %

C. Fracture Permeability (K) = $(3.5 \times 10^8)\left(\frac{1}{A}\right) \sum_{i=1}^{N} (Li \times Wi^3)$

K= (3.5 ×10^8) (1/1962.5) x 223.334

K= 39.83 ×10^6 Darcy

D. Maximum Stress Direction; N09ºW

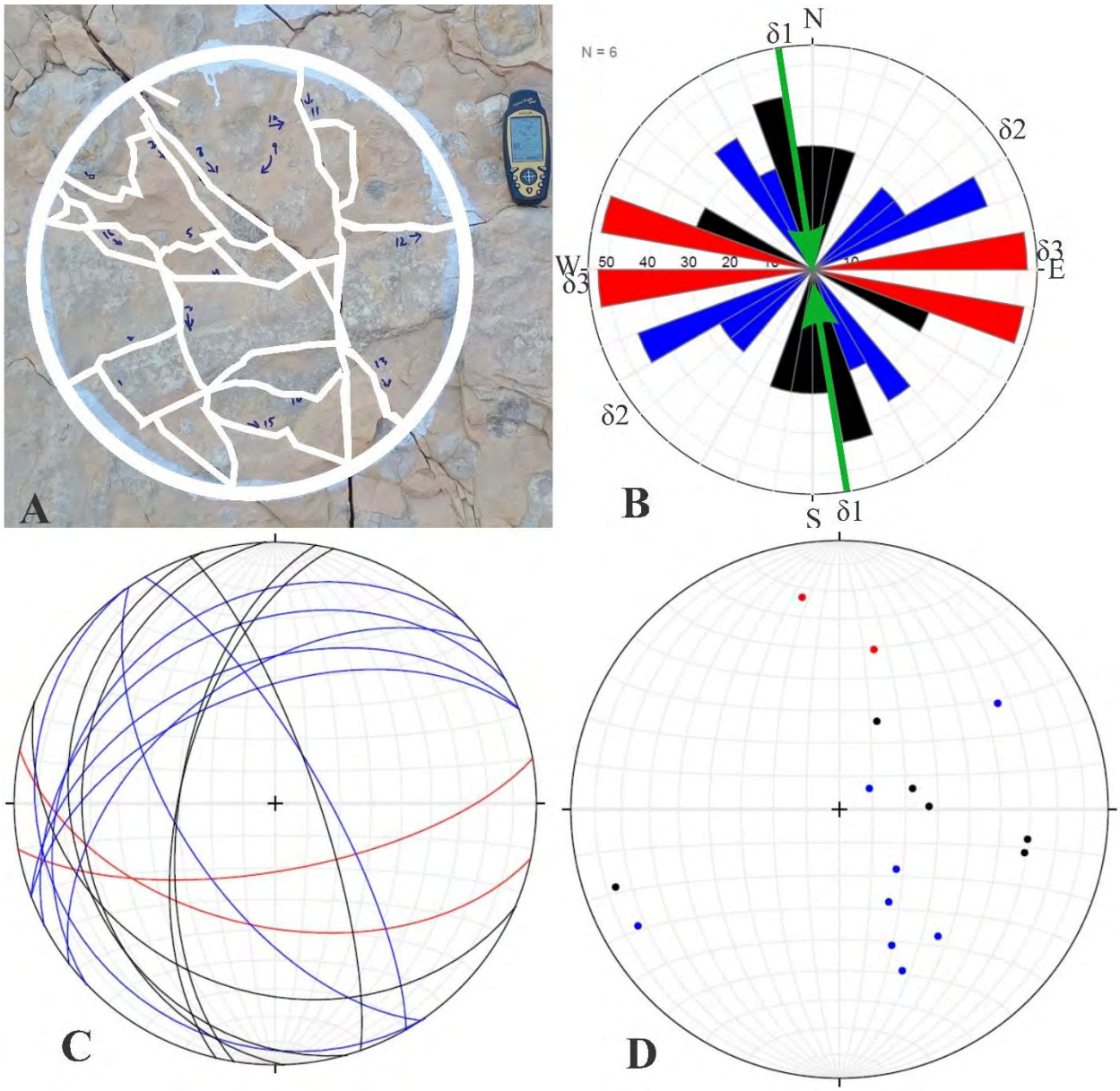

Figure 5. 22 (A) field photograph, (B) Rose diagram of fracture, (C) Plane data of fracture on Stereonet, (D) Poles data of fracture on Stereonet. Number of Release Fractures (Red color) are 02, Conjugate Fractures (Blue color) are 08 whereas Extension Fractures (Black color) are 06.

5.28 Station NO; 03

Area; Surghar Range Location; Mala Khel

Altitude; 1217 GPS Location; 32°55'05.86"N, 71°09'20.75"E

Bed Strike; N88°E Bed Dip; 51°SE

Bed Thickness; Massive Bed Fracture Set; 04

Table 5. 23. Show fracture data of station 23.

S.NO	Strike	Dip	Length (CM)	Width (CM)	Open/Filled or Closed	Filled with	Remarks or Termination	Type
1	S22°W	28°NW	08	0.2	Open		One	Extension
2	S02°W	60°NW	36	01	Open		Continuous	Extension
3	N20°W	78°NE	13	0.5	Open		One	Extension
4	N20°W	74°NE	25	0.5	Open		One	Extension
5	N12°W	71°NE	30	0.6	Open		One	Extension
6	S82°E	65°SW	10	0.5	Open		Both	Release
7	N45°E	81°SE	07	0.5	Open		One	Conjugate
8	N52°W	87°NE	19	0.6	Open		One	Conjugate
9	N55°E	88°SE	38	01	Open		Continuous	Conjugate
10	N36°E	89°SE	20	0.2	Open		Both	Conjugate
11	N47°W	82°NE	18	0.1	Open		Both	Conjugate
12	N20°W	75°NE	14	0.5	Open		Both	Extension
13	S04°W	76°NW	12	0.1	Open		Both	Extension
14	N40°E	86°SE	08	0.5	Open		One	Conjugate
15	N54°E	90°SE	07	0.5	Open		Both	Conjugate
16	N12°E	64°SE	12	0.2	Open		One	Extension
17	S74°W	26°NW	12	0.2	Open		One	Release
18	N10°W	73°NE	11	0.1	Open		One	Extension

Calculation;

A. Fracture Density $(\partial) = (\Sigma L)/\pi\, r^2$

   FD= 300/3.14 $(25)^2$

   FD= 300/1962.5

   FD= 0.152 cm^1 (As all fracture are open, therefore this is both the open and total fracture density)

B. Fracture Porosity % = $\left(\frac{1}{A}\right) \sum_{i=1}^{N} (Li \times Wi) \times 100$

   FP= (1/1962.5) (159.9) x 100

   FP= 8.14 %

C. Fracture Permeability (K) = $(3.5 \times 10^8)(\frac{1}{A}) \sum_{i=1}^{N} (Li \times Wi^3)$

K= (3.5 ×10^8) (1/1962.5) x 95.541

K= 17.03 ×10^6

D. Maximum Stress Direction; N10ºW

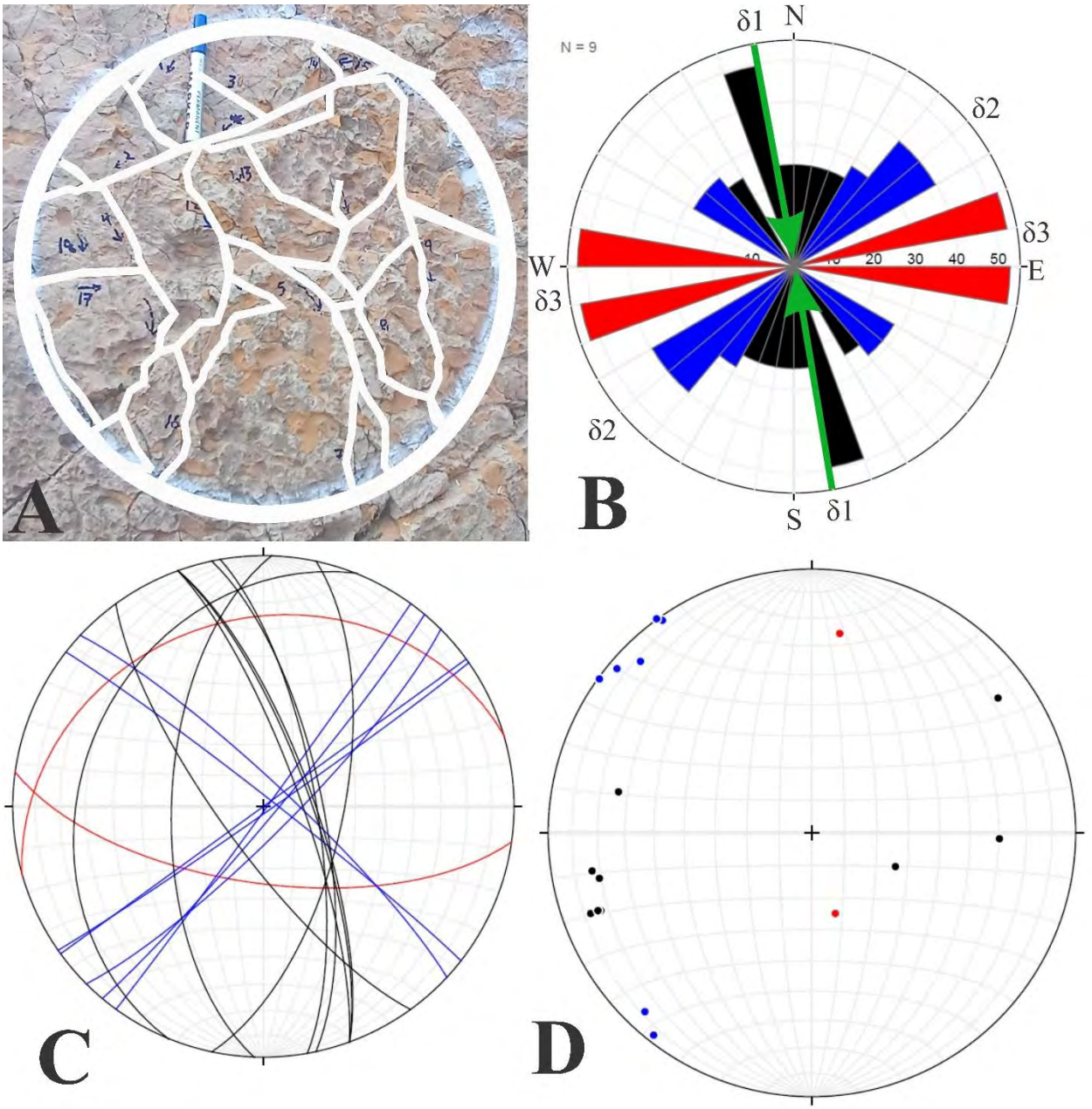

Figure 5. 23 (A) field photograph, (B) Rose diagram of fracture, (C) Plane data of fracture on Stereonet, (D) Poles data of fracture on Stereonet. Number of Release Fractures (Red color) are 02, Conjugate Fractures (Blue color) are 07 whereas Extension Fractures (Black color) are 09.

5.29 Station NO; 04

Area; Surghar Range

Location; Mala Khel

Altitude; 1209

GPS Location; 32°55'04.57"N, 71°09'20.19"E

Bed Strike; S44°W

Bed Dip; 67°NW

Bed Thickness; Massive Bed

Fracture Set; 04

Table 5. 24. Show fracture data of station 24.

S.NO	Strike	Dip	Length (CM)	Width (CM)	Open/Filled or Closed	Filled with	Remarks or Termination	Type
1	N34°W	73°NE	21	01	Open		One	Extension
2	S85°E	78°SW	16	0.2	Filled	Calcite	One	Conjugate
3	S83°W	29°NW	47	1.5	Open		Continuous	Conjugate
4	N19°E	76°SE	11	01	Open		Both	Release
5	S28°E	35°SW	15	0.7	Open		Both	Extension
6	N22°W	77°NE	08	0.3	Filled	Calcite	Both	Extension
7	S36°E	53°SW	50	1.5	Open		Continuous	Extension
8	S67°E	60°SW	08	0.8	Open		Both	Extension
9	N20°W	87°NE	19	1.5	Open		Continuous	Extension
10	S22°W	44°NW	15	0.8	Filled	Calcite	One	Release
11	N09°E	76°SE	24	01	Filled	Calcite	One	Conjugate
12	S33°E	53°SW	35	01	Filled	Calcite	One	Extension
13	N04°W	75°NE	19	0.1	Open		One	Conjugate
14	N10°W	71°NE	14	0.5	Filled	Calcite	One	Conjugate
15	S07°W	70°NW	11	0.5	Open		One	Conjugate
16	N21°W	71°NE	08	00	Closed		Both	Extension
17	N14W	80°NE	18	0.1	Open		One	Conjugate
18	S36°E	52°SW	15	0.2	Open		One	Extension
19	N01°W	62°NE	13	0.2	Open		One	Conjugate
20	N24°W	53°NE	14	0.5	Open		One	Extension

Calculation;

A. Fracture Density $(\partial) = (\Sigma L)/\pi\, r^2$

   FD= 381/3.14 $(25)^2$

   FD= 381/1962.5

   FD= 0.194 cm^1

   Open Fracture Density= 261/1962.5

   FD= 0.132 cm^1

B. Fracture Porosity % = $\left(\frac{1}{A}\right) \sum_{i=1}^{N} (Li \times Wi) \times 100$

   FP= (1/1962.5) (328.3) x 100

FP= 16.72 %

C. Fracture Permeability (K) = $(3.5 \times 10^8)(\frac{1}{A}) \sum_{i=1}^{N}(Li \times Wi^3)$

K= (3.5×10^8) (1/1962.5) x 560.151

K= 99.89 $\times 10^6$ Darcy

D. Maximum Stress Direction; N32°W

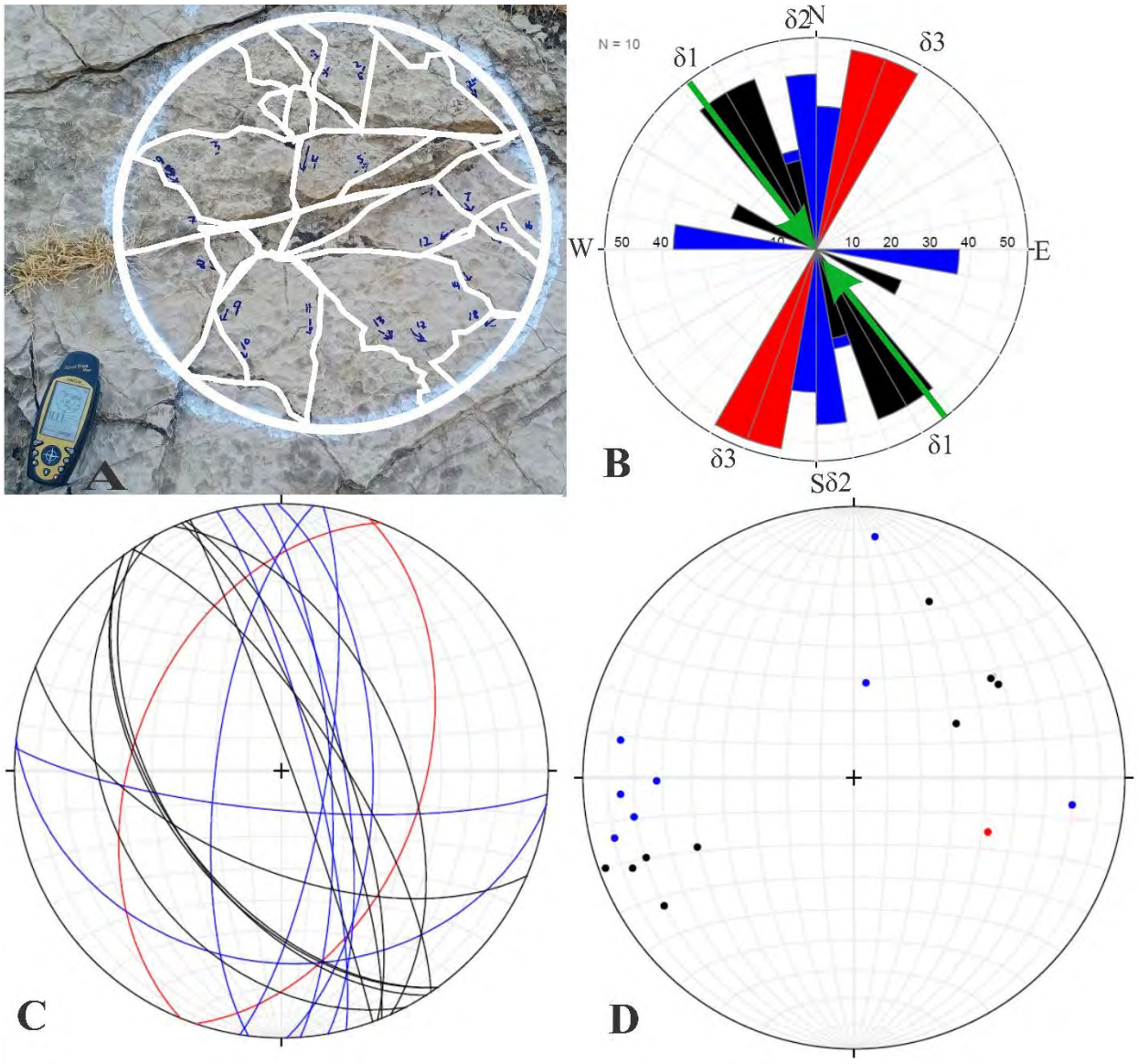

Figure 5. 24 (A) field photograph, (B) Rose diagram of fracture, (C) Plane data of fracture on Stereonet, (D) Poles data of fracture on Stereonet. Number of Release Fractures (Red color) are 02, Conjugate Fractures (Blue color) are 8 whereas Extension Fractures (Black color) are10.

5.30 Station NO; 05

Area; Surghar Range Location; Mala Khel

Altitude; 1212 GPS Location; 32°55'04.75", 71°09'20.56"E

Bed Strike; N82°E Bed Dip; 48°SE

Bed Thickness; Massive Bed Fracture Set; 03

Table 5. 25. Show fracture data of station 25.

S.NO	Strike	Dip	Length (CM)	Width (CM)	Open/Filled or Closed	Filled with	Remarks or Termination	Type
1	S57°W	51°NW	41	02	Open		Continuous	Conjugate
2	S56°W	49°NW	29	1.5	Open		One	Conjugate
3	S24°W	64°NW	27	1.5	Open		Both	Extension
4	S02°E	54°SW	12	01	Open		One	Extension
5	N53°E	85°SE	30	02	Open		One	Release
6	S85°E	61°SW	12	0.5	Open		Both	Release
7	S80°E	62°SW	50	02	Open		Continuous	Release
8	S89°E	72°SW	15	1.5	Open		Both	Release
9	S60°W	46°NW	24	1.5	Open		One	Release
10	S18°W	60°NW	15	0.5	Open		Both	Extension
11	S25°W	57°NW	21	0.2	Open		One	Extension
12	N01°W	78°NE	17	00	Closed		One	Extension
13	S04°W	70°NW	23	01	Open		One	Extension
14	S23°W	62°NW	19	0.2	Open		One	Extension
15	S89°E	68°SW	13	0.5	Open		One	Release
16	S07°W	73°NW	11	0.7	Open		Both	Extension
17	S15°W	64°NW	14	0.2	Open		Both	Extension
18	S17°W	73°NW	23	0.2	Open		Both	Extension
19	S13°W	70°NW	13	0.4	Open		Both	Extension
20	N84°E	56°SE	22	01	Open		Continuous	Release
21	N01°E	83°SE	16	0.2	Open		One	Extension
22	S04°W	77°NW	13	0.2	Open		One	Extension
23	S18°W	67°NW	29	0.2	Open		One	Extension
24	S78°E	56°SW	08	0.3	Filled	Calcite	One	Release

Calculation;

A. Fracture Density $(\partial) = (\Sigma L)/\pi\, r^2$

FD= 497/3.14 $(25)^2$

FD= 497/1962.5

FD= 0.253 cm^1

Open Fracture Density= 472/1962.5

FD= 0.240 cm^{1}

B. Fracture Porosity % = $\left(\frac{1}{A}\right)\sum_{i=1}^{N}(Li \times Wi) \times 100$

FP= (1/1962.5) (503.8) x 100

FP= 25.67%

C. Fracture Permeability (K) = $(3.5 \times 10^{8})\left(\frac{1}{A}\right)\sum_{i=1}^{N}(Li \times Wi^{3})$

K= (3.5 $\times 10^{8}$) (1/1962.5) x 1356.526

K= 241.92 $\times 10^{6}$ Darcy

D. Maximum Stress Direction; N11ºE

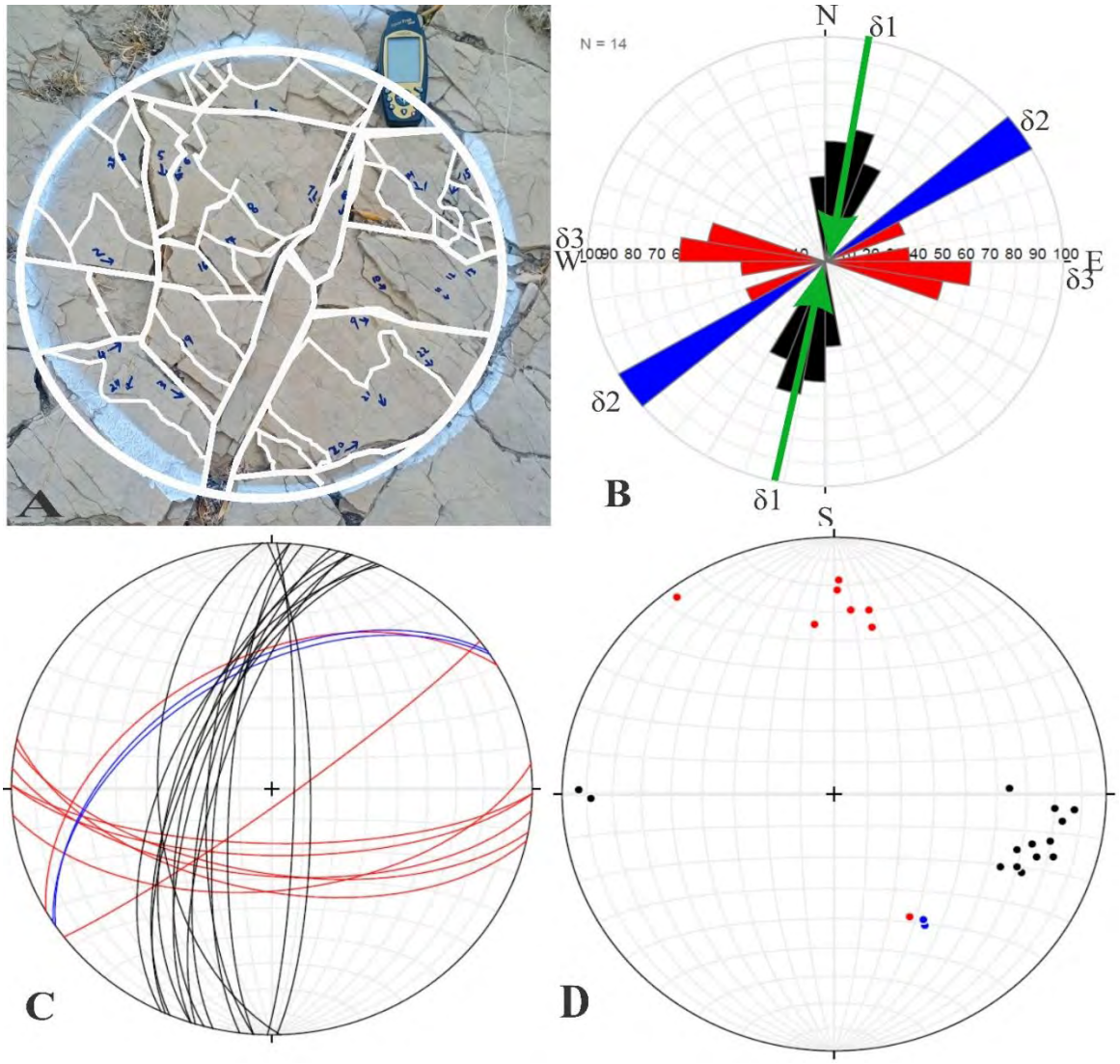

Figure 5. 25 (A) field photograph, (B) Rose diagram of fracture, (C) Plane data of fracture on Stereonet, (D) Poles data of fracture on Stereonet. Number of Release Fractures (Red color) are 08, Conjugate Fractures (Blue color) are 02 whereas Extension Fractures (Black color) are 14.

5.31 Station NO; 06

Area; Surghar Range

Location; Mala Khel

Altitude; 1208

GPS Location; 32°55'04.16"N, 71°09'20.51"E

Bed Strike; N70°E

Bed Dip; 51°SE

Bed Thickness; Massive Bed

Fracture Set; 03

Table 5. 26. Show fracture data of station 26.

S.NO	Strike	Dip	Length (CM)	Width (CM)	Open/Filled or Closed	Filled with	Remarks or Termination	Type
1	N25°W	84°NE	07	0.5	Open		Continuous	Extension
2	S31°W	45°NW	27	01	Open		One	Conjugate
3	N26°W	80°NE	26	0.2	Open		One	Extension
4	S77°W	32°NW	17	0.2	Open		One	Release
5	N04°W	68°NE	23	0.1	Filled	Calcite	One	Extension
6	S60°E	43°SW	18	0.8	Open		One	Conjugate
7	N34°W	86°NE	23	01	Open		One	Extension
8	N20°W	73°NE	14	0.2	Open		Continuous	Extension
9	S84°W	33°NW	50	0.5	Open		Continuous	Release
10	N35°E	80°SE	27	01	Open		Both	Conjugate
11	S43°W	68°NW	28	0.7	Open		One	Release
12	S40°W	63°NW	15	0.2	Open		One	Conjugate
13	S08°E	54°SW	18	0.1	Filled	Calcite	One	Extension
14	S29°W	70°NW	12	0.2	Open		One	Conjugate
15	S30°W	76°NW	22	0.2	Open		One	Conjugate
16	S37°W	42°NW	24	0.2	Open		One	Conjugate
17	S62°E	24°SW	08	0.2	Open		One	Conjugate
18	N13°W	78°NE	09	0.5	Open		Both	Extension

Calculation;

A. Fracture Density $(\partial) = (\Sigma L)/\pi\, r^2$

   FD= 368/3.14 $(25)^2$

   FD= 368/1962.5

   FD= 0.187 cm^1

   Open Fracture Density= 327/1962.5

   FD= 0.166 cm^1

B. Fracture Porosity % = $\left(\frac{1}{A}\right) \sum_{i=1}^{N} (Li \times Wi) \times 100$

   FP= (1/1962.5) (175.7) x 100

   FP= 8.95%

C. Fracture Permeability (K) = $(3.5 \times 10^8)(\frac{1}{A}) \sum_{i=1}^{N}(Li \times Wi^3)$

K= (3.5×10^8) (1/1962.5) x 266.215

K= 47.477 $\times 10^6$ Darcy

D. Maximum Stress Direction; N19°W

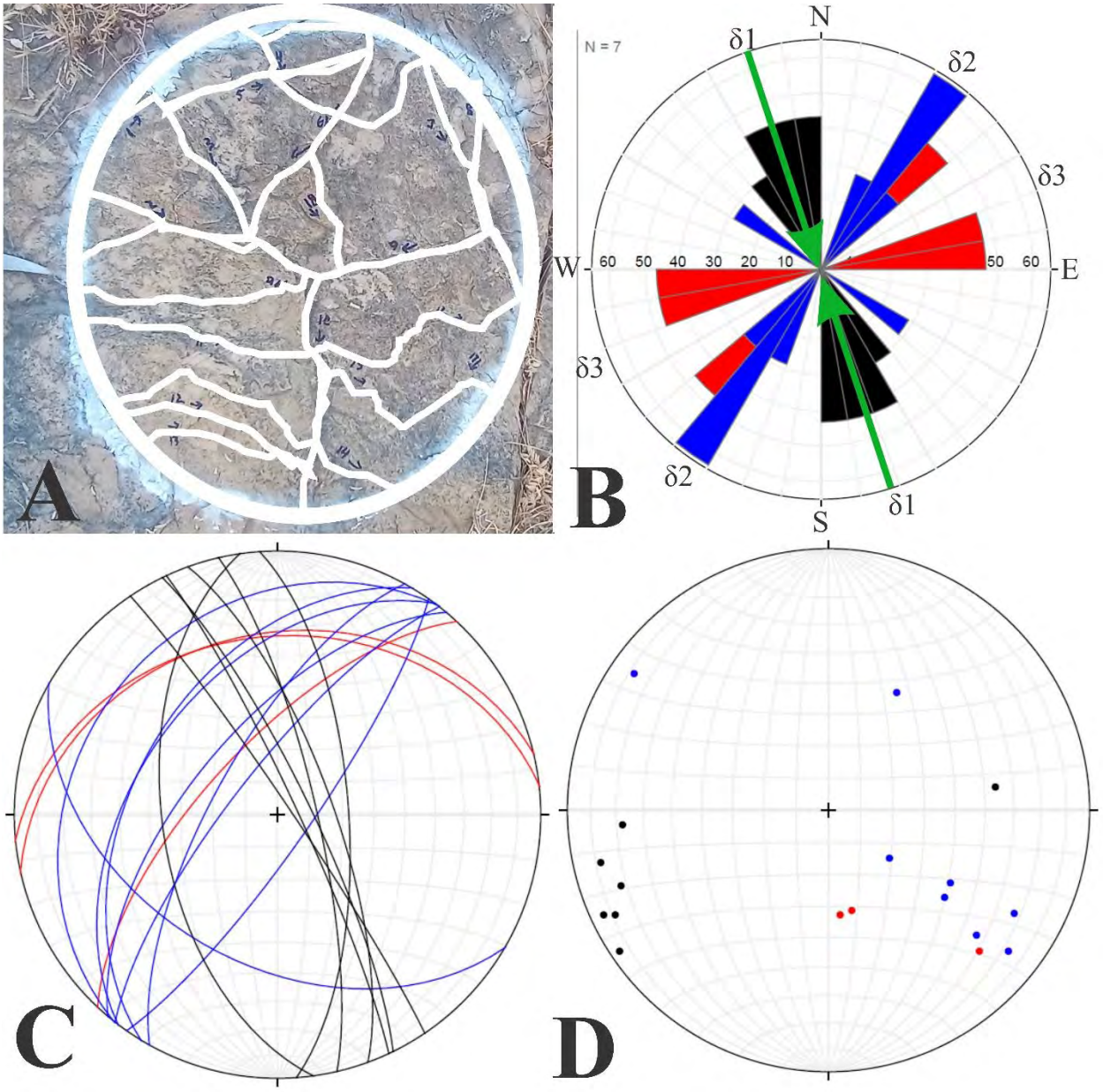

Figure 5. 26 (A) field photograph, (B) Rose diagram of fracture, (C) Plane data of fracture on Stereonet, (D) Poles data of fracture on Stereonet. Number of Release Fractures (Red color) are 03, Conjugate Fractures (Blue color) are 08 whereas Extension Fractures (Black color) are 07.

5.32 Station NO; 07

Area; Surghar Range

Location; Mala Khel

Altitude; 1214

GPS Location; 32°55'04.67"N, 71°09'20.18"E

Bed Strike; S75°W

Bed Dip; 41°NW

Bed Thickness; Massive Bed

Fracture Set; 04

Table 5. 27. Show fracture data of station 27.

S.NO	Strike	Dip	Length (CM)	Width (CM)	Open/Filled or Closed	Filled with	Remarks or Termination	Type
1	N07°W	48°NE	18	0.7	Open		One	Extension
2	N71°W	72°NE	26	01	Open		Continuous	Release
3	N31°W	73°NE	15	01	Open		Both	Conjugate
4	S43°E	33°SW	12	0.2	Open		Both	Conjugate
5	N32°E	86°SE	18	0.3	Open		One	Extension
6	N11°W	61°NE	18	0.1	Open		One	Extension
7	S41°W	32°NW	16	01	Open		Both	Extension
8	S28°W	65°NW	17	0.5	Filled	Quartz	Both	Extension
9	N34°W	73°NE	18	0.8	Open		One	Conjugate
10	N42°W	80°NE	25	0.1	Open		Both	Release
11	S39°E	67°SW	21	0.2	Open		One	Conjugate
12	S73°W	56°NW	16	0.2	Open		Both	Conjugate
13	S88°W	42°NW	24	0.2	Open		One	Release
14	S20°E	48°SW	15	0.2	Filled	Quartz	Both	Conjugate
15	S73°W	51°NW	11	0.2	Filled	Quartz	One	Conjugate
16	S81°W	57°NW	09	0.2	Open		One	Release
17	N60°W	80°NE	19	0.2	Filled	Quartz	One	Release
18	N50°W	74°NE	21	0.2	Filled	Quartz	One	Conjugate

Calculation;

A. Fracture Density $(\partial) = (\Sigma L)/\pi\, r^2$

   FD= 319/3.14 $(25)^2$

   FD= 319/1962.5

   FD= 0.162 cm^1

   Open Fracture Density= 236/1962.5

   FD= 0.120 cm^1

B. Fracture Porosity % = $\left(\frac{1}{A}\right) \sum_{i=1}^{N} (Li \times Wi) \times 100$

   FP= (1/1962.5) (131.8) x 100

   FP= 6.715%

C. Fracture Permeability (K) = $(3.5 \times 10^8)(\frac{1}{A}) \sum_{i=1}^{N}(Li \times Wi^3)$

K= (3.5×10^8) (1/1962.5) x 76.228

K= 13.59 $\times 10^6$ Darcy

D. Maximum Stress Direction; N17ºE

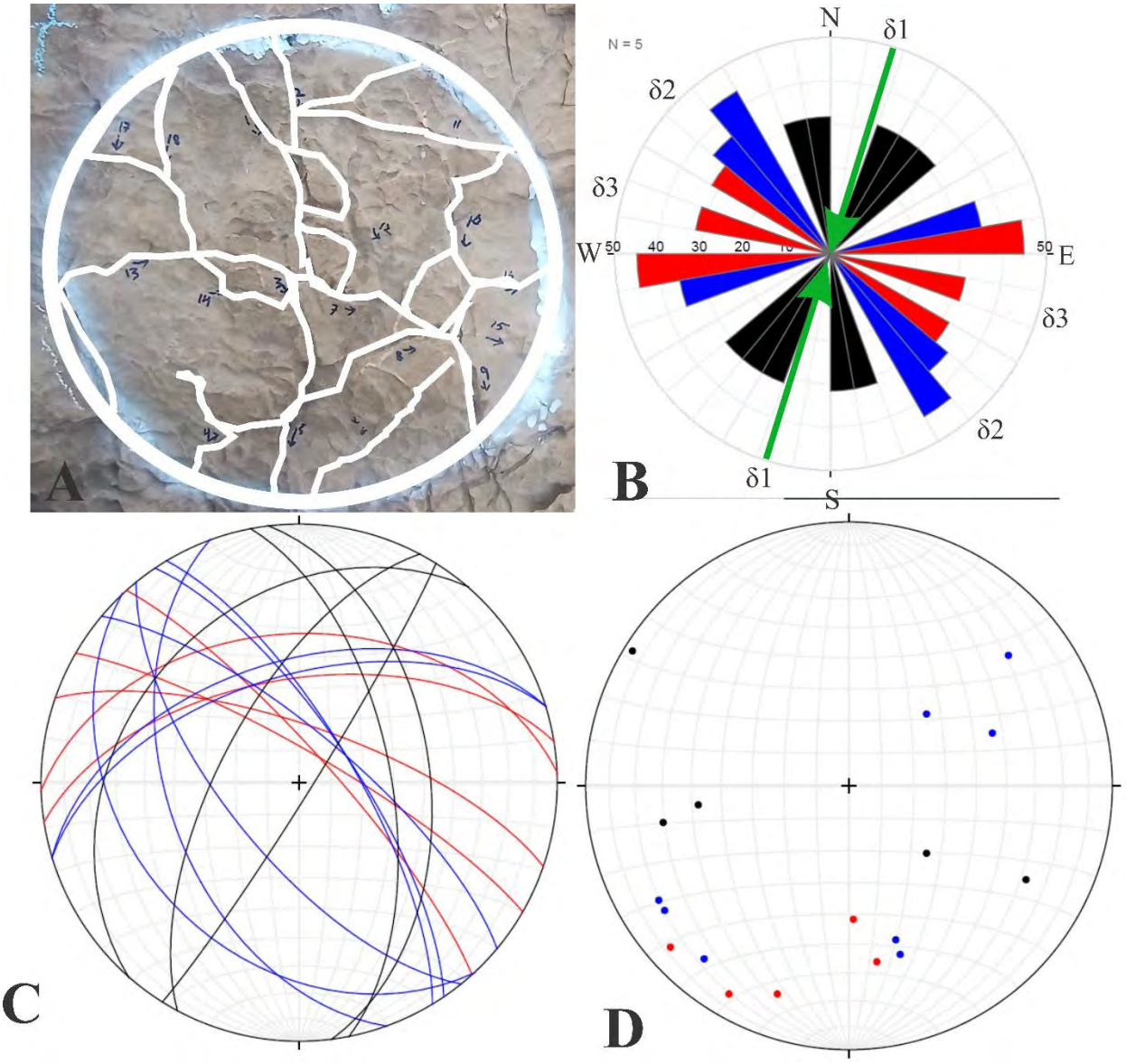

Figure 5. 27 (A) field photograph, (B) Rose diagram of fracture, (C) Plane data of fracture on Stereonet, (D) Poles data of fracture on Stereonet. Number of Release Fractures (Red color) are 05, Conjugate Fractures (Blue color) are 08 whereas Extension Fractures (Black color) are 05.

5.33 Station NO; 08

Area; Surghar Range

Location; Mala khel

Altitude; 1212

GPS Location; 32°55'04.05"N, 71°09'19.70"E

Bed Strike; N87°W

Bed Dip; 40°NE

Bed Thickness; Massive Bed

Fracture Set; 04

Table 5. 28. Show fracture data of station 28.

S.NO	Strike	Dip	Length (CM)	Width (CM)	Open/Filled or Closed	Filled with	Remarks or Termination	Type
1	S04°E	10°SW	22	0.1	Open		One	Extension
2	S09°E	17°SW	28	0.2	Open		Continuous	Extension
3	S24°E	14°SW	30	0.3	Filled	Calcite	Both	Extension
4	N28°W	60°NE	11	0.5	Open		Both	Conjugate
5	S24°W	28°NW	16	0.2	Open		One	Extension
6	N03°E	31°SE	31	0.2	Filled	Quartz	One	Extension
7	N16°W	42°NE	50	01	Open		Both	Extension
8	S18°E	11°SW	13	0.2	Filled	Quartz	Both	Extension
9	N15°E	59°SE	23	01	Open		One	Extension
10	N42°E	76°SE	11	0.2	Open		Both	Conjugate
11	S27°W	72°NW	17	0.2	Open		One	Extension
12	S89°W	70°NW	08	0.2	Open		Both	Release
13	S49°E	73°SW	22	0.5	Open		One	Conjugate
14	N24°E	71°SE	11	0.5	Open		Both	Extension
15	S40°E	33°SW	05	0.5	Open		One	Conjugate
16	N60°E	65°SE	22	0.2	Filled	Calcite	One	Conjugate
17	S34°W	14°NW	11	0.2	Open		One	Conjugate
18	N38°E	19°SE	13	00	Closed		One	Conjugate

Calculation;

A. Fracture Density $(\partial) = (\Sigma L)/\pi\, r^2$

   FD= 344/3.14 $(25)^2$

   FD= 344/1962.5

   FD= 0.175 cm^1

   Open Fracture Density= 235/1962.5

   FD= 0.119 cm^1

B. Fracture Porosity % = $\left(\frac{1}{A}\right) \sum_{i=1}^{N} (Li \times Wi) \times 100$

   FP= (1/1962.5) (140.1) x 100

   FP= 7.138%

C. Fracture Permeability (K) = $(3.5 \times 10^8)(\frac{1}{A}) \sum_{i=1}^{N}(Li \times Wi^3)$

K= (3.5×10^8) (1/1962.5) x 76.228

K= 14.483 $\times 10^6$ Darcy

D. Maximum Stress Direction; N02ºE

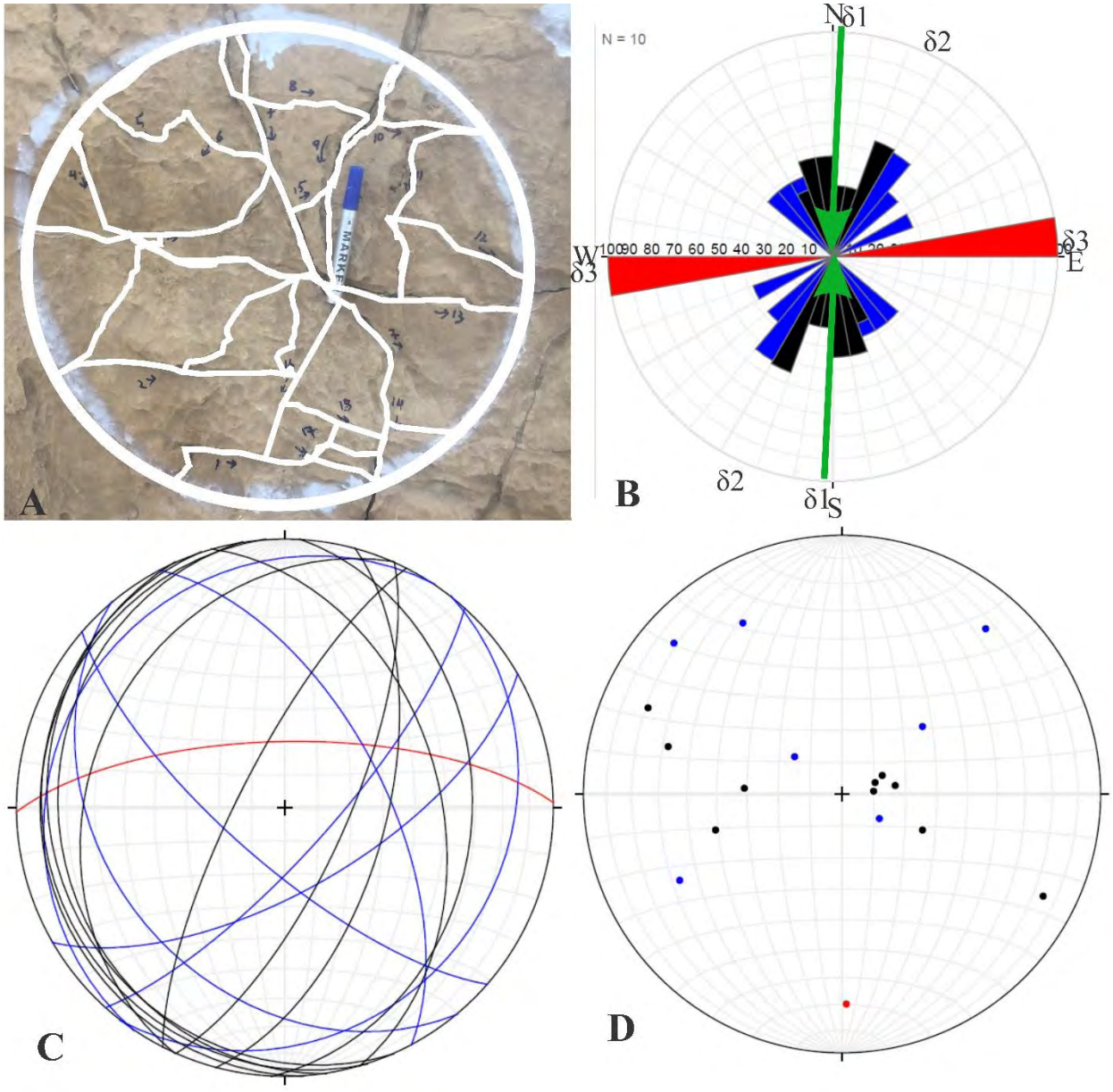

Figure 5. 28 (A) field photograph, (B) Rose diagram of fracture, (C) Plane data of fracture on Stereonet, (D) Poles data of fracture on Stereonet. Number of Release Fractures (Red color) are 01, Conjugate Fractures (Blue color) are 07 whereas Extension Fractures (Black color) are 10.

5.34 Station NO; 09

Area; Surghar Range Location; Mala khel

Altitude; 1216 GPS Location; 32°55'03.77"N, 71°09'19.11"E

Bed Strike; N81°E Bed Dip; 40°SE

Bed Thickness; Massive Bed Fracture Set; 04

Table 5. 29. Show fracture data of station 29.

S.NO	Strike	Dip	Length (CM)	Width (CM)	Open/Filled or Closed	Filled with	Remarks or Termination	Type
1	S84°E	70°SW	12	01	Open		One	Release
2	N04°E	77°SE	13	0.2	Filled	Calcite	One	Extension
3	N14°E	68°SE	08	0.5	One		One	Extension
4	N07°E	70°SE	33	0.2	One		Continuous	Extension
5	S37°E	42°SW	21	0.2	Filled	Calcite	One	Extension
6	S23°E	73°SW	24	0.5	Open		One	Extension
7	S66°W	33°NW	09	0.5	Open		Both	Release
8	S46°W	40°NW	09	0.5	Open		Both	Conjugate
9	S37°E	40°SW	23	0.1	Open		One	Extension
10	S20°W	52°NW	12	0.2	Open		Both	Extension
11	S51°W	45°NW	12	0.2	Open		One	Conjugate
12	S76°W	60°NW	20	0.2	Open		One	Release
13	S37°E	37°SW	19	01	Open		One	Extension
14	S36°W	28°NW	25	1.5	Open		One	Conjugate
15	S54°E	33°SW	06	0.5	Open		One	Conjugate
16	S48°W	34°NW	14	0.5	Open		One	Conjugate
17	S44°W	44°NW	23	0.2	Open		One	Conjugate
18	N15°E	69°SE	12	0.2	Open		Both	Extension

Calculation;

A. Fracture Density $(\partial) = (\Sigma L)/\pi\, r^2$

FD= 295/3.14 $(25)^2$

FD= 295/1962.5

FD= 0.150 cm^1

Open Fracture Density= 261/1962.5

FD= 0.132 cm^1

B. Fracture Porosity % = $\left(\frac{1}{A}\right) \sum_{i=1}^{N} (Li \times Wi) \times 100$

FP= (1/1962.5) (135) x 100

FP= 6.878%

C. Fracture Permeability (K) = $(3.5 \times 10^8)(\frac{1}{A}) \sum_{i=1}^{N}(Li \times Wi^3)$

K= (3.5×10^8) (1/1962.5) x 125.316

K= 22.349 $\times 10^6$ Darcy

D. Maximum Stress Direction; N12ºW

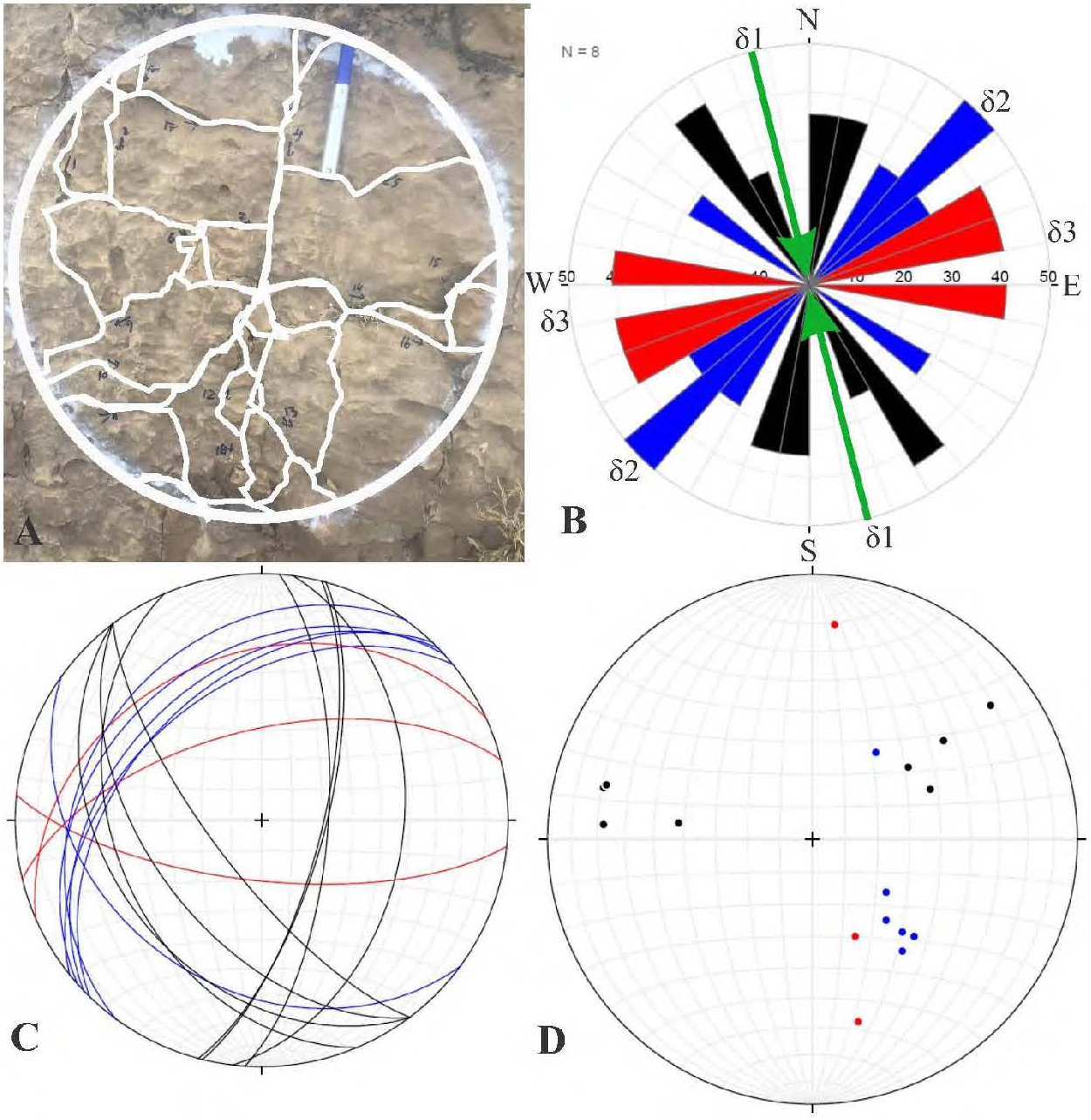

Figure 5. 29 (A) field photograph, (B) Rose diagram of fracture, (C) Plane data of fracture on Stereonet, (D) Poles data of fracture on Stereonet. Number of Release Fractures (Red color) are 03, Conjugate Fractures (Blue color) are 06 whereas Extension Fractures (Black color) are 09.

5.35 Station NO; 10

Area; Surghar Range | Location; Mala khel

Altitude; 1220 | GPS Location; 32°55'04.41"N, 71°09'19.22"E

Bed Strike; N82°W | Bed Dip; 32°NE

Bed Thickness; Massive Bed | Fracture Set; 04

Table 5. 30. Show fracture data of station 30.

S.NO	Strike	Dip	Length (CM)	Width (CM)	Open/Filled or Closed	Filled with	Remarks or Termination	Type
1	S88°W	17°NW	30	1.5	Open		Continuous	Release
2	S58°E	39°SW	11	01	Open		Both	Conjugate
3	S55°W	11°NW	50	1.5	Open		Continuous	Conjugate
4	S68°W	22°NW	21	01	Open		One	Release
5	S50°W	21°NW	16	0.6	Filled	Calcite	Both	Conjugate
6	S50°W	21°NW	14	0.2	Open		Both	Conjugate
7	S31°W	21°NW	10	0.5	Open		One	Extension
8	S33°W	21°NW	08	0.2	Open		One	Extension
9	S41°E	34°SW	11	0.6	Open		One	Conjugate
10	N11°W	45°NE	30	0.8	Open		Continuous	Extension
11	N28°W	51°NE	22	0.6	Open		One	Conjugate
12	N06°E	33°SE	16	0.2	Open		One	Extension
13	N64°W	66°NE	31	01	Open		Continuous	Release
14	S14°W	51°NW	27	01	Open		One	Extension
15	S83°E	64°SW	21	0.5	Open		Both	Release
16	S21°W	21°NW	09	0.5	Open		Both	Extension
17	N38°E	76°SE	06	0.2	Open		One	Extension
18	N42°E	77°SE	06	0.8	Open		One	Conjugate
19	S88°E	60°SW	10	0.5	Filled	Calcite	Both	Release
20	N16°W	31°NE	09	01	Open		Both	Extension
21	S39°E	18°SW	16	0.8	Open		Both	Conjugate

Calculation;

A. Fracture Density $(\partial) = (\Sigma L)/\pi\, r^2$

   FD= 374/3.14 $(25)^2$

   FD= 374/1962.5

   FD= 0.190 cm^1

   Open Fracture Density= 348/1962.5

   FD= 0.177 cm^1

B. Fracture Porosity % = $\left(\frac{1}{A}\right) \sum_{i=1}^{N} (Li \times Wi) \times 100$

FP= (1/1962.5) (323.8) x 100

FP= 16.499%

C. Fracture Permeability (K) = $(3.5 \times 10^8)(\frac{1}{A}) \sum_{i=1}^{N}(Li \times Wi^3)$

K= (3.5 $\times 10^8$) (1/1962.5) x 412.81

K= 73.622 $\times 10^6$ Darcy

D. Maximum Stress Direction; N18ºE

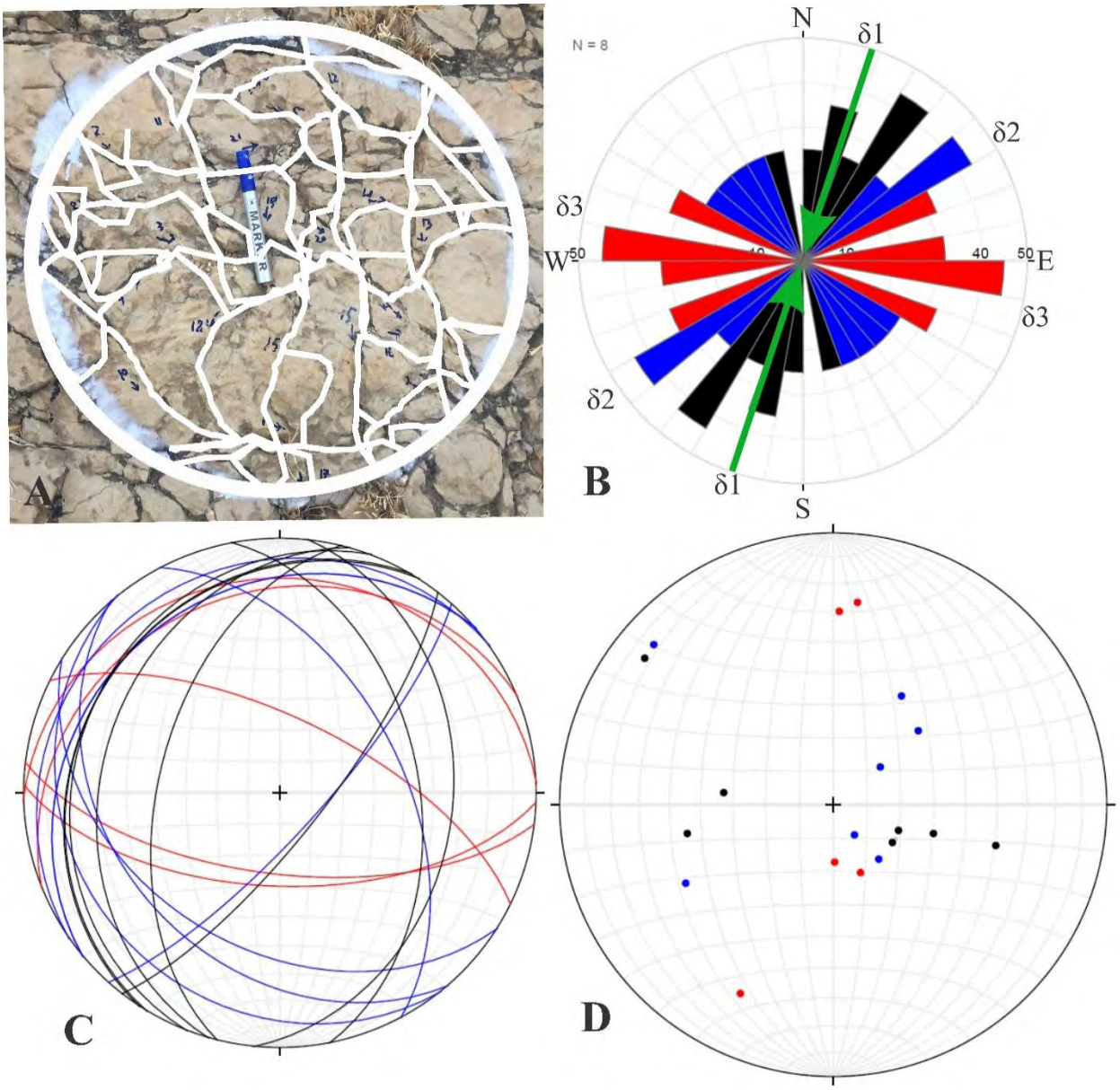

Figure 5. 30 (A) field photograph, (B) Rose diagram of fracture, (C) Plane data of fracture on Stereonet, (D) Poles data of fracture on Stereonet. Number of Release Fractures (Red color) are 05, Conjugate Fractures (Blue color) are 08 whereas Extension Fractures (Black color) are 08.

CHAPTER 06
DISCUSION AND CONCLUSIONS

The different types of fracture such as Release Fracture, Conjugate Fracture, and Extension Fracture are well developed in the study area. The collected data were used to determine the fracture density, fracture porosity and fracture permeability while the stress analysis was carried from rose diagram. For fracture analysis 30 sample stations were used in different sections of the Salt Range including Nammal Gorge, Zaluch Nala and Surghar Range Section. The fracture data i.e., fracture length, width, Orientation, termination, and type were identified from the bedding surface. Only open fracture were used for reservoir characterization while closed and filled fracture do not contribute to fracture porosity and fracture permeability. The circular inventory method was used to collect the fracture data. After calculating all parameters, the reservoir potential of each station were determine.

6.1 Fracture recorded in Salt Range

The fracture analysis of Kingriali Formation in Salt Range were carried out in three different sections Nammal Gorge Section, Zaluch Nala and Sur Ghar Range. A total of 543 fractures were recorded in 30 stations. Among these fractures 492 fractures are opened while the remaining 51 fractures were filled with calcite/quartz or close, this indicates the different chemical dissolution taken place at different strain episode. The Open fractures lack of chemical desolation indicating the low strain region at outcrop. Different types of fracture were recorded including 88 Release fracture, 208 Conjugate Fracture, and 247 Extension Fractures. The collected data in the field were used to calculate fracture density, Fracture Porosity, Fracture Permeability and Maximum stress direction were determined from their Rose diagram at each station.

Rose diagrams are common statistical plot for analyzing the orientation distribution of fractures within study area. The majority of fracture oriented in North-West, and North-East while One station oriented in South-East direction shown in table 6.1.

Section	S.NO	T.F	O.F	F/C.F	R.F	C.F	E.F	T.F.D cm^{-1}	O.F.D cm^{-1}	F.Po (%)	F.Pe (MD)	M.S.D
Nammal gorge	1	11	11	0	2	2	7	0.16	0.16	18.64	321.92	N23°W
	2	13	13	0	3	1	9	0.15	0.15	15.94	128.26	N09°W
	3	17	17	0	6	7	4	0.19	0.19	12.51	77.57	N18°W
	4	21	21	0	8	11	2	0.25	0.25	15.3	181.13	N39°W
	5	11	9	2	0	7	4	0.16	0.15	10.85	26.59	N29°W
	6	12	12	0	0	9	3	0.14	0.14	22.48	109.85	N12°W
	7	15	13	2	0	7	8	0.19	0.18	11.97	238.64	N33°W
	8	15	15	0	4	6	5	0.2	0.2	22.91	222.46	N14°W
	9	17	14	3	2	7	8	0.2	0.13	7.35	40.62	N13°W
	10	15	14	1	3	7	5	0.21	0.2	7.38	46.49	N03°W
Zaluch Nala	11	20	20	0	0	6	14	0.22	0.22	16.1	94.34	N27°W
	12	19	19	0	3	7	9	0.21	0.21	12.28	22.59	N24°W
	13	16	14	2	0	11	5	0.2	0.18	14.49	47.92	N07°W
	14	22	19	3	3	11	8	0.22	0.2	11.06	29.02	N05°W
	15	17	15	2	5	6	6	0.22	0.2	18.06	170.69	N04°W
	16	24	21	3	5	4	15	0.25	0.23	19.99	190.14	N29°W
	17	23	23	0	2	4	17	0.27	0.27	17.61	115.54	N29°W
	18	20	17	3	1	2	17	0.19	0.16	17.07	194.83	N03°E
	19	22	22	0	4	10	8	0.23	0.23	20.95	140.11	S53°E
	20	24	20	4	3	15	6	0.27	0.23	19.67	182.57	N05W

Surghar Range	21	18	18	0	3	6	9	0.18	0.18	9.88	20.46	N11°E
	22	16	14	2	2	8	6	0.18	0.16	10.03	39.83	N09°W
	23	18	18	0	2	7	9	0.15	0.15	8.14	17.03	N10°W
	24	20	14	6	2	8	10	0.19	0.15	16.72	99.87	N32°W
	25	24	22	2	8	2	14	0.25	0.24	25.67	241.92	N11°E
	26	18	16	2	3	8	7	0.19	0.17	8.95	47.47	N19°W
	27	18	13	5	5	8	5	0.16	0.12	6.715	13.59	N17°E
	28	18	13	5	1	7	10	0.17	0.12	7.138	14.48	N02°E
	29	18	16	2	3	6	9	0.15	0.13	6.88	22.35	N12°W
	30	21	19	2	5	8	8	0.19	0.18	16.45	73.62	N18°E

Table 6. 1 Detail of all fracture recorded at each Section and Sampling station. S.NO = Station number, T.F = Total Fracture, O.F = Open Fracture, F/C.F = Filled or Closed Fracture, R.F = Release Fracture, C.F = Conjugate Fracture, E.F = Extension Fracture, F.D = Fracture Density, F.P (%) = Fracture Porosity Percentage, F. Pe (MD) = Fracture Permeability Millidarcy .

6.2 Stress analysis

For stress analysis, fracture orientation data is plotted on a Rose Diagram, which gives a quick visual approximation of the direction of the stress in any given set of data. A concentric circle is typically overlaid on a series of radial lines in a Rose diagram. The maximum stress direction is parallel to the extensional fracture and perpendicular to the release fracture while the conjugate fracture lies in between them. In Nammal Gorge section he maximum stress direction of 10/10 sampling station lies in NW direction, in Zaluch Nala section he maximum stress direction of 8 sampling station lies in NW direction, 1 station lies in NE direction and 1 station lies in SE direction, in Surghar Range section the maximum stress direction of 5 sampling station lies in NW direction and 5 sampling station lies in NE direction. The overall maximum stress direction of 23 stations lies in NW direction, 6 stations in NE direction and 1 station lies in SE direction (figure 6.1). This indicates that the deformation i.e., Fold, fault, joint and fracture in study area is due to the North-South compressional stresses.

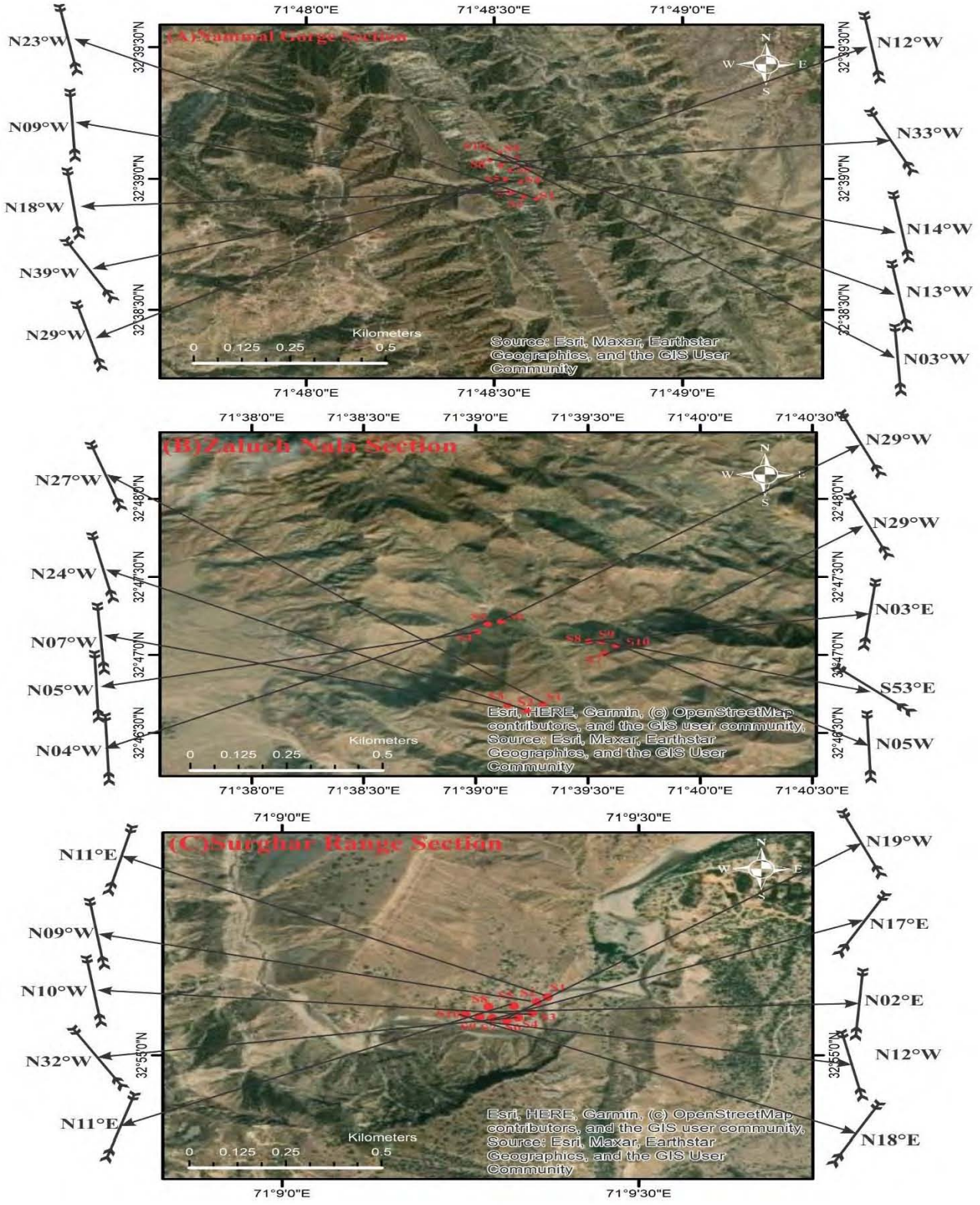

Figure 6. 1 The calculated maximum stress direction at each station shown on google Earth image.

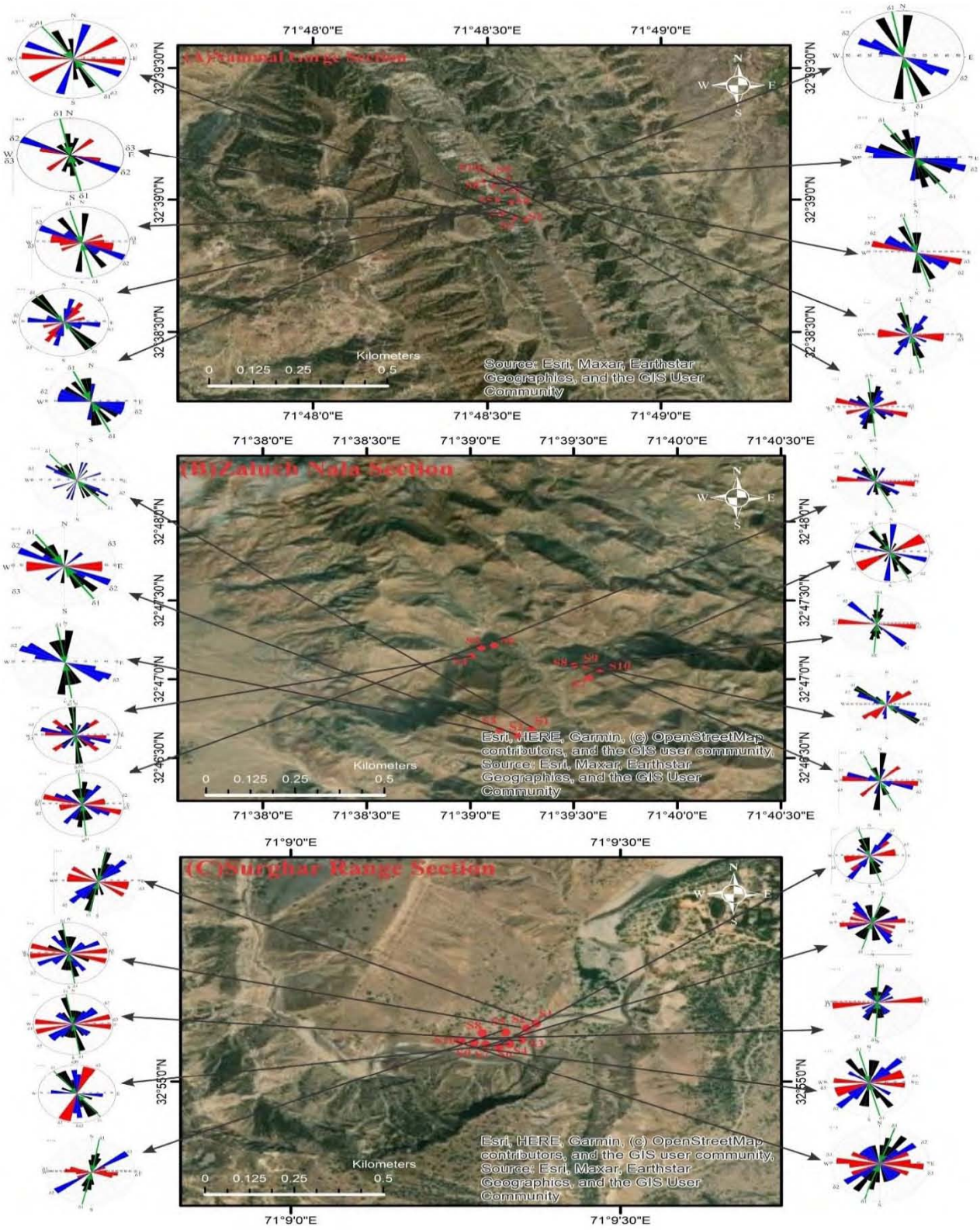

Figure 6. 2 Showing each Station location and their Rose Diagram on Google Earth image.

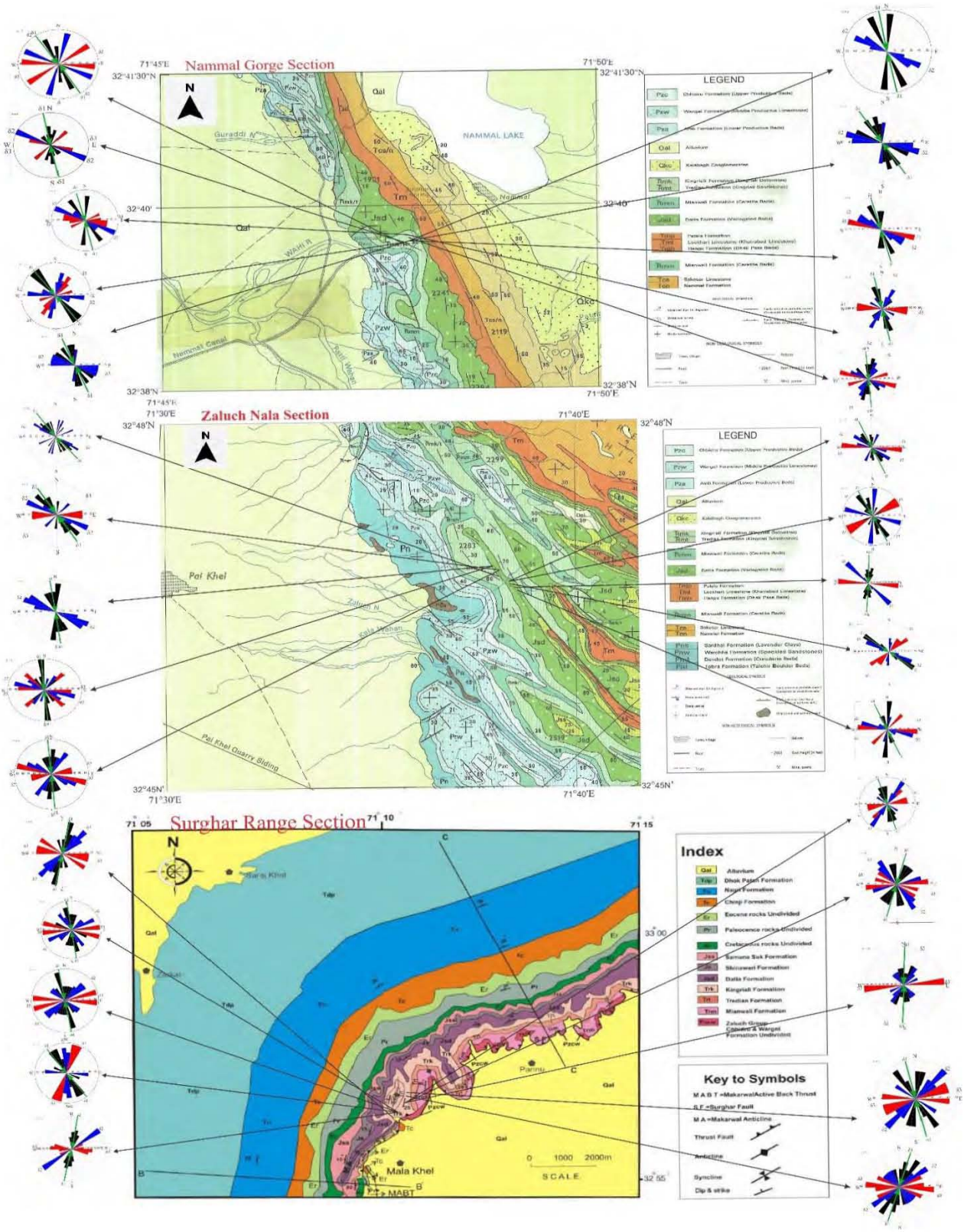

Figure 6. 3 Showing each station location and their rose diagram on geological map (from Gee, 1980; Banks et al., 1985).

6.3 Relationship between Fracture Density (CM^{-1}) and Fracture Porosity (%)

Fracture Porosity and Fracture Density typically have a linear relationship (Baitu et al.,2008). When computed open fracture density and porosity were plotted against one another to determine how they interacted (figure 6.3) the data revealed a weak linear connection. The fracture density entirely dependent on cumulative length of the fracture while fracture porosity depends on fracture width. The cross plot shows some divergence from the ideal positive linear trend because the widths of the open fractures measured at the different sampling points vary. In figure 6.4 The highest fracture porosity (25.67%) at station 25 from Surghar Range section, which is present at the right and top of the graph having relatively low open fracture density (0.24). this show at this station the fracture width is large. Similarly at station 29 from Surghar Section the lowest fracture porosity (6.88) and density (0.13) is present in extreme left and bottom. Generally, the various station sampling of the research area having moderate fracture density and porosity.

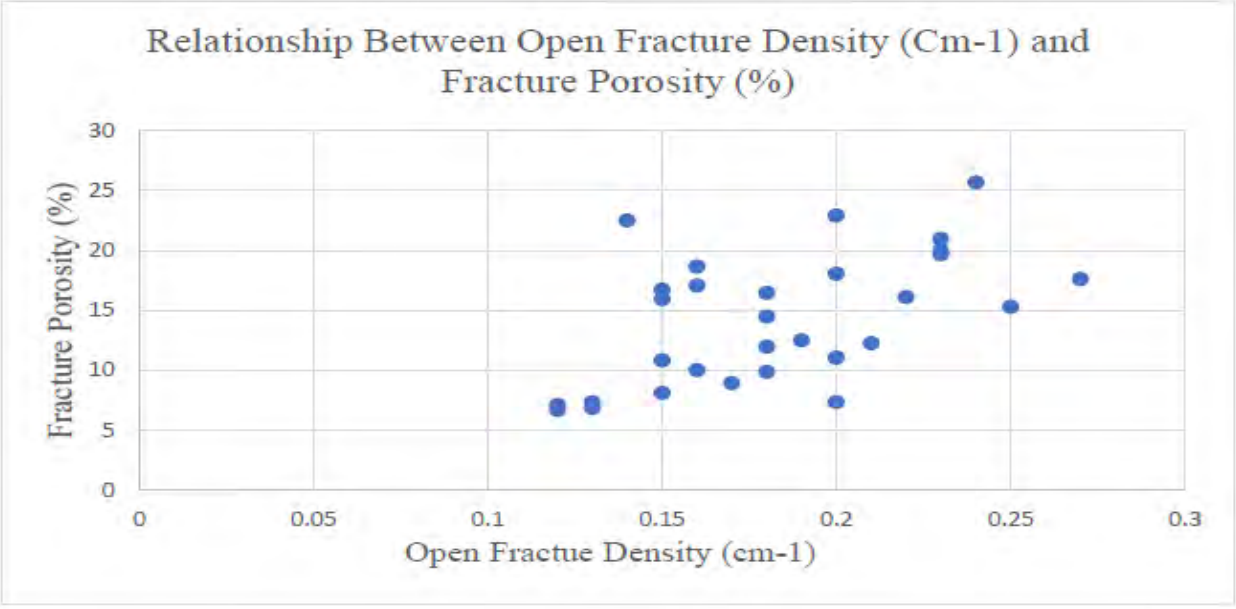

Figure 6. 4 Showing the relationship between Open Fracture Density (CM^{-1}) and Fracture Porosity (%)

6.4 Relationship Between Fracture density (CM^{-1}) and Fracture Permeability (MD)

The calculated fracture density and fracture permeability Results are crossly plotted to get a direct visual interpretation. The data show no relationship between these Parameters. The highest fracture permeability (338.64) determined at station NO 07 Nammal Gorge Section having lower

fracture density (0.19) (figure 6.5). It may be due to fracture width (table 6.1), as the fracture width increase the fracture permeability increase.

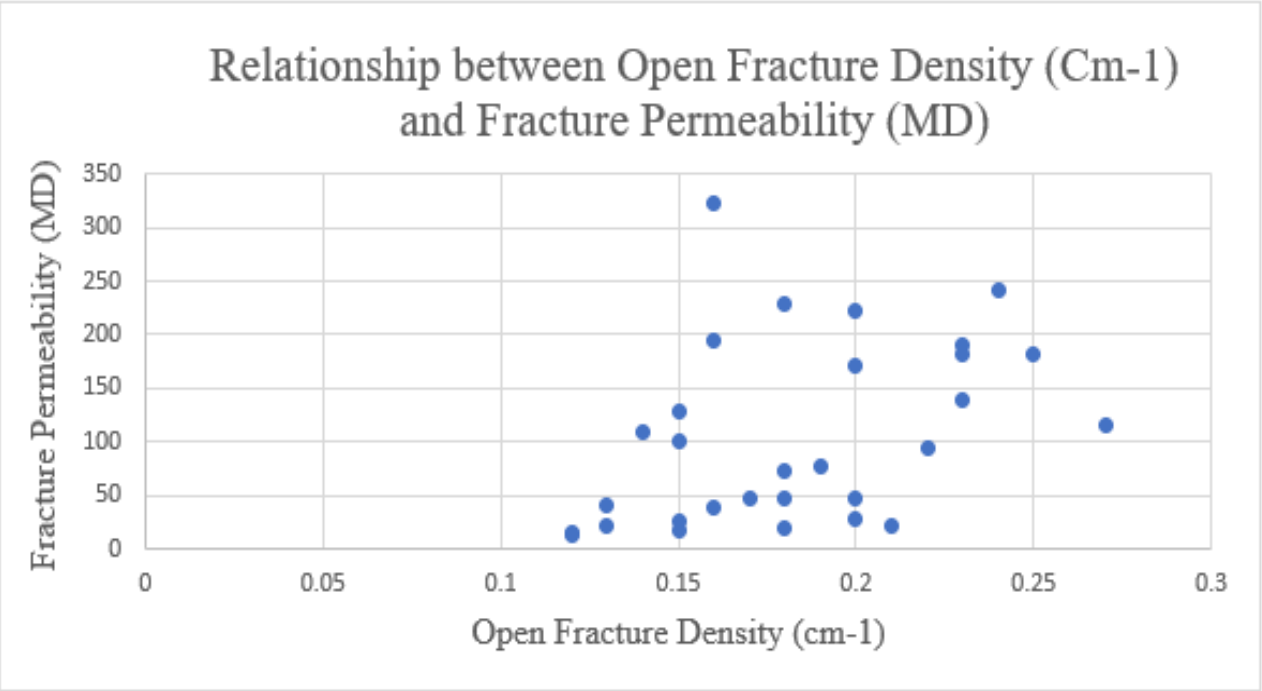

Figure 6. 5 Showing relationship between Open Fracture Density (CM^{-1}) and Fracture Permeability (MD)

6.5 Relationship between Fracture Porosity and Fracture Permeability

Fracture porosity depends on the width of fracture in inventory circle, while fracture permeability is dependent on the fracture connectivity. The permeability was calculated by multiplying the length of each individual fracture by cube of width, or (W^3), and dividing that result by the circumference of the inventory circle. As a result, there may be some variability in the trend of the displayed data, but generally, fracture permeability and fracture porosity show a modest positive association (figure 6.6)

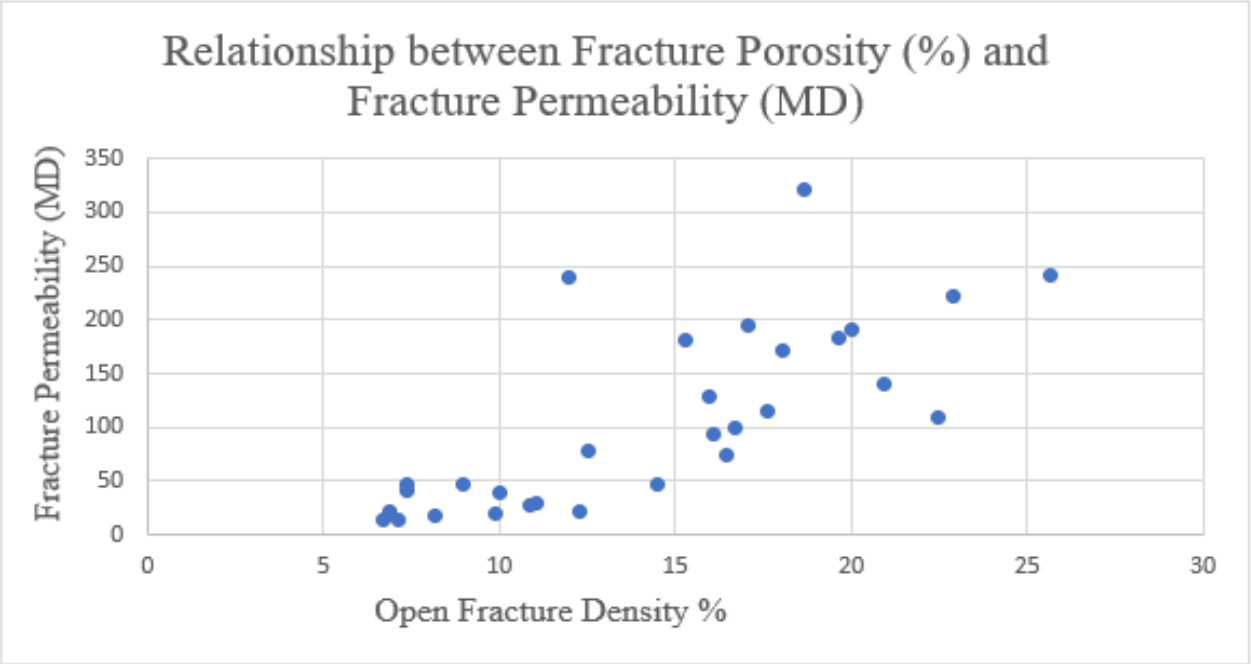

Figure 6. 6 Showing relationship between Fracture Porosity (%) and Fracture Permeability (MD)

6.6 Reservoir potential of each Section

Using the data and estimated results for each section, the reservoir potential has been determined. All of the sections were qualitatively assessed based on relative amounts in accordance with Nelson's, (2001) classification of the naturally fracture reservoir (NFR) system. In this classification, the permeability value of < 1 Mega Darcy (MD) is categorized in Type-4 category, 1-99 MD in Type-3, 100-200 MD in Type-2 and > 200 MD in Type-1 category (Table. 6.2).

Section	Open fracture Density cm^{-1}	Fracture Porosity (%)	Fracture Permeability (106 Darcy)	Type of Naturally Fracture Reservoir Rocks (NFR)
Nammal Gorge	0.12-0.25	7.35-22.91	26.56-321.64	Type-3 to Type-1
Zaluch Nala	0.16-0.27	9.88-20.95	20.46-194.83	Type-3 to Type -2
Surghar Rang	0.12-0.24	6.71-25.67	13.59-241.92	Type-3 to Type-1

Table 6. 2 Qualitative classification of each section according to Nelson, (2001) NFR category based on quantitative data.

6.6.1 Nammal Gorge Section

The data collected from Nammal Gorge section at 10 different stations, which have 3 stations type-1, 3 Stations type-2 and 4 Stations type-3 reservoir NFR classifications (Reservoir NFR Classifications= Type-3 to Type-1) (Table 6.3). According to the NFR classification Kingriali Formation in this section is a good reservoir. The Open Fracture Density, Fracture Porosity and fracture permeability data of Nammal Gorge section is given in table 6.3. the relationship between Open Fracture Density and Fracture Porosity is plotted in figure 6.7, while the relationship between Fracture porosity and Fracture Permeability data is denoted in figure 6.8.

Station No	Open fracture density cm^{-1}	Fracture porosity (%)	Fracture permeability (10^6 Darcy)	Type of Naturally fracture reservoir Rock (NFR)
1	0.16	18.64	321.92	Type-1
2	0.15	15.94	128.26	Type-2
3	0.19	12.51	77.57	Type-3
4	0.25	15.3	181.13	Type-2
5	0.15	10.85	26.59	Type-3
5	0.14	22.48	109.85	Type-2
7	0.18	11.97	238.64	Type-1
8	0.2	22.91	222.46	Type-1
9	0.13	7.35	40.62	Type-3
10	0.2	7.38	46.49	Type-3

Table 6. 3 Qualitative classification of Nmmal Gorge Section according to Nelson, (2001) NFR classification on the basis of quantitative data.

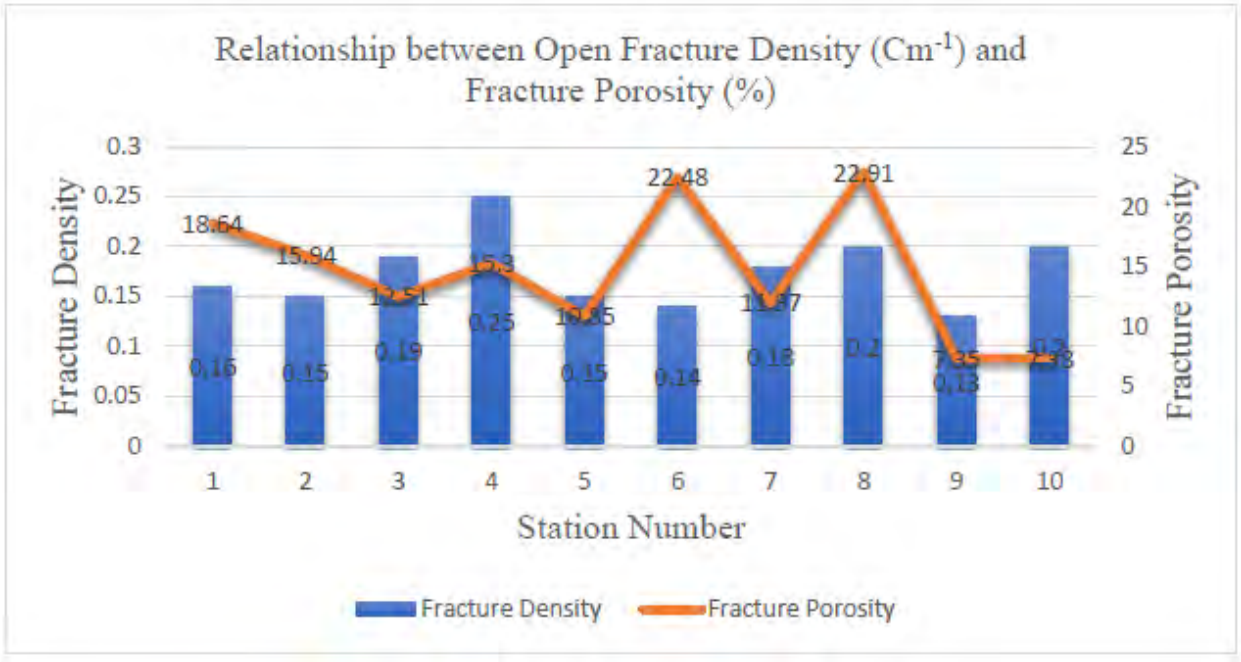

Figure 6. 7 Showing the relationship between Open Fracture Density (CM^{-1}) and Fracture Porosity (%)

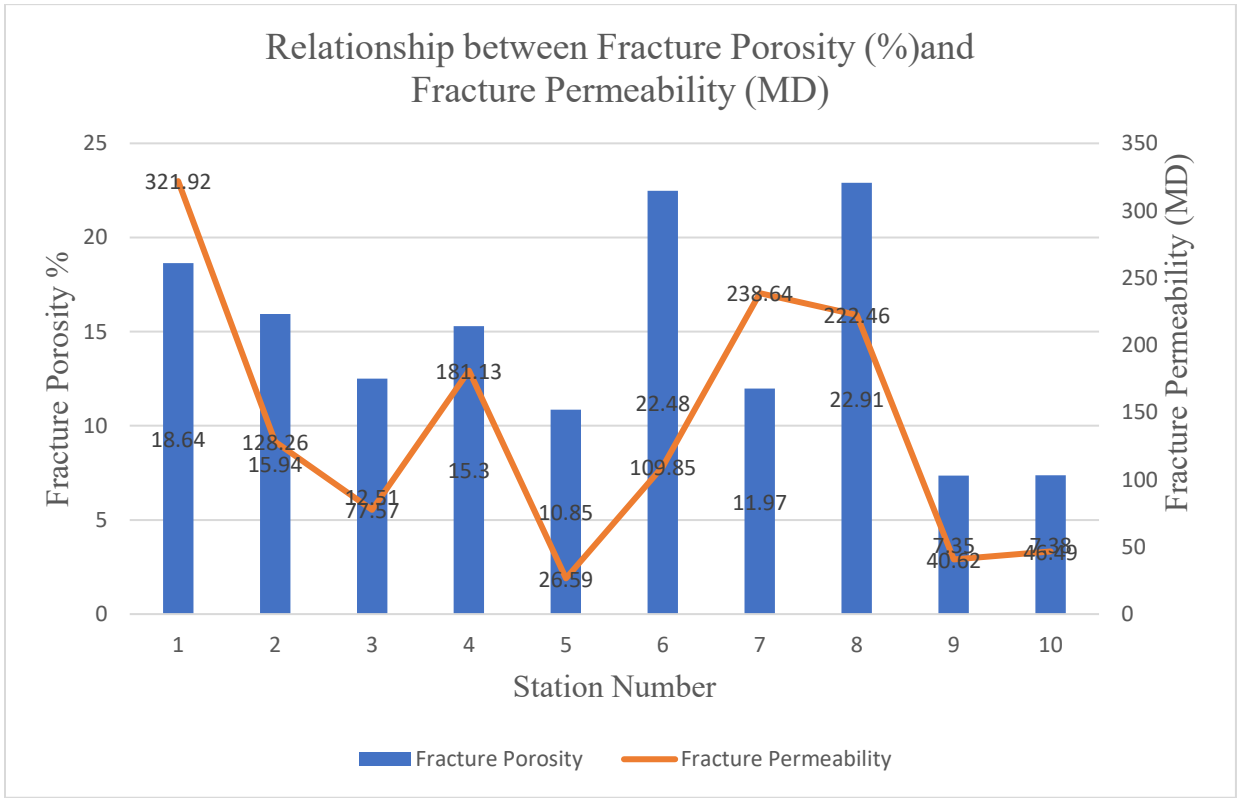

Figure 6. 8 Showing relationship between Fracture Porosity (%) and Fracture Permeability (MD)

6.6.2 Zaluch Nala Section

The data collected from Zaluch Nala section at 10 different stations, which have 4 stations type-3, and 6 Stations Type-2 reservoir NFR classifications (Reservoir NFR Classifications= Type-3 to Type-2) (Table 6.4). According to the NFR classification Kingriali Formation in this section is a good reservoir. The Open Fracture Density, Fracture Porosity and fracture permeability data of Zaluch Nala section is given in table 6.4. the relationship between Open Fracture Density and Fracture Porosity is plotted in figure 6.9. while the relationship between Fracture porosity and Fracture Permeability data is denoted in figure 6.10.

Station No	Open fracture density cm^{-1}	Fracture porosity (%)	Fracture permeability (10^6 Darcy)	Type of Naturally fracture reservoir Rock (NFR)
1	0.22	16.1	94.34	Type-3
2	0.21	12.28	22.59	Type-3
3	0.18	14.49	47.92	Type-3
4	0.2	11.06	29.02	Type-3
5	0.2	18.06	170.69	Type-2
5	0.23	19.99	190.14	Type-2
7	0.27	17.61	115.54	Type-2
8	0.16	17.07	194.83	Type-2
9	0.23	20.95	140.11	Type-2
10	0.23	19.67	182.57	Type-2

Table 6. 4 Qualitative classification of Zaluch Nala Section according to Nelson (2001) NFR classification on the basis of quantitative data.

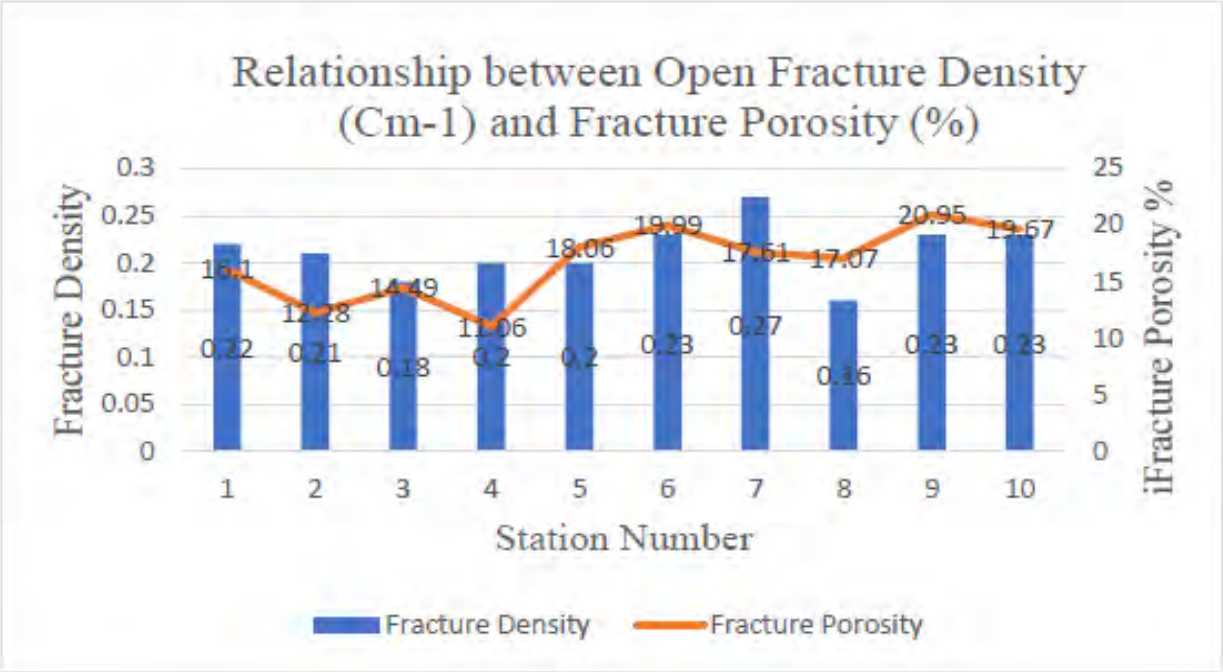

Figure 6. 9 Showing the relationship between Open Fracture Density (CM^{-1}) and Fracture Porosity (%)

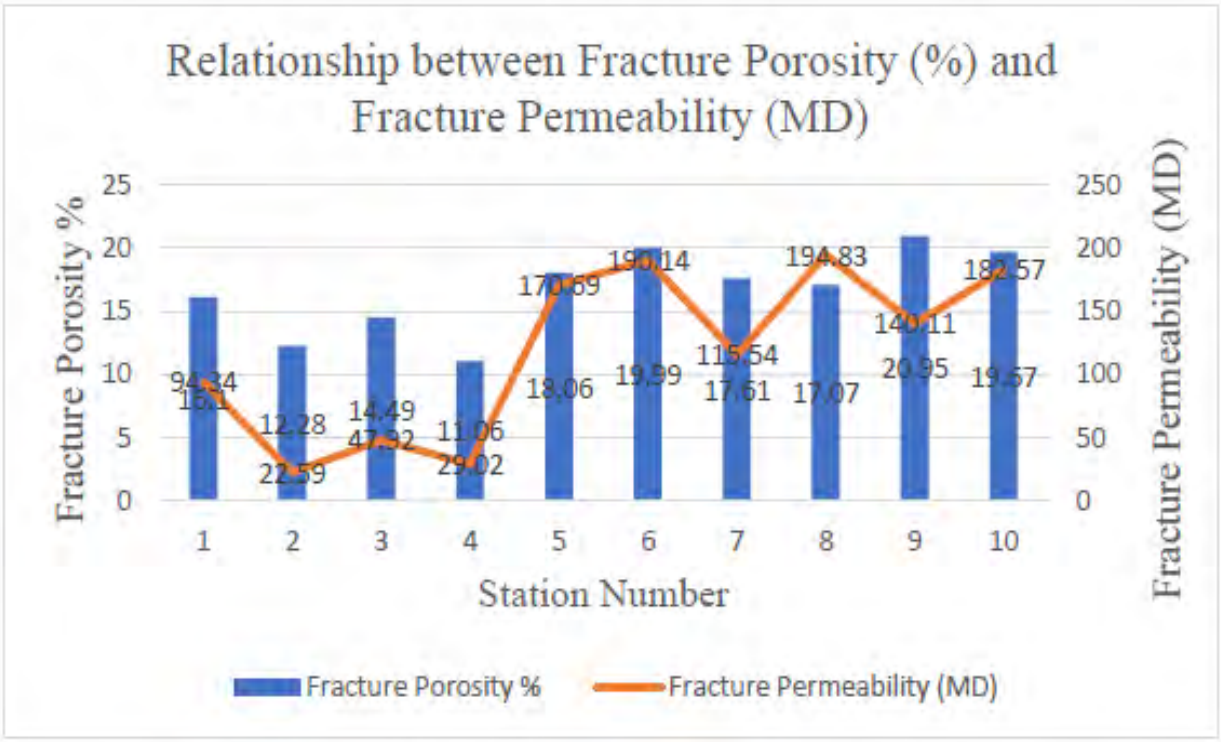

Figure 6. 10 Showing relationship between Fracture Porosity (%) and Fracture Permeability (MD*)*

6.6.3 Surghar Range Section

The data collected from Surghar Range section at 10 different stations, which have 1 stations type-1, and 9 Stations Type-3 reservoir NFR classifications (Reservoir NFR Classifications= Type-3 to Type-1) (Table 6.5). According to the NFR classification Kingriali Formation in this section is a good reservoir. The Open Fracture Density, Fracture Porosity and fracture permeability data of Surghar Range section is given in table 6.5. The relationship between Open Fracture Density and Fracture Porosity is plotted in figure 6.11. while the relationship between Fracture porosity and Fracture Permeability data is denoted in figure 6.12.

Station No	Open fracture density cm^{-1}	Fracture porosity (%)	Fracture permeability (10^6 Darcy)	Type of Naturally fracture reservoir Rock (NFR)
1	0.18	9.88	20.46	Type-3
2	0.16	10.03	39.83	Type-3
3	0.15	8.14	17.03	Type-3
4	0.15	16.72	99.87	Type-3
5	0.24	25.67	241.92	Type-1
5	0.17	8.95	47.47	Type-3
7	0.12	6.715	13.59	Type-3
8	0.12	7.138	14.48	Type-3
9	0.13	6.88	22.35	Type-3
10	0.18	16.45	73.62	Type-3

Table 6. 5 Qualitative classification of Surghar Range Section according to Nelson (2001) NFR classification on the basis of quantitative data.

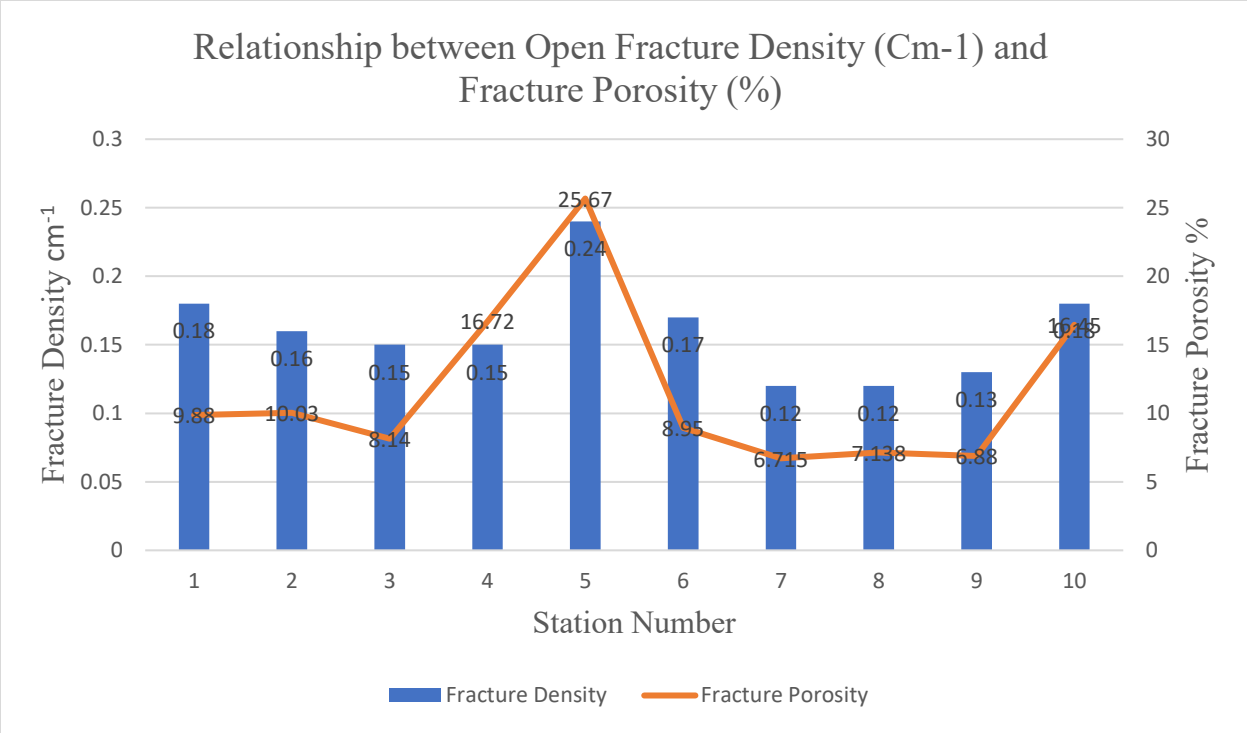

Figure 6. 11 Showing the relationship between Open Fracture Density (CM^{-1}) and Fracture Porosity (%)

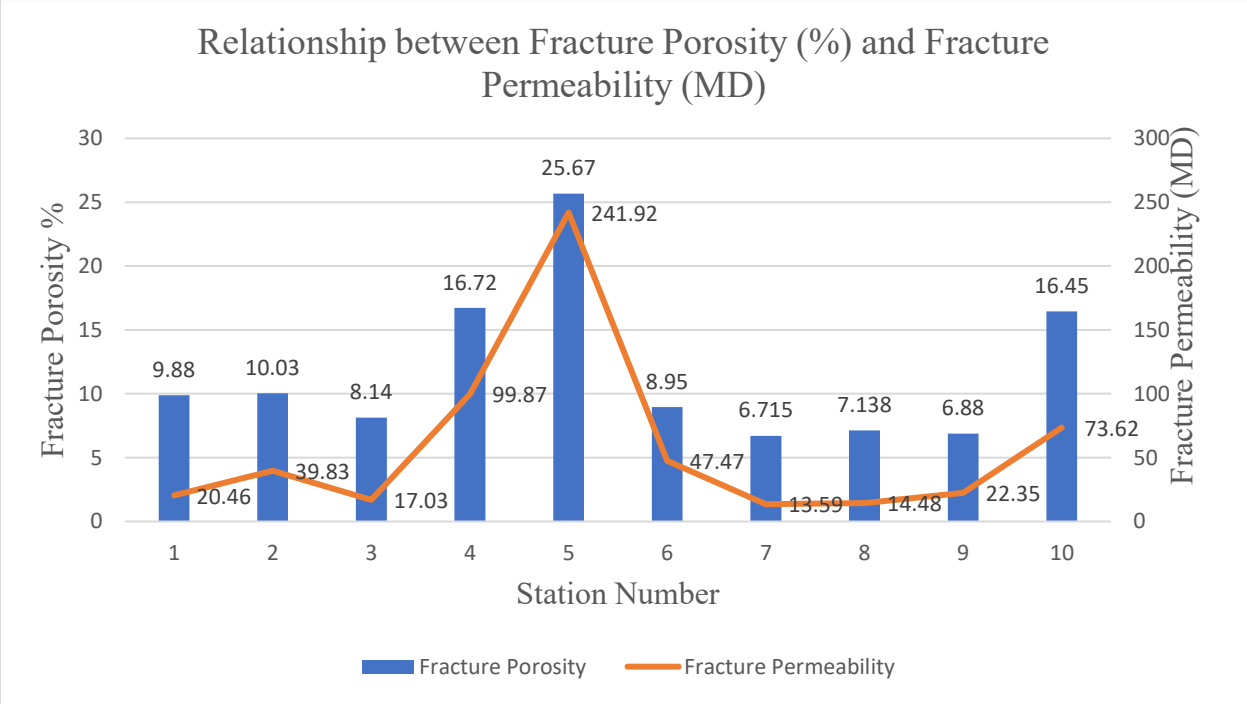

Figure 6. 12 Showing relationship between Fracture Porosity (%) and Fracture Permeability (MD).

CONCLUSION

The Research area has undergone extensive deformation, as shown by the numerous faults and folds (thrust belt) brought on by compressional forces. In study area Fracture porosity and fracture permeability are determined only from open fracture data. The maximum stress direction of each station is determined from the strike data plotted on Rose diagram. The principal findings of the research are described below.

1. The regional compressional stresses in the study area are primarily oriented in the NW-SE direction.
2. The research area a total of fracture 543 fracture was recorded which have 492 Open fractures while the remaining 51 fractures are closed or filled with quartz and calcite.
3. Different types of fracture were recorded including 88 Release fracture, 208 Conjugate Fracture, and 247 Extension Fractures.
4. The order of structural Deformation is an ascending order from Zaluch Nala section, Surghar Range section, and Nammal Gorge section.
5. According to the fracture data Nammal Gorge and Surghar Range Section have the highest reservoir potential while Zaluch Nala have comparatively low reservoir potential.
6. The filled fracture affects secondary permeability, which in high stress region is filled with calcite and quartz.

REFERENCES

Abdulghani, A.; Ghazi, S.; Riaz, M.; Zafar, T. Sedimentary fabrics and diagenetic features of the Late Triassic Kingriali Formation, Khisor-Marwat ranges, Pakistan. *Indian J. Geo-Mar. Sci.* **2020**, *49*, 954–964.

Ahmad, I., & Jehan, N., Occurrence of a melange along the Malakand pass north of Dargai, northern Pakistan. *Journal of Himalayan Earth Sciences*, **2006**, *39*, 55-59.

Ahmad, I., Shah, M. M., Janjuhah, H. T., Trave, A., Antonarakou, A., & Kontakiotis, G. (2022). Multiphase Diagenetic Processes and Their Impact on Reservoir Character of the Late Triassic (Rhaetian) Kingriali Formation, Upper Indus Basin, Pakistan. *Minerals*, *12*(8), 1049.

Ahmad, S, A Comparative study of Structural Styles in the Kohat Plateau, NW Himalayas, NWFP, Pakistan: University of Peshawar, 2003.

Ahmad, S., Hamidullah, S., Irfan, M., and Ali, A., Structural transect of the western KohatFold and Thrust Belt between Hangu and Basia Khel, NWFP, Pakistan, PAPG: ATC, conference proceedings, 2004.

Aitchison, J. C., Ali, J. R., & Davis, A. M., When and where did India and Asia collide?. *Journal of Geophysical Research: Solid Earth*, **2007**, *112*(B5).

ALAM, I. (2008). *STRUCTURAL AND STRATIGRAPHIC FRAMEWORK OF THE MARWAT-KHISOR RANGES, NW. FP, PAKISTAN* (Doctoral dissertation, University of Peshawar).

Alam, I., Ahmad, S., Ali, A., & Irfan, M. (2005). Fold-thrust styles in the Marwat-Khisor Ranges, NWFP, Pakistan. In *PAPG, ATC 2005, conference proceedings* (pp. 80-93).

Alam, I., Structural and Stratigraphic framework of the Marwat-Khisor ranges, NWFP, Pakistan, *Unpublished Ph. D. thesis, NCEG, University of Peshawar, Pakistan,* **2008**.

Alam, I.; Ahmad Sr, S.; Ali, F.; Khan, M.W. Architecture of fold-thrust assemblages in the Marwat-Khisor ranges of the outer Himalayan Orogenic Belt of Pakistan. *J. Himal. Earth Sci.* **2015**, *48*, 9.

Ali, A., Structural Analysis of the Trans-Indus Ranges: Implications for the hydrocarbon potential of the NW Himalayas, Pakistan: University Of Peshawar, Peshawar, 2010.

Ali, F., Khan, M. I., Ahmad, S., Rehman, G., Rehman, I., & Ali, T. H. (2014). Range front structural style: an example from Surghar Range, North Pakistan. *Journal of Himalayan Earth Sciences*, *47*(2), 193.

Argles, T. W. (2000). The evolution of the Main Mantle Thrust in the Western Syntaxis, Northern Pakistan. *Geological Society, London, Special Publications*, *170*(1), 101-122.

Baitu, A. H., Sheikh, R. A., Ahmad, N. A. Z. I. R., Javed, A., Rehman, A., & Wahab, A. B. D. U. L. (2008). Fracture analysis of Eocene Sakesar limestone Mardwal anticline, Soan-Sakesar valley, western part of central Salt Range, district Khushab, Pakistan. *Geol. Bull. Punjab Univ*, *43*, 121-130.

Baitu, A. H., Sheikh, R. A., Ahmad, N. A. Z. I. R., Javed, A., Rehman, A., & Wahab, A. B. D. U. L. (2008). Fracture analysis of Eocene Sakesar limestone Mardwal anticline, Soan-Sakesar valley, western part of central Salt Range, district Khushab, Pakistan. *Geol. Bull. Punjab Univ*, *43*, 121-130.

Baitu, A.; Sheikh, R. A.; Ahmad, N.; Javed, A.; Rehman, A.; Wahab, A. Fracture analysis of Eocene Sakesar limestone at Mardwal Anticline, Soan-Sakesar valley, Western part of Central Salt Range, District Khushab, Pakistan. *Geological Bulletin, University of Punjab,* **2008**, *43*, 121-130.

Bannert, D., Khan, Moin R, Indian Plate Collision in Pakistan and Myanmar and its Impact on Hydrocarbon Prospectivity, AAPG International Conference: Milano, Italy, 2012.

Bellahsen, N.; Fiore, P.; Pollard, D. D. The role of fractures in the structural interpretation of Sheep Borneman, N. L., Hodges, K. V., Van Soest, M. C., Bohon, W., Wartho, J. A., Cronk, S. S., & hafee, T. Age and structure of the Shyok suture in the Ladakh region of northwestern India: implications for slip on the Karakoram fault system. *Tectonics*, **2015**, *34*(10), 2011-2033.

Bouilhol, P., Jagoutz, O., Hanchar, J. M., & Dudas, F. O., Dating the India–Eurasia collision through arc magmatic records. *Earth and Planetary Science Letters*, *366*, **2013**, 163-175.

Chatterjee, S., India‘s Northward Drift from Gondwana to Asia During the Late Cretaceous-Eocene, *Proceedings of the Indian National Science Academy,* **2017**, *82*, (3), 479-487.

Chaudhry, M. N., & Ghazanfar, M. (1993). Some tectonostratigraphic observations on northwest Himalaya. Pakistan. *Pakistan Journal of Geology*, *1*(2), 1-19.

Chemenda, A. I., Burg, J. P., & Mattauer, M., Evolutionary model of the Himalaya–Tibet system: geopoem: based on new modelling, geological and geophysical data. *Earth and Planetary Science Letters*, **2000**, *174*(3-4), 397-409.

Cosgrove, J. Forced folds and fractures: An introduction. *Geological Society, London, Special Publications,* **1999**, *169*, (1), 1-6.

Cotter, G. D. P. (1933). The geology of the part of the Attock district west of longitude 72 45 E. *Memoirs of the Geological Survey of India*, *55*(2), 63-161.

Cotter, G. D. P. (1933, July). Notes on the Geological Structure and Distribution of the Oil-Bearing Rocks of India and Burma. In *World Petroleum Congress* (pp. WPC-1003). WPC.

Crupa, W. E., Khan, S. D., Huang, J., Khan, A. S., and Kasi, A., Active tectonic deformation of the western Indian plate boundary: A case study from the Chaman Fault System, *Journal of Asian Earth Sciences,* **2017**, *147*, 452-468.

Danilchik, W. (1961). The iron formation of the Surghar and western Salt Range, Mianwali District, West Pakistan. *US Geol Surv Prof Pap*, *424*, 228-231.

Danilchik, W., & Shah, S. M. (1975). *Stratigraphic nomenclature of formations in the Trans-Indus Mountains, Mianwali District, Pakistan* (No. 75-622). US Geological Survey,

Danilchik, W., & Shah, S. M. I. (1967). Stratigraphic nomenclature of formations in TransIndus Mountains Mianwali District, West Pakistan. *US. Geological Survey Project Report*, 33-45.

Dasti, N., Akram, S., Ahmad, I., & Usman, M. (2018). Rock fractures characterization in Khairi Murat Range, Sub Himalayan fold and thrust belt, North Pakistan. *The Nucleus*, *55*(3), 115-127.

Dasti, N.; Akram, S.; Ahmad, I.; Usman, M. Rock Fractures Characterization in Khairi Murat Range, Sub Himalayan Fold and Thrust Belt, North Pakistan. *The Nucleus,* **2018**, *55*, (3), 115-127.

Davies, L. M. (1930). The fossil fauna of the Samana Range and some neighbouring areas, The Palaeocene Foraminifera/by LM Davies.

Davies, L. M., & Pinfold, E. S. (1937). The Eocene beds of the Punjab, Salt Range: Mem. Geol. Surv. India, Pal. Indica. *New Ser*, *24*(1), 1-79.

Davis, G. H.; Reynolds, S. J.; Kluth, C. F. *Structural geology of rocks and regions*: John Wiley & Sons: **2011**.

Dunbar, C. O. (1933). *Stratigraphic Significance of the Fusulinids of the Lower Products [sic] Limestone of the Salt Range...*

Faisal, S., & Dixon, J. M. (2015). Physical analog (centrifuge) model investigation of contrasting structural styles in the Salt Range and Potwar Plateau, northern Pakistan. *Journal of Structural Geology*, *77*, 277-292.

Fatmi, A. N., & MR, C. (1972). EARLY JURASSIC CEPHALOPODS FROM KHISOR-MARWAT RANGES (SHAIKH BUDIN HILLS) DERA ISMAIL KHAN DISTRICT, NWFP, PAKISTAN.

Gaetani, M.; Garzanti, E. Multicyclic history of the northern India continental margin (northwestern Himalaya). *AAPG Bull.* **1991**, *75*, 1427–1446.

Gee, E. R., & Gee, D. G. (1989). Overview of the geology and structure of the Salt Range, with observations on related areas of northern Pakistan. *Geological Society of America special paper*, *232*, 95-112.

Gee, G., Higginson, W. C. E., Levesley, P., & Taylor, K. J. (1959). 266. Polymerisation of epoxides. Part I. Some kinetic aspects of the addition of alcohols to epoxides catalysed by sodium alkoxides. *Journal of the Chemical Society (Resumed)*, 1338-1344.

Golonka, J., *Paleozoic paleoenvironment and paleolithofacies maps of Gondwana*; AGH University of Science and Technology Press: 2012.

Green, O. R., Searle, M. P., Corfield, R. I., & Corfield, R. M., Cretaceous-Tertiary carbonate platform evolution and the age of the India-Asia collision along the Ladakh Himalaya (northwest India). *The Journal of Geology*,**2008**, *116*(4), 331-353.

Gross, M. R.; Eyal, Y. Throughgoing fractures in layered carbonate rocks. *Geological Society of America Bulletin,* **2007**, *119*, (11-12), 1387-1404.

Hemphill, W. R., and Kidwai, A. H., Stratigraphy of the Bannu and Dera Ismail Khan areas, Pakistan, **1973**, 2330-7102.

Hennings, P. H.; Olson, J. E.; Thompson, L. B. Combining outcrop data and three-dimensional structural models to characterize fractured reservoirs: An example from Wyoming. *AAPG bulletin,* **2000**, *84*, (6), 830-849.

Hinsbergen V., D. J., Lippert, P. C., Dupont-Nivet, G., McQuarrie, N., Doubrovine, P. V., Spakman, W., & Torsvik, T. H., Greater India Basin hypothesis and a two-stage Cenozoic collision between India and Asia. *Proceedings of the National Academy of Sciences*, **2012**, *109*(20), 7659-7664.

Hunt, L., Chopra, S., Reynolds, S., & Hadley, S. (2009). On calibrating curvature data to fracture density: causes. *CSEG Recorder*, *34*(10), 27-32.

Hussain, B. R. (1967). Saiduwali Member, a new name for the lower part for the Permian Amb Formation, West Pakistan. Karachi University Studies. *Science and Technology*, *4*, 88-95.

Hussain, H., & Zhang, S. (2018). Structural evolution of the Kohat Fold and thrust Belt in the shakardarra area (south eastern Kohat, Pakistan). *Geosciences*, *8*(9), 311.

Iqbal, S., Jan, I. U., & Hanif, M. (2014). The Mianwali and Tredian formations: An example of the Triassic Progradational deltaic system in the low-latitude western Salt Range, Pakistan. *Arabian Journal for Science and Engineering*, *39*, 5489-5507.

Iqbal, S.; Wagreich, M.; Bibi, M.; Jan, I.U.; Gier, S. Multi-Proxy Provenance Analyses of the Kingriali and Datta Formations (Triassic–Jurassic Transition): Evidence for Westward Extension of the Neo-Tethys Passive Margin from the Salt Range (Pakistan). *Minerals* **2021**, *11*, 573.

Irving, R. W., Leather, P., & Gusfield, D. (1987). An efficient algorithm for the "optimal" stable marriage. *Journal of the ACM (JACM)*, *34*(3), 532-543.

Jadoon, I. A., Bhatti, K. M., Siddiqui, F. I., Jadoon, S. K., Gilani, S. R., & Afzal, M. (2005, November). Subsurface fracture analysis in carbonate reservoirs: kohat/potwar plateau, north Pakistan. In *SPE/PAPG Pakistan Section Annual Technical Conference* (pp. SPE-111051). SPE.

Jadoon, W. A., Shami, B. A., & Abbasi, I. A. (2003, October). Fracture analysis of Khaur anticline and its implications on subsurface fracture system. In *PAPG-SPE annual technical conference and oil show* (pp. 3-5).

Jadoon, W. A.; Shami, B.; Abbasi, I. A. In *Fracture analysis of Khaur anticline and its implications on subsurface fracture system*, PAPG-SPE Annual Technical Conference and

Jain, A., When did India–Asia collide and make the Himalaya?, *Current Science,* **2014**, 254-266.

Kayal, J. R., *Microearthquake seismology and seismotectonics of South Asia*. Springer Science & Business Media, 2008.

Kazmi, A. H., & Jan, M. Q. (1997). Geology and tectonics of Pakistan.

Khan, M. A., Hussain, S. R. J., Ali, B., Ali, S., Khan, M. J., & Mehmood, S. (2017). Microfacies analysis and depositional setting of the late Permian Wargal limestone exposed at Nammal Gorge, Western Salt Range, Pakistan. *Bahria University Research Journal of Earth Sciences*, *2*, 46-51.

Khan, M. I., Ahmad, S., Khan, A. A., & Ali, A. (2007). Fracture network analysis of Samana anticline: a fault-related fold at the front of Samana Range, Orakzai Agency, NWFP, Pakistan. *Pakistan Journal of Hydrocarbon Research*, *17*, 103-114.

Khan, N.; Jan, I.U.; Iqbal, S.; Swennen, R.; Hersi, O.S.; Hussain, H.S. Bulk organic geochemical and palynofacies analyses of the Hettangian Datta Formation (Potwar Basin, Pakistan): Regional comparison with the time equivalent Lathi Formation (Jaisalmer Basin, India). *J. Earth Syst. Sci.* **2021**, *130*, 148.

Khan, S. D., Walker, D. J., Hall, S. A., Burke, K. C., Shah, M. T., & Stockli, L., Did the Kohistan-Ladakh island arc collide first with India?. *Geological Society of America Bulletin*, **2009**, *121*(3-4), 366-384.

Kugler, F., & Waagen, G. F. (1879). *Handbook of Painting: The German, Flemish, and Dutch Schools*. J. Murray.

Kümmel, H., Mattauch, J. H. E., Thiele, W., & Wapstra, A. H. (1966). A new mass law with shell and deformation corrections. *Nuclear Physics*, *81*(2), 129-154.

Kutschera, U., Symbiogenesis, natural selection, and the dynamic Earth, *Theory in Biosciences,* **2009**, *128*, (3), 191.

Lavé, J., & Avouac, J. P. (2000). Active folding of fluvial terraces across the Siwaliks Hills, Himalayas of central Nepal. *Journal of Geophysical Research: Solid Earth*, *105*(B3), 5735-5770.

Lewis, G. E. (1937). Taxonomic syllabus of Siwalik fossil anthropoids. *American Journal of Science*, *5*(200), 139-147.

Lewis, M. A., Cheney, C. S., & O Dochartaigh, B. E. (2006). Guide to permeability indices.

Lillie, R. J., Johnson, G. D., Yousuf, M., Zamin, A. S. H., & Yeats, R. S. (1987). Structural development within the Himalayan foreland fold-and-thrust belt of Pakistan.

Malinconico, L.L., The structure of the Kohistan-Arc terrane in northern Pakistan as inferred from gravity data. *Tectonophysics*, **1986**, *124*(3-4), 297-307.

Malkani, M.S.; Mahmood, Z. Stratigraphy of Pakistan. *Geol. Surv. Pak. Mem.* **2017**, *24*, 1–134.

Marshak, S., & Mitra, G. (1988). Basic methods of structural geology.

Mountain Anticline, Wyoming. *Journal of Structural Geology,* **2006**, *28*, (5), 850-867.

Muskat, M. (1949). The theory of potentiometric models. *Transactions of the AIME*, *179*(01), 216-221.

Muttoni, G., Kent, D. V., Garzanti, E., Brack, P., Abrahamsen, N., & Gaetani, M., Early Permian Pangea ‗B'to Late Permian Pangea ‗A'. *Earth and Planetary Science Letters*, **2003**, *215*(3-4), 379-394.

Mynatt, I., Seyum, S., & Pollard, D. D. (2009). Fracture initiation, development, and reactivation in folded sedimentary rocks at Raplee Ridge, UT. *Journal of Structural Geology*, *31*(10), 1100-1113.

Mynatt, I.; Seyum, S.; Pollard, D. D. Fracture initiation, development, and reactivation in folded sedimentary rocks at Raplee Ridge, UT. *Journal of Structural Geology,* **2009**, *31*, (10),

Nelson, R. A. (2001). Evaluating fractured reservoirs. *Geologic analysis of naturally fractured reservoirs*, 1-100.

Neumayer, J., Wiesmayr, G., Janda, C., Grasemann, B., & Draganits, E., Eohimalayan Fold and Thrust Belt in the NW-Himalaya (Lingti-Pin Valleys): Shortening and Depth to Detachment Calculation. **2004**.

Noetling, F. (1901). *Beiträge zur Geologie der Salt Range, insbesondere der permischen und triassischen Ablagerungen*. E. Schweizerbart'sche Verlagsbuchhandlung (E. Nägele).

Oil Show, **2003**; 3-5.

Olson, J. Fracture aperture, length and pattern geometry development under biaxial loading: a numerical study with applications to natural, cross-jointed systems. *Geological Society, London, Special Publications,* **2007**, *289*, (1), 123-142.

Parvez, M.K. *Petroleum Geology of Kohat-Bannu Plateau, Northwest Frontier Province, Pakistan*; University of South Carolina: Carolina, SC, USA, 1992.

Pilgrim, G. E. (1913). The correlation of the Siwalik with mammal horizons of Europe. *Rec. Geol. Surv. India*, *43*, 264-325.

Pivnik, D. A., & Sercombe, W. J. (1993). Compression-and transpression-related deformation in the Kohat Plateau, NW Pakistan. *Geological Society, London, Special Publications*, *74*(1), 559-580.

Salam, M. U., Mahalder, B. K., Bhandari, H., Kabir, M. S., Sarkar, M. A. R., Nessa, B., & Ali, M. A. (2019). Policy directions toward increasing rice productivity—lessons from Bangladesh. In *Advances in Rice Research for abiotic stress tolerance* (pp. 895-913). Woodhead Publishing.

Sayab, M., & Jadoon, Q. K. (2005). Kinematics of tectonic fracture development during regional folding in sandstones of the Kamlial Formation, Khushalgarh, northern Pakistan. *Geological Bulletin, University of Peshawar*, *38*, 65-79.

Scotese, C. R., Earth System History Geographic Information System. *Version 02b (PALEOMAP Project, Arlington, TX),* **2001**.

Searle, M. P., & Phillips, R. J. (2007). Relationships between right-lateral shear along the Karakoram fault and metamorphism, magmatism, exhumation and uplift: evidence from the K2–Gasherbrum–Pangong ranges, north Pakistan and Ladakh. *Journal of the Geological Society*, *164*(2), 439-450.

Seeber, L., and Armbruster, J., Seismicity of the Hazara arc in northern Pakistan: decollement vs. basement faulting, *Geodynamics of Pakistan,* **1979**, *131*, 142.

Shah, S. A., & Qadir, A. (2020). Fracture Analysis of Rocks for Slope Stability Assessment in SiriKot Area, District Haripur, Khyber Pakhtunkhwa, Pakistan. *International Journal of Economic and Environmental Geology*, *11*(3), 53-56.

Shah, S. I. (1977). Stratigraphy of Pakistan..

Singhal, B. B. S., & Gupta, R. P. (2010). *Applied hydrogeology of fractured rocks*. Springer Science & Business Media.

Sorkhabi, R. Fracture, Fracture Everywhere: Part I. GEOExPro: Geo education, **2014**, *11***,** (3), 86-88.

Spath, L. F. (1930). *The Fossil Fauna of the Samana Range and Some Neighbouring Areas: The Lower Cretaceous Ammonoidea; with Notes on Albian Cephalopoda from Hazara*. Government of India.

Teichert, C. (1966). Stratigraphic nomenclature and correlation of the Permian “Productus limestone”, Salt Range, West Pakistan. *Geological Survey of Pakistan*, *15*(1), 1-19.

Teichert, C. (1967). Nature of the Permian glacial record, Salt Range and Khisor Range, West Pakistan. *Neues Jahrbuch für Geologie und Paläontologie, Abhandlungen*, *129*(2), 167-184.

Thakur, V. C., Active tectonics of Himalayan frontal thrust and seismic hazard to Ganga Plain. *Current science*, **2004**, *86*(11), 1554-1560.

Valdiya, K. Northern and North-western Continental Margin: Mesozoic Stratigraphy. In *The Making of India*; Springer: Berlin/Heidelberg, Germany, 2016; pp. 509–545.

Waagen, W. H., & Wynne, A. B. (1872). *The Geology of Mount Sírban, in the Upper Punjâb*.

Wadia, A. R. (1919). Mr. Joachim's Coherence-Notion of Truth. *Mind*, *28*(112), 427-435.

Watkins, H.; Healy, D.; Bond, C. E.; Butler, R. W. Implications of heterogeneous fracture distribution on reservoir quality; an analogue from the Torridon Group sandstone, Moine Thrust Belt, NW Scotland. *Journal of Structural Geology,* **2018**, *108*, 180-197.

Yeats, R. S., & Hussain, A. (1987). Timing of structural events in the Himalayan foothills of northwestern Pakistan. *Geological society of America bulletin*, *99*(2), 161-176.

A DETAILED FRACTURE ANALYSIS OF TRIASSIC KINGRIALI FORMATION IN THE WESTERN SALT RANGE AND TRANS INDUS RANGES (SURGHAR RANGE), PAKISTAN

ORIGINALITY REPORT

8%	4%	4%	4%
SIMILARITY INDEX	INTERNET SOURCES	PUBLICATIONS	STUDENT PAPERS

PRIMARY SOURCES

1	Submitted to Higher Education Commission Pakistan Student Paper	4%
2	www.mdpi.com Internet Source	1%
3	Muhammad Yaseen, Muhammad Zeeshan, Jawad Ahmad, Abbas Ali Naseem. "Recognizing and classifying the naturally fractured reservoirs (NFRs) system for the cretaceous carbonate formation exposed along the Bagnotar-Baragali Section, north Pakistan: Implications from surface fractures, petrography and geochemistry", Research Square Platform LLC, 2022 Publication	1%
4	journal.kiu.edu.pk Internet Source	<1%
5	www.slideshare.net Internet Source	<1%